PTAF

Polygon Tessellation to Approximate Frame.
A Method for the Design and Analysis of Complex Frames

by
Richard Mui

A thesis
presented to the University of Waterloo
in fulfillment of the
thesis requirement for the degree of
Master of Architecture

Waterloo, Ontario, Canada, 2019.

AUTHOR'S DECLARATION

I hereby declare that I am the sole author of this thesis. This is a true copy of the thesis, including any required final revisions, as accepted by my examiners.

I understand that my thesis may be made electronically available to the public.

ABSTRACT

Complex frames are difficult to model because there are so many elements and redundant load paths. In order to explore the realm of complex frames, there needs to be a technique for approximate modelling to allow for rapid analysis with dependable accuracy. This thesis proposes the Polygon Tessellation to Approximate Frame (PTAF) method for rapid structural analysis of the Living Architecture Systems (LAS) group's complex frames.

The PTAF method uses the LAS composition design polygons as inputs for a parametric script that generates a simplified frame model. This model can be used for Finite Element Analysis (FEA) because it has perfect connectivity. By simplifying the model, the analysis can be run quickly on conventional computer hardware. In this way, structural performance can be evaluated without significant time investment. Especially in the early stages of the design process, it is important to quickly receive reasonably accurate predictions of performance because the design is constantly evolving.

To simplify the model, each component of the frame are reduced to a few beam elements that closely approximate the behaviour of much more detailed models. The process of linear FEA relates the force exerted on a model to the displacement it will undergo by its stiffness. The detailed and coarse models were subjected to the same support and loading conditions so that the displacement could be measured, and a function of error between the two displacements could be made. By minimizing the error between detailed and course models, values for the equivalent stiffness of each component can be derived. By enforcing continuity, the behaviour at the component scale can be used to predict behaviour at the global scale. In this way, the global simplified model will approximate the behaviour of the frame.

This research started through a collaboration with the LAS on the Amatria installation at Luddy Hall. The goal of the collaboration was to add value to the project through the addition of structural analysis in the design process. The frame of Amatria was immensely complex, full analysis of the frame would be prohibitively expensive, and add an unreasonable amount of time to the design process. This research was able to benefit the project by analyzing key components to ensure adequate strength and stiffness to facilitate ease of construction. Lessons learned from this projected helped inform this method's development.

This research provided the possibility of self-supporting LAS structures, based on the system of components currently being used in LAS testbeds.

A pavilion study was used as a thought experiment of how the combination of parametric modeling and approximate analysis could be used to design a free standing pavilion with LAS component construction. Participation in future testbeds will undoubtedly provide invaluable information to refine this method.

ACKNOWLEDGMENTS

I would like to thank my thesis supervisor Philip Beesley for providing the best research environment for exploring this interdisciplinary subject, and for his incredible patience through the whole process.

Thank you to my committee member Robert Gracie for providing expert guidance in the field of finite elements.

Thank you to my committee member Jonathan Enns for providing critical comments on the organization and presentation of the thesis.

Thank you to my external readers Scott Walbridge and Dave Bowick for taking time out of your busy schedules to be available for my review at such short notice.

Thank you to the members of the Living Architecture Systems Group for making me feel welcome in your studio.

Thank you to Elizabeth English for creating and championing the structural certificate. I would not be able to undertake this research or pursue my current career path without this certificate program.

Thank you to Andrea Atkins for providing continuing mentorship and trailblazing the path for myself and future structural certificate graduates.

Finally, a huge thank you to my family for your love and support.

DEDICATION

For my parents Linda and Dan Mui, my brother Aaron, and
my wife Soo Jung Woo, without whom nothing would be possible.

TABLE OF CONTENTS

LIST OF FIGURES

Part 4

THESIS ORGANIZATION

This thesis is structured in five chapters, the first introduces the problem of analyzing complex frames. The Polygon Tessellation to Approximate Frame (PTAF) method, which focuses on balancing speed, accuracy, and interface with typical architectural design software, is proposed as the solution. The second chapter provides relevant background information relating to: analytical tools, the design process, and an explanation of structural analysis techniques. The third lays out the PTAF method explicitly for the LAS system. The fourth chapter presents two explicit project studies: the first is Amatria, an LAS installation at Luddy hall, and the second is a hypothetical pavilion. The fifth and final chapter lays out areas for future improvement and application of PTAF.

The second chapter has four sections: the first is economic motivation. The second presents context of the development of structural analysis informed architectural exploration methods. The third shows a few specific case study projects which integrate structural analysis into their conceptual methods. The fourth section details the finite element analysis (FEA) method analysis technique behind PTAF.

The third chapter is divided into four sections which explain the PTAF method in detail. The first part describes the parametric scripts used to generate an approximate frame model of a LAS sphere unit from its representative polygon. The second part shows how structural approximation was applied to the spars. The third section shows how similar approximation was applied to the connections. The final part demonstrates how all these parts come together to create a structural analysis model of the entire frame.

The fourth chapter has two parts: Amatria at Luddy hall and the hypothetical pavilion. Amatria was the primary research collaboration through which PTAF was developed. Throughout the process, it became clear that building a FEA model of the frame was not possible with current desktop computer hardware limits. Furthermore, even with sufficient hardware, such models would be too cumbersome to update and maintain through the iterative design process. On the other hand, the project showed great potential for how structural analysis could improve the quality of the architecture. Engineering of the components for greater stiffness lead to an easier erection process through increased maneuverability and handling. The pavilion projects the capabilities of PTAF and how it might be interwoven into an iterative design workflow.

The final chapter overviews all that has been presented, then lays out the

different avenues for the future development of the PTAF method.

part 1

INTRODUCTION

1.1 PROBLEM STATEMENT

Figure 1-1: Amatria installation at Luddy Hall.

Recent developments in digital modeling and manufacturing have allowed architects to explore increasingly complex structures; however, while many design aids exist allowing for rapid design of rectilinear frames, there are yet similar methods for complex frames[1]. Complex frames are difficult to model because there are so many elements and redundant load paths, and they require tremendous amounts of computer processing power to run simulations on.

The design of complex frames are a cornerstone of the Living Architecture Systems (LAS) group's work. In order to explore the realm of complex frames, there needs to be a technique for approximating complex frames for rapid analysis with dependable accuracy. This could augment the group's design process with structural performance data, opening up more design possibilities.

1.2 INTRODUCTION

The LAS uses polygons to represent clusters of frame elements called spars in configurations known as sphere units. These polygons are used to study compositions of sphere units throughout the design process. Full spar geometry is not often used in studies because it is extremely taxing on computer hardware. Even in instances where detailed three dimensional models are built, the designers do not attempt to align all the connections accurately. Since the spars are made of thin material, and connected in a complex network, the physical elements can flex significantly during

installation in order to fit together in the desired arrangement. This results in models which are unsuitable for structural analysis because analytical models require member connectivity to be perfectly modeled. Even when the time required to model the frame is invested, these structures are so complex that it is physically impossible to run the simulations on regular workstation grade computer hardware. This was proved during a research collaboration between the author and the LAS on the Amatria test bed. To address these problems, this thesis proposes the Polygon Tessellation to Approximate Frame (PTAF) method for rapid approximate structural

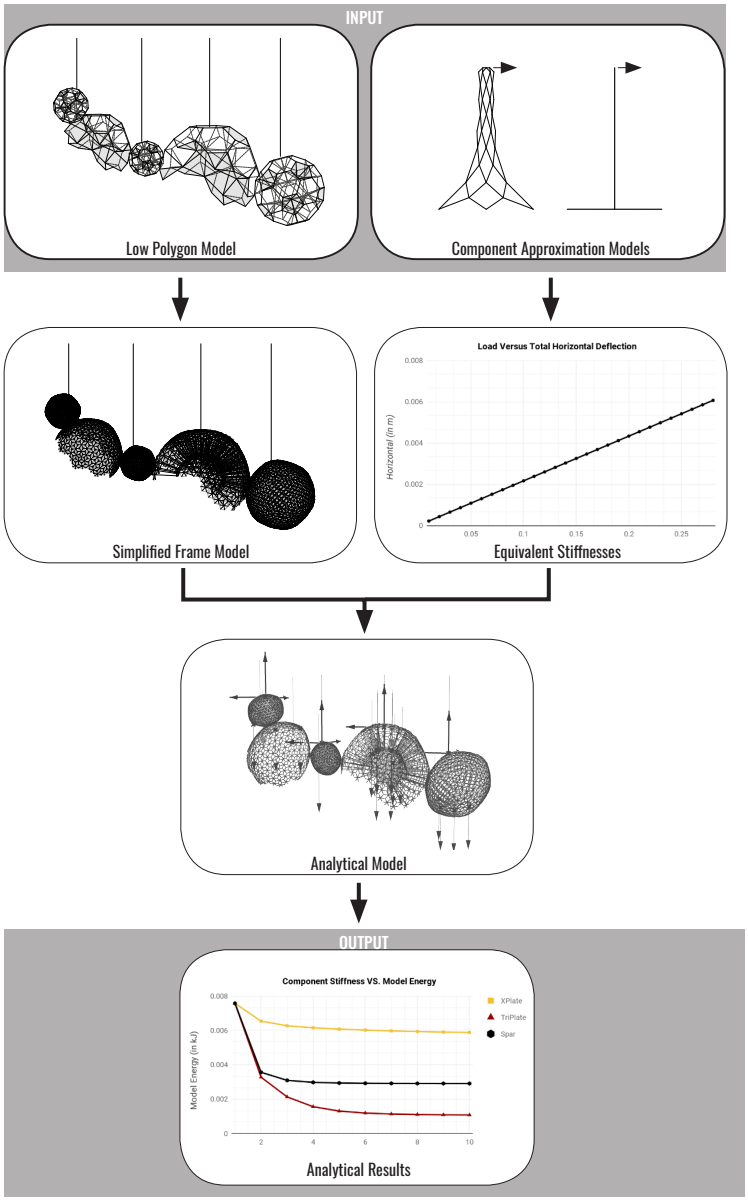

Figure 1-2: Concept diagram of the PTAF process.

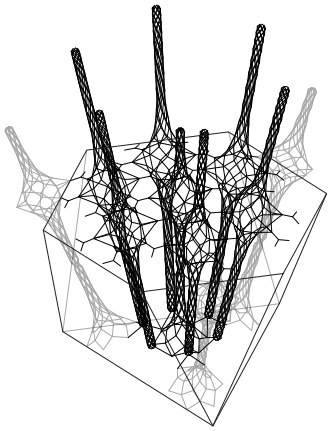

Figure 1-3: Composition Polygon with the Sphere Unit overlain.

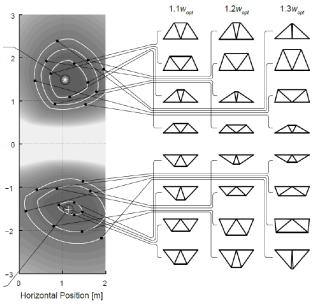

Figure 1-4: StructureFIT diagram showing variety of near optimal truss shapes.

analysis of complex frame structures.

The PTAF method solves these problems by using the original composition polygons as inputs in a parametric script which generates a simplified frame model. This model has perfect connectivity so it can be used as a direct input for Finite Element Analysis (FEA). By simplifying the model, the analysis can be run quickly on conventional computer hardware. In this way, structural performance can be evaluated without significant time investment. Especially in the early stages of the design process, it is important to receive reasonably accurate predictions of performance very quickly because the design is constantly evolving. This is particularly important for LAS projects because the structural elements are clearly visible and constitute a significant portion of the project's body.

There is also economic value in this proposal because it circumvents the process of trial and error. While almost all human innovation is rooted in this technique, it is costly to iterate through physical prototypes. This is all the more important in the case of buildings because the method of trial and error can be very dangerous to execute.

Architectural design processes augmented with structural analysis have a long history. Architects like Antonio Gaudi and Frei Otto have used analogue form finding models in order to achieve architectural forms which were previously not possible[2]. The tools they used, such as weighted catenary models, were insightful in that they created an intuitive link between building form and structural performance. The reason designers do not continue to use these models today is that analogue models are too expensive to be effective in the contemporary design industry. Contemporary form finding software tools which cater to both design and engineering are only employed in highly specialized applications such as tensile structure design.

In academia, the work of the Digital structures research group at MIT is of particular interest to this research because they are focused on creating a set of tools that are made for multi-objective structural optimization, and have the promise of delivering speed, analysis, and intuitive interfaces[3]. Furthermore, these tools are being developed for Grasshopper and Rhinoceros 3D software because these software are typically employed by architects for conceptual design.

Some contemporary projects use topology optimization software to incorporate structural information into their design process. These

software work efficiently in situations where the problem is well defined, such as Kociecki's optimization of the Ottawa train station roof gridshell[4]. Similarly, the Akutagawa Office and Qatar National Convention center have clear boundaries where the topology optimization question is defined[5]. The Block Research Group (BRG) at the ETH in Zurich created bespoke software to formfind lightweight shell structures. The efficacy of their research is demonstrated in their HiLo penthouse roof project on the NEST building at ETH[6]. Their software considered architectural criteria, such as door placements and headroom, in conjunction with stress reduction in the generation of the form. It was clear from these projects that any method developed for a hybrid structural and architectural design process should be made for a specific type of structure to be effective.

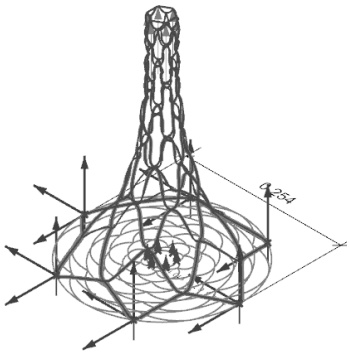

Figure 1-5: Parametric non-linear spar expansion model.

In order to achieve faster analysis, the structural analysis process itself had to be explored in detail. The most widely used analytical technique in engineering today is the finite element analysis (FEA) method utilizing beam elements, also known as the direct stiffness method. This technique relates the forces exerted on a beam to the displacements it will undergo by the stiffness. The stiffness is a function of the beam's material and geometric properties. A frame can be represented as an amalgamation of beams. In order to model the behaviour of a frame, the geometry of the frame should be modeled as accurately as possible.

Yet, as explained earlier, it is unreasonable to model a complex frame in its entirety. The solution was to represent a spar with as few beam elements as possible; while maintaining its geometric connectivity within the frame. Going back to basics, the stiffness is all that is needed to execute accurate analysis. It is possible to derive a numeric value for the equivalent net stiffness of a spar frame. In this way, even though the approximation models of the spars are not geometrically accurate representations of the spars, they can still be used to produce reasonably accurate results. By dramatically simplifying spar geometry, it is possible to create a Grasshopper script which converts the simple geometry used in the architectural model, into line models for FEA input. The more difficult part of the process is determining whether or not this simplified model is reasonably accurate. In this research, this was achieved by minimizing the error in deflection between more accurate representative models and the coarse approximation models, for each of the components which constitute the assembly.

The research collaboration with the LAS on the Amatria at Luddy Hall installation was seminal to developing the PTAF method. The goal of

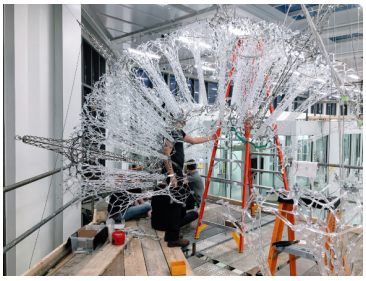

Figure 1-6: Amatria installation process.

Figure 1-7: Finished installation of Amatria at Luddy Hall.

the collaboration was to add value to the project through the addition of structural analysis in the design process. The frame of Amatria was immensely complex, full analysis of the frame would be prohibitively expensive, and add an unreasonable amount of time to the design process. The solution at the time was to analyze key components to ensure adequate strength and stiffness to facilitate ease of construction.

The next project, a hypothetical pavilion design, projects how the PTAF can be integrated into an architectural design study work flow. In this example, model strain energy is used in conjunction with visual appraisal, in order to give another lens to compare different design options. The goal is not to use as little material as possible, but rather to achieve the most value in between design quality and efficiency.

While the PTAF method was successfully outlined through this research, significant work needs to be done in each aspect of the PTAF process. Each portion can become its own research topic of significant depth. New types of spar combination polygons and their combinatorics could be explored. Topology optimization algorithms could potentially be employed to approximate input surfaces as tessellations of several input polygon types. These tools would open the door to more design exploration.

The metal expansion process, relating the cut pattern to expanded form, of the Spar elements would require a series of lab tests in order to calibrate further numerical analysis. Additionally, torsion and other equivalent stiffnesses should be worked into each approximate spar and connection model for increased accuracy. This makes it more difficult to derive the equivalent stiffness because the function of error between the approximate and true frame becomes multidimensional.

One of the most difficult, but important pieces of information to add to the output of PTAF is prediction of structure yielding. Unfortunately, since yield criterion is related to geometry, it is not possible to get it directly from PTAF models. A suggestion would be to research the specific nodal displacements associated with yield of the spar geometry and store this information in a table. A program could be written to cross reference this table to see if any nodes have exceeded the specified yield displacement. Substantial investigation must be made on this front to produce a solution.

Further research should also consider nonlinear behaviour of the entire frame. The behaviour of the frame is nonlinear because the effective stiffness changes while the body is deforming. The current model does not

take advantage of this and might lead to over designed frames.

Future research can be conducted on these discrete areas in relative isolation because their relevance to the method is relatively well defined by this outline. The ultimate goal is to see this process utilized and evolve organically through its implementation in future LAS work.

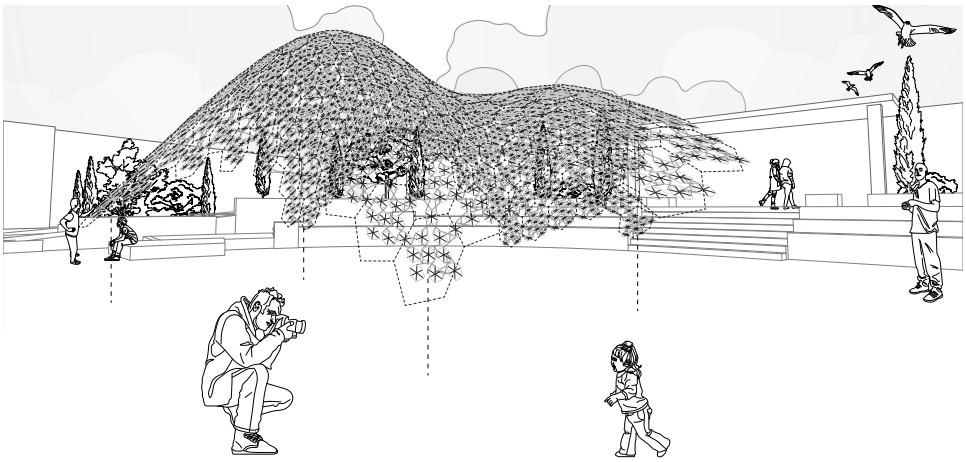

Figure 1-8: Rendering of generated pavilion.

Endnotes

1 Canadian Wood Council, *The Span Book: Span Tables for Canadian Dimension Lumber and Glued-Laminated Timber*, 6th ed. (Ottawa, Ontario.: Canadian Wood Council, 2009)

2 Block, Philippe. "Thrust Network Analysis Exploring Three-dimensional Equilibrium," *Massachusetts Institute of Technology*, 2009, accessed October 3, 2017, https://dspace.mit.edu/handle/1721.1/49539. 37.

3 Danhaive, Renaud, and Caitlin T. Mueller. "Combining Parametric Modeling and Interactive Optimization for High-Performance and Creative Structural Design," *Proceedings of the IASS Symposium 2015*, Digital Structures, Accessed November 11, 2017, http://digitalstructures.mit.edu/files/2015-09/iass2015-524698.pdf.

4 Kociecki, Maggie, and Hojjat Adeli. "Two-phase Genetic Algorithm for Size Optimization of Free-form Steel Space-frame Roof Structures." *Journal of Constructional Steel Research* 90 (2013): 283-96. doi:10.1016/j.jcsr.2013.07.027.

5 Januszkiewicz, Krystyna, and Marta, Banachowicz. "Nonlinear Shaping Architecture Designed with Using Evolutionary Structural Optimization Tools." *IOP Conference Series: Materials Science and Engineering* 245 (2017): 082042. doi:10.1088/1757-899x/245/8/082042.

6 Veenendaal, Diederik, Jack Bakker and Philippe Block. "Structural Design of the Flexibly Formed, Mesh-reinforced Concrete Sandwich Shell Roof Of Nest HiLo," *Journal of the International Association for Shell and Spatial Structures 58*, no.1(2017): accessed November 2, 2017, http://www.block.arch.ethz.ch/brg/files/Jiass_2017_vol58_no1_08_Veenedaal_Mesh-reinforced-sandwich-shell-roof-NEST-HiLo_1491482576.pdf.

part 2
CONTEXT

2.1 INTRODUCTION TO SECTION

This research is situated in the larger narrative between the engineering and architectural design disciplines. The goal of this section is to provide the context of that narrative, as well as provide the necessary engineering background to understand PTAF. This chapter has four sections which serve these goals. The first is background on the value proposition of engineering. The second is the context of the development of structural analysis informed architectural exploration methods. The third presents a few specific precedent study projects that integrate structural analysis with architectural conceptualization. The fourth section details the FEA method which is the analysis technique behind PTAF.

The value proposition of engineering is that it should provide direct economic value because it circumvents the process of trial and error. This section introduces this proposition in the structural engineering of buildings. It then zooms in on what value PTAF, as a hybrid engineering process, could bring to the LAS.

The second section of this chapter looks at how structural analysis fits into the intuitive design process. Early analogue form finding models, such as the weighted catenary models Antonio Gaudi and his team constructed to inform the shapes of the vaults of the Sagrada Familia, were analytical and intuitive; however they were expensive. Modern form finding software are fast and analytical, but they are not intuitive and do not integrate into the architect's open ended problem solving workflows. Software that promotes user participation, such as CADenary and StructureFIT, are fast, intuitive, and somewhat analytical, but are independent applications that do not integrate well with typical architectural CAD software. The most significant precedent for PTAF is work of the Digital structures research group at MIT. The group is focused on creating a set of tools which are made for multi-objective structural optimization that have the promise of delivering fast analysis through an intuitive interfaces. Furthermore, these tools are being developed for Grasshopper and Rhinoceros 3D software because they are typically employed by architects for conceptual design. Although many specific details differ, these major aspects helped inform the development of PTAF.

The third section explores a series of project precedents which incorporate a structurally informed design process. These projects all utilize topology optimization software in order to generate form and increase material efficiency. The issue is topology optimization software only work efficiently in situations where the problem is well defined, such as Kociecki's optimization of the roof gridshell of a train station in Ottawa. Since the

technique is well suited for defined problems, buildings designed with these software tends to lean toward a particular design aesthetic, such as the Akutagawa Office and Qatar National Convention center. A solution to software authorship is the creation of bespoke software for a specific class of projects. The Block research group at the ETH in Zurich exemplify this approach in their creation of formfinding software for lightweight shell structures. The efficacy of their research is demonstrated in their project for the design of the HiLo roof to be used on the penthouse of the experimental NEST building on the ETH campus. It was clear that, in order to maintain the aesthetic of the LAS, PTAF had to be developed specifically for LAS installations.

The final part of this chapter presents important background information necessary to understanding the limitations and opportunities of contemporary structural analysis software. FEA is the most commonly used structural analysis method in the industry. The goal of the FEA method is to find approximate solutions to differential equations, the reason why this is valuable is because the method makes it possible to solve conditions that could not be solved by other methods. Nonlinear FEA is discussed because the process of forming sheet metal into spars breaks the assumptions of linear analysis, making linear FEA invalid.

2.2 ECONOMIC MOTIVATION

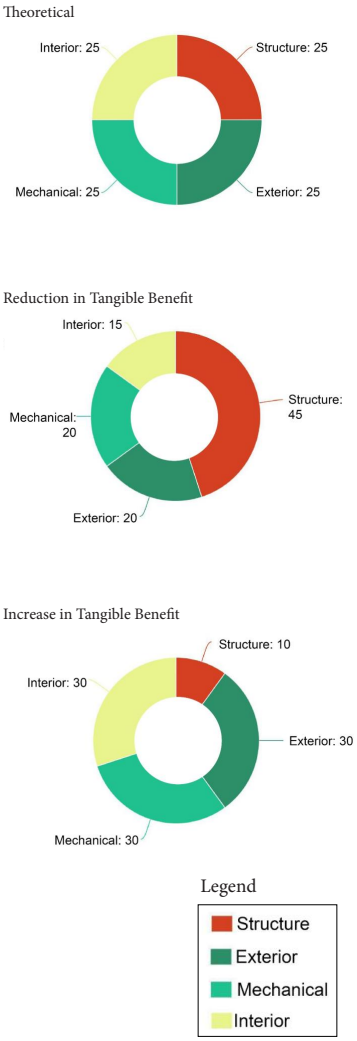

Figure 2-1: Conceptual cost breakdown of a building

The engineer Arthur Wellington famously said that "an engineer can do for a dollar what any fool can do for two[1]." This statement highlights that the proposition that engineers can save resources by using their knowledge to circumvent trial and error. For buildings in particular, engineers become mandatory because these structures are too dangerous to design through trial and error. The practice of structural engineering has become a careful balance between providing economic efficiency and occupant safety[2].
The cost of a building can be approximated as one quarter structure, one quarter exterior, one quarter mechanical systems, and one quarter for interior elements[3]. It is known that structure is important to safety, but after a building is safely standing, spending more money on it does not effect the quality of life within. Considering the other three: spending extra money on creating a better insulated and air tight building exterior will save energy and thus reduce the environmental impact of the building. Spending extra money on mechanical systems allows the building to have more efficient systems, similarly reducing environmental impact. Better mechanical systems can also lead to an increase in occupant comfort. Spending on interior finishes and quality directly increases the user experience and enjoyment of the occupants. Structure is the only aspect where excess spending does not directly effect occupants; furthermore, any excess spending on structure directly takes away from the other three parts that do.

Since the industrial revolution, architectural design has diverged into many uniquely skilled professionals[4]. In particular, there is the architect involved with aesthetic and user focused design criteria as well as overall project coordination, and there is the structural engineer who is focused on the design and specification of a building's structural framing elements to ensure occupant safety. The issue is that geometry has the greatest impact on structural efficiency, but the geometry is set by architects who do not consider structural performance criteria. On the other hand, engineers propose framing layouts without considering key architectural criteria. Since each professional is working in their own silo, it is only natural that large discrepancies occur. This leads to many increases in the cost of super structure as a direct result of poor coordination. In this way, many materially inefficient structures have been created in the last few decades. There needs to be methods for integrating both criteria in the early design stage.

For the installations of the LAS, the value proposition of structural engineering is seemingly less obvious than structural engineering for conventional buildings. Part of the reason is the scale of LAS projects are

sufficiently small so that trial and error can be used. Furthermore, analysis of such complex frames is so difficult that it results in a design process that is slower than using trial and error. Even so, in order to create larger scale, self supporting projects, the LAS must employ engineering technique.

The structures that the LAS create can be classified as free form space frames, The largest controlling factor of these structure is the number of unique components. The danger of an unintegrated engineering process is the requirement for many unique components. Individually fabricating components for a unique design comes at a significant economic disadvantage. Thomas Fischer describes two approaches to creating irregular trusses: the first is to design a set of components that can be used in various combinations to create many unique designs, and the second is to take an irregular design and try to rationalize it into as few unique components as possible[5]. Both of these techniques deviate from truly freeform designs, thus some landmark projects forgo these procedures. The roof extension to the British Museum by Foster and Partners and utilized 5000 unique beams and 1500 unique nodes to create the structure. When it comes to inhabited structures, there is undoubtedly a need for engineering, the question becomes how and where to integrate engineering technique in the process of design.

2.3 THE ROLE OF ANALYSIS IN CONCEPTUAL DESIGN

Current architectural practices that truly integrate structural analysis in the earliest stages of their design are few and far between. Historically, Antonio Gaudi and Frei Otto have been two significant architects who have created masterworks based on this pairing. Gaudi famously used an analogue model for the formfinding of his church the Sagarda Familia in Barcelona. In his model, he utilized strings loaded with weights proportional to the loads that the structure would be subjected to once built[6]. By Hooke's famous discovery "the sagging cable inverted so stands the rightful arch" Gaudi and his team were able to design a structure which was beautiful and structurally efficient. Otto and the institute for lightweight structures in Stuttgart utilized a sophisticated electronically measured and actuated hanging cable model for the design of the Multihalle in Mannhiem Germany[7]. In principle, albeit much more advanced, Otto's hanging catenary model was similar to the one utilized by Gaudi a century earlier. The advantage of analogue models that approximate structural behaviour is that they allow simultaneous structural analysis and formal exploration. The disadvantage is that these models are expensive to construct and maintain, furthermore, once the model becomes significantly complex, it becomes very tedious to implement changes.

Today's designers largely work with digital tools, Caitlin Mueller, in her 2014 PhD dissertation for MIT, discusses how current architectural modeling tools create geometry in absence of performance, while engineering software requires the input of already determined geometric form. Yet structural performance is most affected by geometric form; in the current paradigm, opportunities to achieve innovative and structurally efficient designs have been lost[8]. The negative effects of current post analyzed processes are exacerbated in the design of complex frames Danhaive and Muller critique typical black-box optimizers because they limit the authorship of designers. Interactive optimization algorithms, on the other hand, would allow designers to input and influence the optimization process of a field of options, thus allowing them to retain their creative freedom[9].

A particularly useful optimization software is Galapagos, which is a built-in evolutionary solver for Grasshopper. It provides easy to use tools for designers to integrate evolutionary optimization techniques in their parametric models. The problem is Galapagos only provides solutions that optimize a single value; which is unacceptable in architectural conceptual design. On the other hand, Stormcloud, developed by the Digital Structures team at MIT, provides evolutionary optimization with the goal of maximizing variation. Based on an input seed and parameters

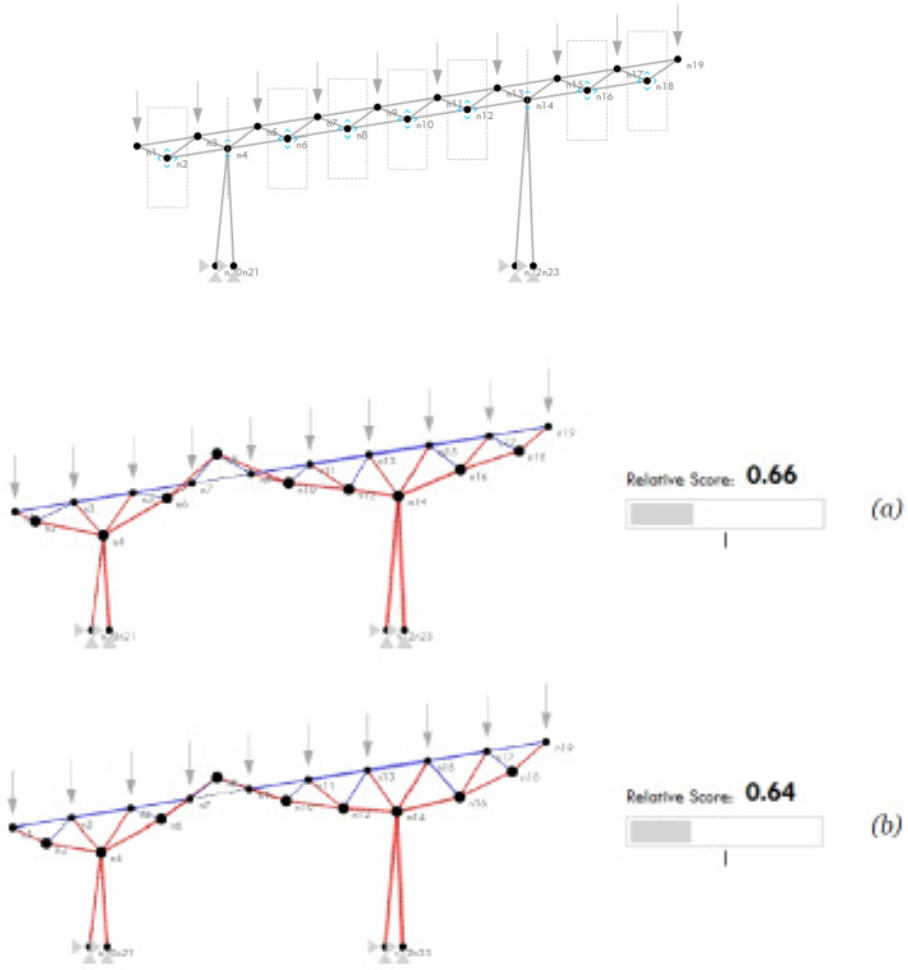

Criteria	How is it expressed?	How is it measured?
Structure weight	Numeric score	Relative to a baseline
Daylighting	In drawing	Not measured

Figure 2-2: Topology optimization of a roof truss from StructureFIT.

to optimize, the program will generate a field of designs which are near optimal whilst maximizing difference in geometric form[10].

A further benefit of the integration of analysis in conceptual design is the possibility of discovering unforeseen options. To explore this possibility, Mueller created an interactive evolutionary software she had developed called StructureFit. In an exemplary exercise, she utilized the software to develop the design of a roof truss. One of the options that was generated was not only 34% more efficient in steel usage, it provided for the new architectural opportunity of a skylight in the space[11]. Mueller's study proves bringing structural considerations into conceptual architectural design not only serve economic benefit, but also opens up new unforeseen architectural forms.

There is other research that focuses on the building intuition through live feedback. To this end, Kilian and Ochsendorf explore a particle-spring Runge-kutta solver for the use of equilibrium formfinding of two and three dimensional funicular forms[12]. The key advantage of this technique is that users can change form and forces in real time while the solution is calculating. The environment is fully dynamic, allowing an intuitive manipulation of the form as opposed to a quantitative one. This solver, and other similar intuitive form finding software, are typically applications of dynamic relaxation, because applying this method to computer models with kinetic dampening allows the effect of changes to be viewed in an interactive way. As stated by Barnes, the integration of specific knowledge of the system of assembly, such as: a cable net, gridshell, or space frame, is important as these will affect the allowable deformation of the structure[13]. While the addition of material behaviour to such solvers is undoubtedly important, integrating these applications directly into typical architectural software would be fundamental for the adoption of such techniques in practice.

There are also software that integrate directly with architectural software. For example, Kangaroo, a physics simulation plug-in for the visual based coding environment Grasshopper for Rhinoceros 3D, allows architects to simulate analogue catenary modeling and soap-film like minimum surfaces within the Rhino modeling environment. The software integrates a real-time dynamic solver allowing designers to see how their changes can affect the design in real time. The problem with Kangaroo, and similar applications is that it does not utilize realistic units for forces; rather users will input seemingly arbitrary magnitudes on a relative scale. Another issue is that users are not able to easily adjust specifics of the solving algorithm,

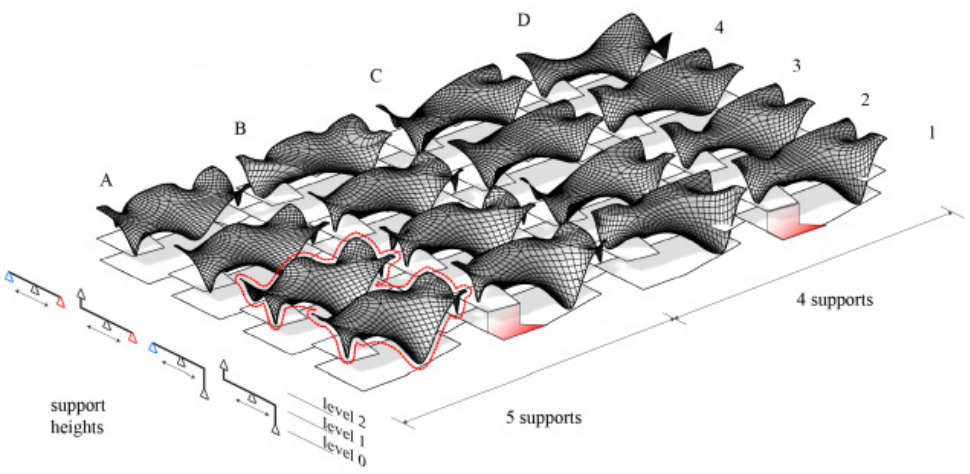

$$\text{minimize } E\left(f\left(x,s,h,q\right)\right)$$

subject to

$$\begin{aligned}
\sigma &\le 20 \text{ N/mm}^2, \\
\delta &\le 30 \text{ mm}, \\
0.11 &\le x_4 \le 0.45, \\
0.60 &\le x_3 \le 0.90, \\
1.10 &\le x_2 \le 1.90, \\
2.10 &\le x_1 \le 2.43, \\
3.45 &\le x_5 \le 3.90, \\
0 &\le s_{1\ldots5} \le 10, \\
0 &\le h \le 5, \text{ and} \\
1 &\le q_{1\ldots11} \le 10.
\end{aligned}$$

Criteria	How is it expressed?	How is it measured?
Structure weight	Numerically	Proportional to bending energy
Geometric boundary conditions, example avoid supports near corners	Numeric domain	Constraint on solver

Figure 2-3: Topology optimization of the concrete shell roof of the HiLo Penthouse.

rendering the software a block-box solver.

Commercial engineering software such as Strand7 provides a full finite element analysis suite for general application, opposite to Kangaroo; the tool is heavily analytic based. As previously discussed, the tool has the ability to realistically predict the behaviour of non-linear structures with a great degree of precision[14]. The big drawback of Strand7 is that models are exceptionally time consuming to build and big design changes are similarly tedious to integrate. These qualities render the tool unsuitable for use in conceptual design.

There is yet a practical workflow for designers to incorporate structural performance in early explorations. While providing a general software applicable to all project types is still elusive, aspects of this research informs the specific PTAF method for the LAS spar unit system.

2.4 STRUCTURAL OPTIMIZATION AND THE ARCHITECTURAL DESIGN PROCESS

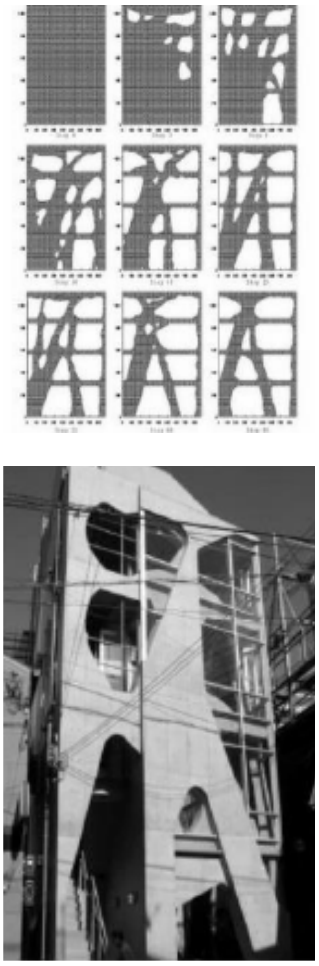

Figure 2-4: Akutagawa River Side in Takatsuki, Japan. Top: topology optimization of the facade, bottom: view of the building from the street.

The following projects serve as precedents that incorporate design informed by structural analysis. All these projects utilize some form of topology optimization. Topology optimization is most effective when the problem is well defined; however, there is a reciprocal relationship between articulating design concepts and defining the design problem. Wael Abdelhameed summarized that architectural design ideas can be generated from: the architect and their creativity, subjective interpretation of design-problem context, personal prejudice of design thinking and individual style[15]. Application of topology optimization is project and architect specific. The first application of topology optimisation in the design of a building was in the 2004 Akutagawa building in Takatsuki Japan designed by architect Hiroyuki Futai and Iijima structural design office (figure 2-4)[16]. Extended evolutionary structural optimisation (EESO) was used to determine the void patterns of the walls of the building. The optimisation accounted for dead, live, and dynamic earthquake loads[17]. The architectural merit of the application of EESO is the ability to read the force distribution within the structure on the facade.

The first major volumetric implementation of EESO was in the Qatar National Convention Center, conceived of by architect Arata Isoaki and engineer Matsuro Sasaki in 2008 (Figure 2-5). The building features two EESO derived structural trees which support a 250 meter long entrance canopy[18]. This is still the largest EESO generated structure today. That being said, the specific topology of the structure's organic skin is largely formal in nature, since the structure is not made or reinforced concrete, and the fluid form of the structural trees is created by a complex series of cladding panels. The interior structure consists of octagonal tubes welded from flat plate. In this way, the thickening and thinning of the structure does not truly represent any efficiency in material distribution.

Research into explicit use of topology optimization to achieve material efficiency has been undertaken by ARUP. The company conducted a research project into creation of a structural node for a tension structure, based on a previous design. The complex geometry of the structure called for many unit nodes, thus reducing the economy of conventional production techniques. ARUP researched the potential of additive manufacturing in the production of unique nodes. Researchers realized that this technology had the potential to create complex geometries, and therefore was feasible to use in conjunction with topology optimisation (figure 2-6). Resulting node designs reduced the weight almost in half. The current costs of additive manufacturing are prohibitively expense, and the

generation of node geometry is also highly labour intensive for engineers.

The crematorium in Kakamigahara Gifu Japan, designed by architect Toyo Ito and engineering Mutsuro Sasaki utilized EESO to rationalize the roof's free-flowing form. The roof balances functional programing, structural requirements, servicing, and the architect's aesthetics requirements.

In academia, there is research on the integration of stress analysis and material distribution. Inspired by the methods that water spiders use to weave their underwater webs, researchers at the ICD and ITKE at the University of Stuttgart designed a pavilion that was to be constructed by a robotic arm inside of an inflated dome. The inflated dome would act as formwork for the robotic arm to lay carbon fibre reinforcements. Analysis of the dome using finite element techniques allowed the engineers and designers to align the placement patterns of carbon fibre with principal stress. In a similar vein, the design of the NEST HiLo shell roof by the block research group at ETH Zurich utilized digital catenary form finding in the conceptual stage. Utilizing an integrated parametric model for multi-objective evolutionary shape optimization of the shell, researchers of the Block research group were able to integrate processes of form finding and analysis into a multi-phased approach. The process starts with the generation of boundary curves, then a topology is generated within the boundaries, afterwards a form is generated using the linear force density method. Loads are applied and then the form is subjected to early optimization, which yields multiple optimal designs. These designs are cycled iteratively between increasingly complex structural analysis and architectural scrutiny.

Figure 2-5: Images Qatar National Convention Centre in Doha. Clockwise descriptions: Exterior view, topology optimization output model, axonometric view of the structure, framing and cladding strategy, view of branching support.

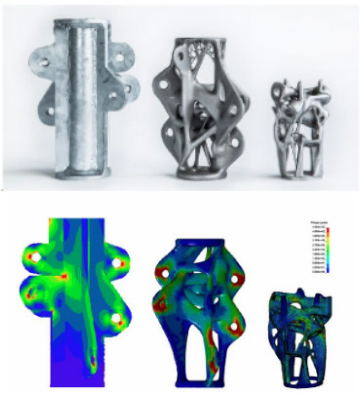

Figure 2-6: Top: node fabricated from plate and two nodes produced by additive manufacturing, bottom: FEA of nodes showing reduction in underutilized material

The projects and techniques reviewed in this section make it clear that technology is still far from being able to create fully automated general purpose structural design software. It is possible; however, to create efficient solvers for well defined problems. It requires several iterations in order to establish the scope of an engineering problem. Furthermore, these techniques are valid only within a preset domain. Formfinding, the process of defining domains, is an important part of architectural design. Unlike optimisation problems, formfinding is an open ended problem that is subject to objective and subjective constraints. The iterative design approach is still the most valuable method for approaching these types of problems; however, utilizing analysis will provide insight that might be valuable to defining efficient and beautiful forms. Topology optimisation can also be useful for reducing the time it takes to generate options. Each of these techniques are tools, and their usefulness depends on the specific

Figure 2-7: Images of Crematorium in Kakamigahara Fifu, Japan. Top: view from exterior, bottom: view looking outwards.

design problem, as well as the designer's background knowledge and subjective biases. This particular research is interested in using a limited combination of parts to create space frame structures. The boundary surface of these frames will be defined by their functional and structural criteria. The distribution of set components becomes a sufficiently well defined problem to solve. Design of these components and boundary surfaces will be driven by insight from numerical analysis.

2.5 ANALYTICAL TECHNIQUES

2.5.1 THE DIRECT STIFFNESS METHOD

Although purely symbolic methods of structural analysis exist, contemporary engineers largely employ numerical methods because they can be readily executed by computers[19]. The principle of virtual work, a classical mechanic theory based on newton's law of motion, underpins all numeric methods of structural analysis. Virtual work is based on real work; however, instead of considering a real distance, we consider a differential distance, that is to say a distance of almost zero. The fundamental theorem of calculus allows us to deal with values that are effectively zero; these values are called differentials. If we consider a deformable body in static equilibrium, we can use the principle of virtual work in a way to solve for the internal forces within all of the members subjected to external forces and constraints. First, we define the internal virtual work equal to the internal forces through the virtual displacement differential x; where x is a vector. Next, we define the external virtual work equal to the virtual force through the real displacement. Finally, since the body is in equilibrium, we know that the external virtual work must equal the internal virtual work. By this equality, we can solve for the internal forces and well as the external displacement.

Most steel frames can be classified as slender and behave like collections of beams. Given that the members of a steel frame are sufficiently thin, we can model their behavior with Euler-Bernoulli beam theory where torsion and shear deformation can be considered negligible[20]. Commercial structural analysis software use collections of beam elements, in what is known as the stiffness method, in order to compute the member forces and displacements. In order to understand the stiffness method, a few topics need to be introduced first, namely: strain, stress, and linear elasticity. Strain is deformation per unit length, essentially the units of deformation in a body. Stress is the force per unit area, that is to say the units of force in a body. Linear elasticity is when a system; its arrangement, and its materials, obey Hooke's law. In the linear elastic case, this law relates stress as linearly proportional to strain:[21]

$$F = -kx \tag{2.1}$$

The linear elastic assumption holds true for small deformations, which is convenient because building users typically do not want their buildings to visibly deform. Euler-Bernoulli beam theory relates force to displacement in a beam using Hooke's law.

$$EI_{yy}\frac{d^2u_2(x)}{dx^2} = -M_y(x) \tag{2.2}$$

Full derivation of the stiffness method can be found in the textbook: A First Course on Finite Elements by Belytschko and Fish chapter ten; however, key points will be summarized below in the following text[22]. If we consider a beam in two dimensions only and assume that the beam is relatively thin, we can consider it to be in a state of plane stress, thus only strain ε_{xx} is not zero. Therefore, we may derive the following strain equation by using beam theory:

$$\varepsilon_{xx} = \frac{\partial u_x^M}{\partial x} - y\frac{\partial^2 u_y}{\partial x^2} \tag{2.3}$$

Using Hooke's law and the theory of normal stress due to moment from solid mechanics and applying them to 2.2, we can arrive at the following expression for the moment in the beam.

$$m = E\frac{d^2u_y(x)}{dx^2}\int_A y^2 dA = EI\frac{d^2u_y(x)}{dx^2} = EI\kappa \tag{2.4}$$

If we imagine that the beam divided into infinitesimally small slices or slices of differential width, we can consider the equilibrium of each of these elements. We know that, since the system is in equilibrium, each sub-element is also in equilibrium. By taking the sum of the moments and the sum of the vertical forces in this slice, we can arrive at the following equation:

$$\frac{d^2m}{dx^2} - p = 0 \tag{2.5}$$

We already derived another equation for moment earlier, so we can substitute (2.3) into (2.4) to give us:

$$EI\frac{d^2u_y}{dx^4} - c = 0 \tag{2.6}$$

This equation is known as the governing differential equation or strong form equation of Euler-Bernoulli beams. This is a very significant equation, because it relates the vertical deformation of a beam to its internal moment. Using this equation, we are able to predict the amount of sag a beam will experience when subjected to a load, as well as its internal bending and shear stress, so long as we don't violate the linear elastic assumption. This is a general differential equation, so to solve it for a specific case, we must include it's boundary conditions. Solving an equation without boundary conditions is akin to imagining a beam floating in the vacuum of space. This situation is not very useful to designers of buildings on earth, therefore we need to consider how the beam is attached to the ground and or other parts of the structure. Furthermore, we should consider the entire of system of beams in the frame, in order to predict its performance. Therein lies the problem, once we consider the entire system, the problem because impossible to solve symbolically for all but the most simple of situations.

This is where we can use a numeric approximation technique called finite element discretization. The process is as follows: convert the strong form equation to a weak form equation, break the beam up into a finite number of pieces, create approximate solutions for each piece, and reassemble all the pieces together to get an approximation of the entire beam's behaviour. First, we will derive the weak form by taking the strong form, multiplying by a weight function, integrate by parts, and applying the boundary conditions to arrive at:

$$\int_\Omega \frac{d^2w}{dx^2} EI \frac{d_y^{2u}}{dx^2} dx = \int_\Omega wpdx + \left(\frac{dw}{dx}\,\bar{m}\right)\Big|_{\Gamma_m} + (w\bar{s})|_{\Gamma_s} \; for\; \forall w \in U_0 \tag{2.7}$$

Next, we need to cut the beam into small pieces, but unlike before, we will cut it into a definite number of pieces. The more pieces we cut the beam into, the closer our answer will be to the theoretical answer; however, we are limited by the processing power of computers. Therefore, it is important to choose the number of elements that balances appropriate accuracy with reasonable computation time. Next, at the element level, we can approximate the force as a linear combination of polynomial functions.

The advantage of using a linear combination of polynomials is that even an incredible quantity of linear equations can be solved systematically with linear algebra. In this way, a computer can readily solve thousands, or even millions, of simple linear equations. To construct these linear combinations of polynomials, we can use the form of Hooke's law (2.1). We know that force equals the displacement multiplied by the stiffness. The displacement is what we are solving for, so that leaves the stiffness to be approximated. To get to this point, we can represent u_y and w as the following linear combinations:

$$u_y^e = \boldsymbol{N}^e \boldsymbol{d}^e, \qquad w^e = \boldsymbol{N}^e \boldsymbol{w}^e \tag{2.8}$$

Where the bold type is used to signify that the variable is in fact a matrix of linear equations. The exponent e is used to signify that it is an element level equation. Now we can substitute these approximations into (2.7). The left hand side gives us the forces in the form of force times displacement. The exact process will not be covered here, but the left hand side shows us K in the form below:

$$\boldsymbol{K}^e = \int_\Omega EI \boldsymbol{B}^{e^T} \boldsymbol{B}^e dx \tag{2.9}$$

Similarly, the force can be found by substitution of our approximations into the first two terms of the right side of (2.7). This give us the following:

$$\boldsymbol{f}^e = \underbrace{\int_\Omega \boldsymbol{N}^{e^T} \rho dx}_{\boldsymbol{f}_\Omega^e} + \underbrace{\left(\boldsymbol{N}^{e^T} \bar{s}\right)|_{\Gamma_s} + \left(\frac{d\boldsymbol{N}^{e^T}}{dx} \bar{m}\right)\Bigg|_{\Gamma_m}}_{\boldsymbol{f}_\Gamma^e} \tag{3.0}$$

Using these forms, and re assembling our element level equations into a global equation, we can find the equation in the form:

$$\boldsymbol{K}\boldsymbol{d} = \boldsymbol{f} + \boldsymbol{r} \tag{3.1}$$

This form of the equation can finally be solved easily by a computer. This entire process is known as the Stiffness Method, which can give us the member forces and displacements of arbitrarily complex arrangements of beams. The stiffness method is generally quite accurate for predicting the displacement and moment within a beam; however, insufficient elements

can lead to large inaccuracy in shear prediction. This is manageable by the fact that long slender members are typically controlled by moment and deflection.

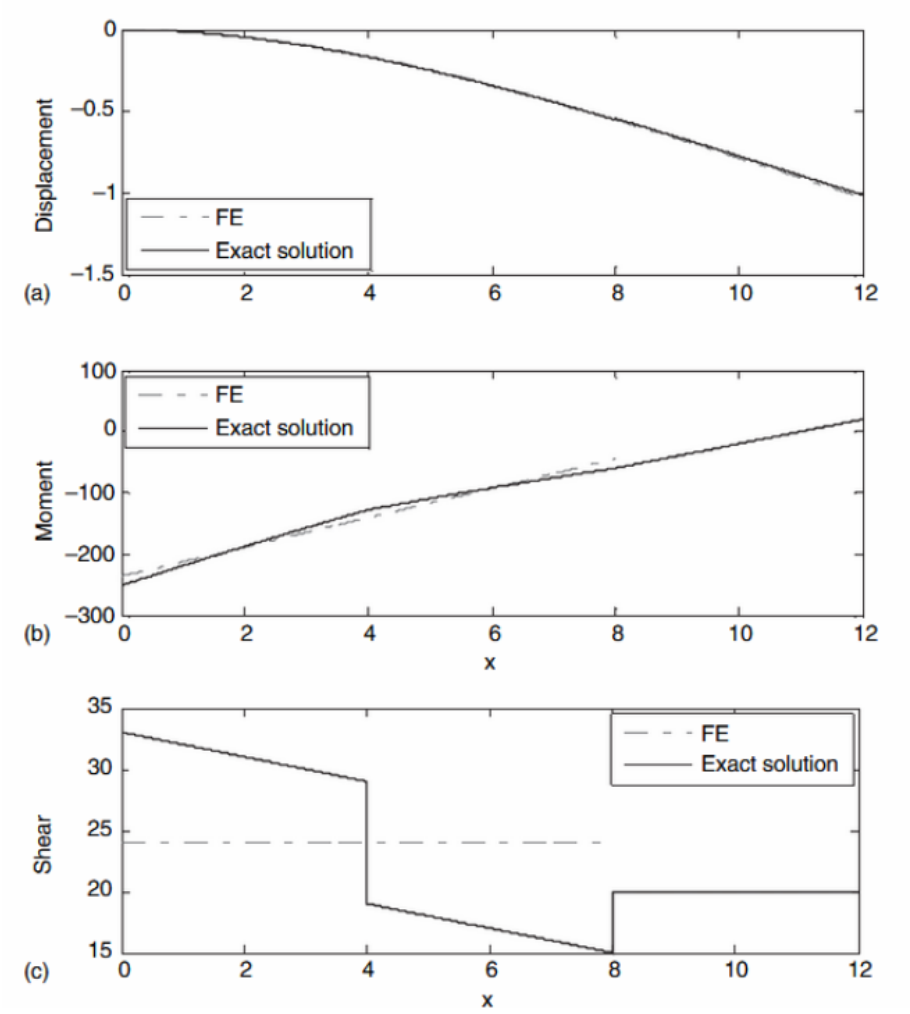

Figure 2-8: Accuracy of beam elements predicting a simple cantilevered beam.. (Fish, Jacob, and Ted Belytschko)

2.5.2 THE FINITE ELEMENT METHOD

The direct stiffness method, is a very useful method for analyzing complex frames of slender members, but if we try to apply it to non-slender members it proves to be completely inaccurate. The reason is members that are not slender cannot be assumed to have uniform stress over their cross sections[23]. In order to analyze these types of elements we can apply finite element discretization to solve the elasticity differential equation. This method is known as the Finite Element Method or Finite Element Analysis, shortened to FEM or FEA. More specifically, we are considering the FEM applied to linear elasticity. Linear elasticity has four basic assumptions: the deformations are small, the behavior of the material is linear, dynamic effects ignored, there are no cracks in the solid[24]. The Direct Stiffness method is actually as special application of the FEM, so solving linear elasticity through the FEM is quite similar. The equilibrium equation for linear elasticity is:

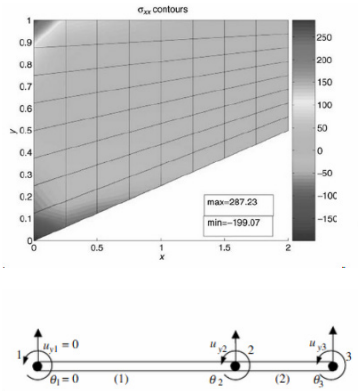

Figure 2-9: Top: a tapered cantilever divided into two dimensional quadrilateral elements, right: a cantilever divided into one dimensional beam elements.

$$\nabla_S^T \boldsymbol{\sigma} + \boldsymbol{b} = \mathbf{0} \tag{3.2}$$

The ∇ denotes the gradient, which is the function of partial derivatives in all basis vectors of σ. σ is the matrix of linear elastic stress equations in all basis vectors; which are most frequently x,y, and z Cartesian coordinate vectors. By considering more dimensions, it is possible to break the body under analysis into elements across its depth and width as well as length.

In this way, we are able to predict values of stress throughout a member's depth and width. In practice, it is impractical to model complex structures with solid elements, because it would take far too many elements to yield a reasonable answer[25]. For this reason, many engineers choose to use shell elements that are often based on Kirchoff-Love shell theory. Shell elements can accurately predict the behaviour of thin surfaces such as the metal panels on a car's body.

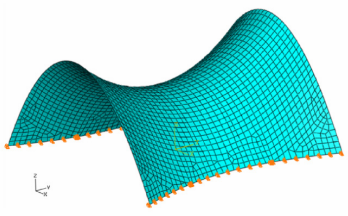

Figure 2-10: Shell element model of a saddle shaped structure.

2.5.3 NON-LINEAR FINITE ELEMENT ANALYSIS

All techniques previously mentioned were linear, meaning that they are only valid for linear material behaviour, and when the loads only induce small deformations on the structure, but what about nonlinear material solids undergoing large deformations? There exist many types of analysis that are able to predict these types of behaviour which exist under the umbrella term Nonlinear FEA. These types of analyses are significantly more complex than linear ones, therefore engineers try to use linear elastic models whenever applicable. Figure 2-11 shows that the solution for nonlinear and linear FEA is convergent for small deformations; however, the inaccuracy of linear FEA is clear when the material is undergoing large deformations. Another complication of nonlinear analysis is that it is a system of analyses. It is possible to use all types of nonlinearities: nonlinear material behaviour, large displacements and rotations, and large strains, in one generalized model; however, this would not tell the engineer which factor of these factors is dominating the design. In the words of Bathe "the complete process of analysis can be likened to a series of laboratory experiments in which different assumptions are made in each experiment- in the finite element analysis these experiments are performed on the computer with a finite element program[26]."One particular situation where nonlinear analysis is warranted is when predicting metal forming processes; whereby the point of such processes is to greatly deform a solid into a desired shape.

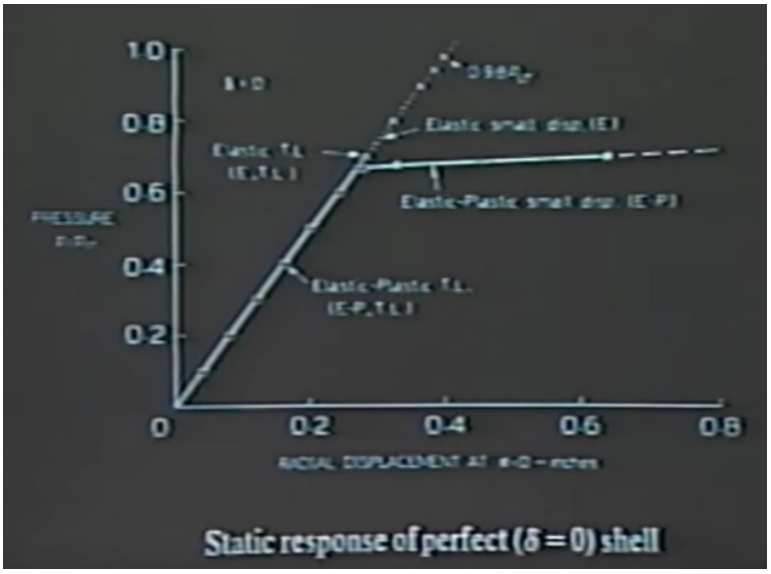

Figure 2-11: Elastic, elastic small deformation, elastic- plastic small deformation, and elastic-plastic pressure versus displacement models of a static shell

2.5.4 NUMERIC ANALYSIS OF STEEL SPACE FRAME STRUCTURES

The expanded-metal cellular frames considered in this thesis behave similarly to steel space frames. As explained in the previous section, steel frames are most efficiently analyzed with the Direct Stiffness method. Modeling frames consisting of many slender members with solid elements would not yield valuable enough information to warrant implementation of linear elastic FEA. There are many widely used commercial software that are capable of Direct Stiffness analysis such as: SAP2000, Autodesk Robot Structural Analysis, and Ansys to name a few. Dr. Muller of the Digital Structures Research group at MIT argues that development of these tools are focused on accuracy and speed, yet they are largely incapable of generating geometry. In this way, these tools "relegate engineers to the tasks of verifying the form and sizing of members[27]." The issue with the last statement is that the latter takes significant effort. Analysis is selecting a mathematical model of a physical problem, and solving that specific problem[28]. If the mathematical model does not sufficiently approximate the behaviour of the physical phenomenon in question, the answer is equally useless. Much like design, the process of analysis is also an iterative process; which can be summarized in the diagram from Bathe (figure 2-12)

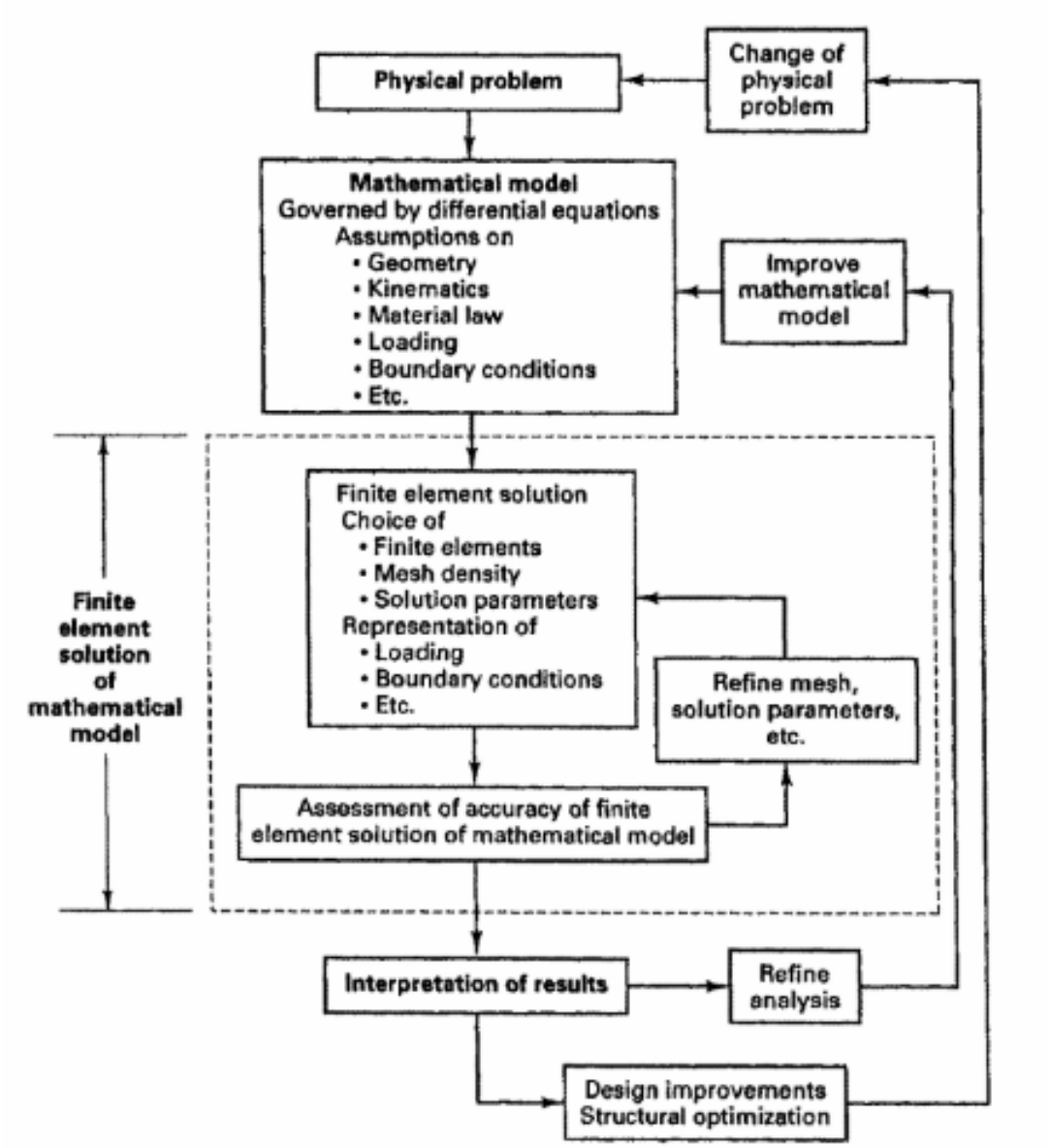

Figure 2-12: Flow chart of the Finite Element Analysis study process.

Analysis can never exactly predict the physical problem because of the extraordinary amount of conditions affecting even basic frames. These analysis provide insight to allow the engineer to make informed design choices. In this way, we have a dilemma; we cannot make meaningful design predictions without significant analysis, but significant analysis cannot be done until the problem is well defined.

In the case of this thesis, the problem is the design of steel frames in shell and freeform surface configurations. The research reviewed in this section look to illustrate the current relationship between geometry generation and mechanical insight. Genetic algorithms have been used to successfully optimize steel frame design. Use of such algorithms have surged since the 1990s, and have since developed to encompass AISC code specifications[29]. The disadvantage preventing the widespread adaptation of such algorithms is their long computation time. Kociecki et al. presented a possible solution to this problem in the design of a steel frame roof for a light rail train station in Ottawa, Canada. This design was a theoretical exercise, based on an actual design by the author. The resulting design resulting from the genetic algorithm was an average of roughly 10% lighter then the actual design, and computed over a shorter time period then the original manual iterative design. The issue is the problem is already well defined, and the author already has significant insight into the problem, therefore she could create an accurate and efficient mathematical model to optimize. Total structural weight was defined as a function to optimize, and the geometry was already set, therefore the optimization was limited "to rearranging members within the given shape to achieve a more efficient design[30]." This use of genetic algorithms touches on the large field of topology optimization; which is a series of techniques used to search for optimal material distribution within a design domain given specific constraints. This type of exercise was explored in a theoretical cantilever by Changizi at el. The boundary conditions where a frame fixed to the ground and a single corner load[31]. The topology optimization lead to the frame in the right of (figure 2-13). These types of analyses can be very powerful for reducing the amount of time to reach an optimal solution.

Figure 2-13: Topology optimization of a two dimensional frame subjected to a lateral load.

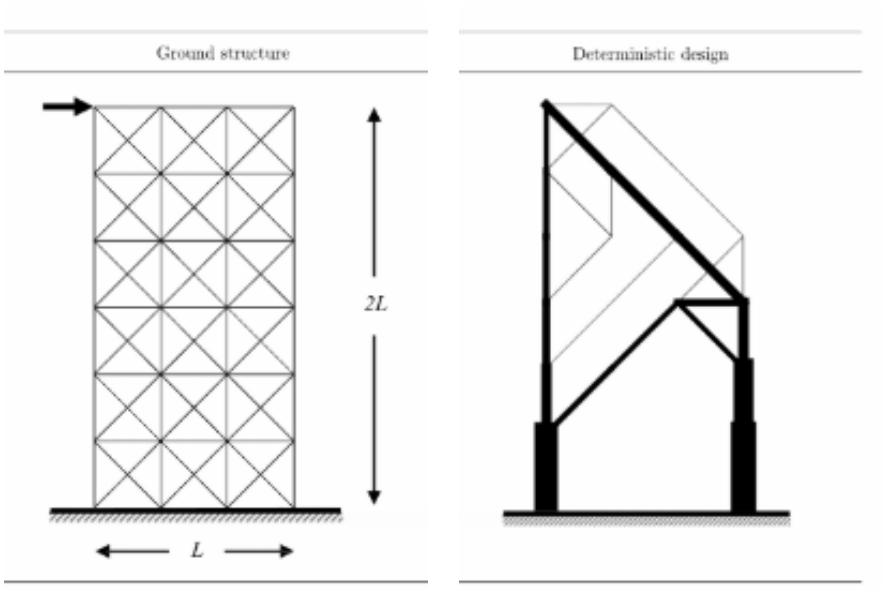

Endnotes

1 Wellington, Arthur M. *The Economic Theory of the Location of Railways: An Analysis of the Conditions Controlling the Laying out of Railways to Effect the Most Judicious Expenditure of Capital* (New York: J. Wiley & Sons, 1887).

2 "R.R.O. 1990, Reg. 941: General," *Government of Ontario,* made March 23, 2018, https://www.ontario.ca/laws/regulation/900941

3 "Comparative Building Costs," *Buildings*, accessed June 18, 2019, https://www.buildings.com/news/industry-news/articleid/21528/title/comparative-building-costs.

4 Eyre, Jim. "Architecture or Engineering." *WilkinsonEyre*. Accessed June 18, 2019. https://www.wilkinsoneyre.com/thoughts/essays/architecture-or-engineering.

5 Fischer, Thomas. "Generation of Apparently Irregular Truss Structures," *Computer Aided Architectural Design Futures* 2005 (2005): 229-238, doi:10.1007/1-4020-3698-1_21.

6 Block, Philippe. "Thrust Network Analysis Exploring Three-dimensional Equilibrium," *Massachusetts Institute of Technology*, 2009, accessed October 3, 2017, https://dspace.mit.edu/handle/1721.1/49539. 37.

7 Block, Philippe. "Thrust Network Analysis Exploring Three-dimensional Equilibrium," 38

8 Mueller, Caitlin T. "Computational Exploration of the Structural Design Space," *Massachusetts Institute of Technology*, June 2014. accessed October 3, 2017, http://hdl.handle.net/1721.1/91293.

9 Danhaive, Renaud, and Caitlin T. Mueller. "Combining Parametric Modeling and Interactive Optimization for High-Performance and Creative Structural Design," *Proceedings of the IASS Symposium 2015*, Digital Structures, Accessed November 11, 2017, http://digitalstructures.mit.edu/files/2015-09/iass2015-524698.pdf.

10 Danhaive, Renaud, and Caitlin T. Mueller. "Combining Parametric Modeling and Interactive Optimization for High-Performance and Creative Structural Design,"

11 Mueller, Caitlin T. "Computational Exploration of the Structural Design Space,"

12 Kilian, Axel, and John Ochsendorf. "Particle-Spring Systems for Structural Form Finding," *Journal of the International Association for Shell and Spatial Structures* 46, no.147, 2005, accessed November 11, 2017, http://designexplorer.net/newscreens/cadenarytool/KilianOchsendorfIASS.pdf.

13 Barnes,Michael. "Form Finding and Analysis of Tension Structures by Dynamic Relaxation," *International Journal of Space Structures* 14 No. 2, 1999, accessed November 2, 2017, http://journals.sagepub.com.proxy.lib.uwaterloo.ca/doi/abs/10.1260/0266351991494722

14 Hui, Deng, Li Hongyang, Su Cheng and Yiping Jiang. "Monitoring and Analyzing Displacement of Large-Span Spoke-Type Cable Structure Roof," *Journal of Surveying Engineering* 142, no.4, 2017, accessed November 2, 2017, http://ascelibrary.org/doi/10.1061/%28ASCE%29SU.1943-5428.0000237

15 Abdelhameed, Wael. "Reciprocal Relationship of Conceptualization and Design Problem Definition." *CAAD Futures 2009* (2009): 410-422, http://papers.cumincad.org/cgi-bin/works/paper/cf2009_410.

16 Bialkowski, Sebastian. "Structural Optimisation Methods as a New Toolset for Architects." *Proceedings of the 34th ECAADe Conference 2* (2016): 255-264, http://papers.cumincad.org/cgi-bin/works/paper/ecaade2016_098.

17 Januszkiewicz, Krystyna, and Marta, Banachowicz. "Nonlinear Shaping Architecture Designed with Using Evolutionary Structural Optimization Tools." *IOP Conference Series: Materials Science and Engineering* 245 (2017): 082042. doi:10.1088/1757-899x/245/8/082042.

18 Januszkiewicz, Krystyna, and Marta, Banachowicz. "Nonlinear Shaping Architecture Designed with Using Evolutionary Structural Optimization Tools," 6

19 Hibbeler, Russell C. Structural Analysis, 10th ed. (Upper Saddle River, N.J: *Pearson Prentice Hall*, 2017),23

20 Fish, Jacob, and Ted Belytschko. *A First Course in Finite Elements* (Pacific Grove, CA: Content Technologies, 2007), 27

21 Hibbeler, Russell C., and Kai Beng Yap, *Mechanics of Materials* (Harlow, United Kingdom: Pearson, 2018)

22 Fish, Jacob, and Ted Belytschko. *A First Course in Finite Element*, 250.

23 Reddy, J.N., *Introduction to the Finite Element Method*. (Europe: McGraw-Hill Education, 2018)

24 Fish, Jacob, and Ted Belytschko. *A First Course in Finite Element*, 250.

25 Fish, Jacob, and Ted Belytschko. *A First Course in Finite Element*, 250.
26 Bathe, Klaus-Jürgen. *Finite Element Procedures* (Utgivningsort Okänd: Utgivare Okänd, 2006), 629.
27 Mueller, Caitlin T. "Computational Exploration of the Structural Design Space," *Massachusetts Institute of Technology*, June 2014. accessed February 08, 2019, http://hdl.handle.net/1721.1/91293.
28 Bathe, Klaus-Jürgen. *Finite Element Procedures*, 3.
29 Kociecki, Maggie, and Hojjat Adeli. "Two-phase Genetic Algorithm for Size Optimization of Free-form Steel Space-frame Roof Structures." *Journal of Constructional Steel Research* 90 (2013): 283-96. doi:10.1016/j.jcsr.2013.07.027.
30 Kociecki, Maggie, and Hojjat Adeli. "Two-phase Genetic Algorithm for Topology Optimization of Free-form Steel Space-frame Roof Structures with Complex Curvatures." *Engineering Applications of Artificial Intelligence 32* (2014): 218-27. doi:10.1016/j.engappai.2014.01.010.
31 Changiz, Navid, and Mehdi Jalalpou. "Robust topology optimization of frame structures undergeometric or material properties uncertainties," *Structural and Multidisciplinary Optimization* 56, Issue 4, (2017): 791–807. Accessed January 12, 2018. doi:10.1007/s00158-017-1686-4

part 3

FRAME MODELING

3.1 FRAME COMPOSITION AND PARAMETRIC MODELING

Figure 3-1: Top: spar frame element mid expansion, right: x-plate connection element.

Numerical simulation is used to test the effect of different variables on a system. In this way, it is very similar to physical testing. In order to ensure optimal accuracy, it is best validate tests with physical data, then extrapolate to more complex conditions. A hanging system will be used as the basis of analysis. In accordance with the process of analysis laid out by Bathe referred to in 2.5.4 (figure 2-13), the baseline model and assumption will be defined in the following section. Afterward, several control variables can be defined and the effect of each on the structural integrity can be observed.

The designers of the LAS have used polygon representations of sphere units consisting of: spars, x-plates, and tri-plates (figure 3-1) in order to manage the overall composition of elements. The goal of the analytical model is to create a link between the architectural design and the structural performance. For this reason it was important to create a parametric model capable of quickly adapting to new changes of the complex frame. The plan is to use the low-polygon composition models as inputs for a parametric script that outputs a thin line frame model that can be readily used for direct stiffness analysis (figures: 3-2, 3-3).

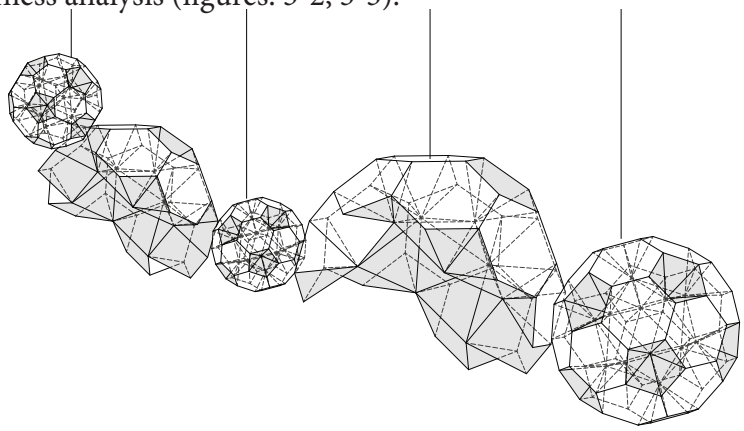

Figure 3-2: Low-polygon approximation model.

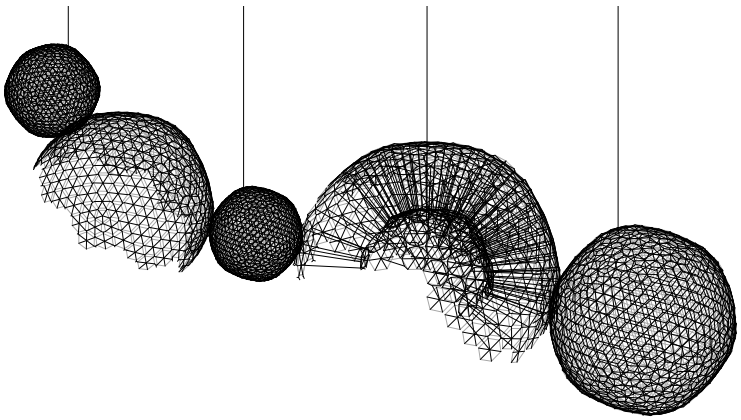

Figure 3-3: Thin line approximation model.

Each of these low-polygon or low-poly units represents a radial array of long spars around a central double spar. Around these spars are three double spars located at three sides of the hexagon outer face of the polygon. The outer layer of these units, the layer of spar connections at the hexagon face of each polygon, is connected with three-way connections know as triangle-plates. The inner layer, the layer of spar connections at the triangle face of each polygon, is connected with four-way connections known as x-plates (figures: 3-4, 3-5).

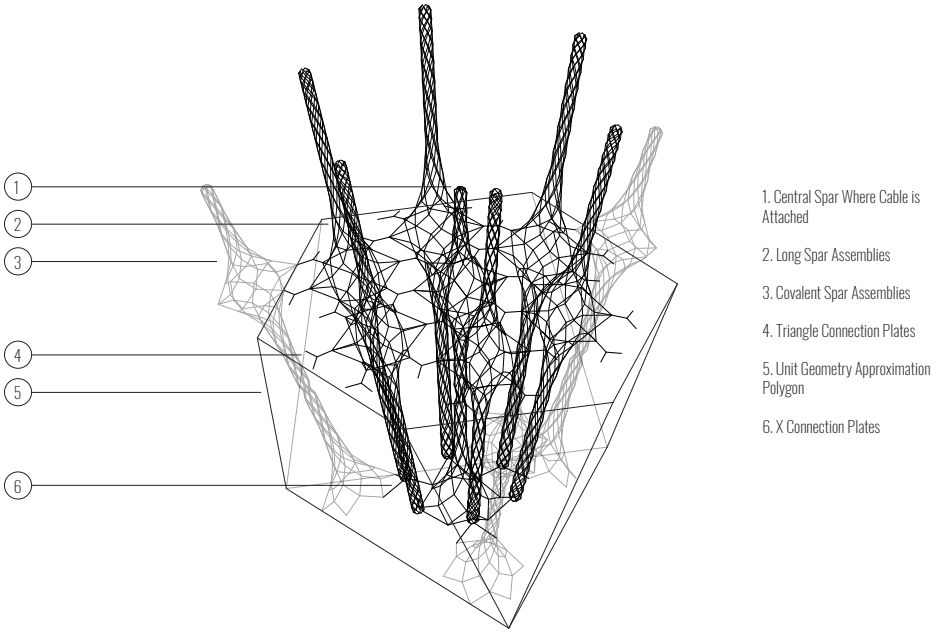

Figure 3-4: 3 dimensional view of a sphere unit and the arrangement of spars it represents.

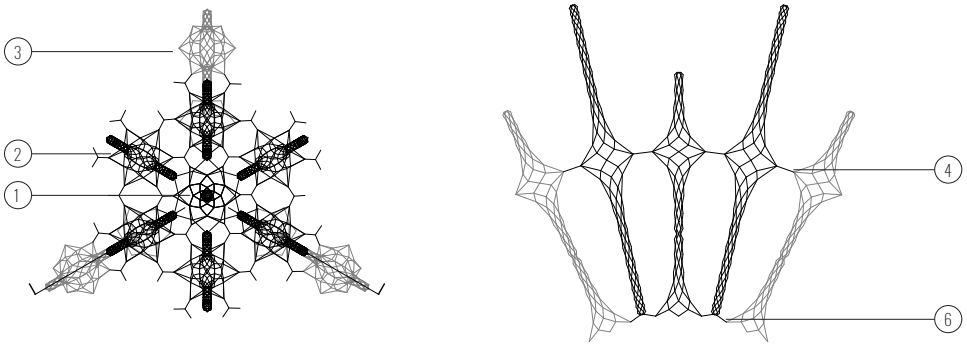

Figure 3-5: Left: plan view, right: section view of sphere unit.

This particular organization is known as a double shell because it has two connection planes: one at the hexagonal face and one at the triangular face. Figure 3-6 shows a section of a double shell. The hexagonal face of the unit is known as the outer shell, while the triangular face is known as the inner shell. Another combination is the single shell, where the spars follow the same organization, but are only connected on the outer shell plane.

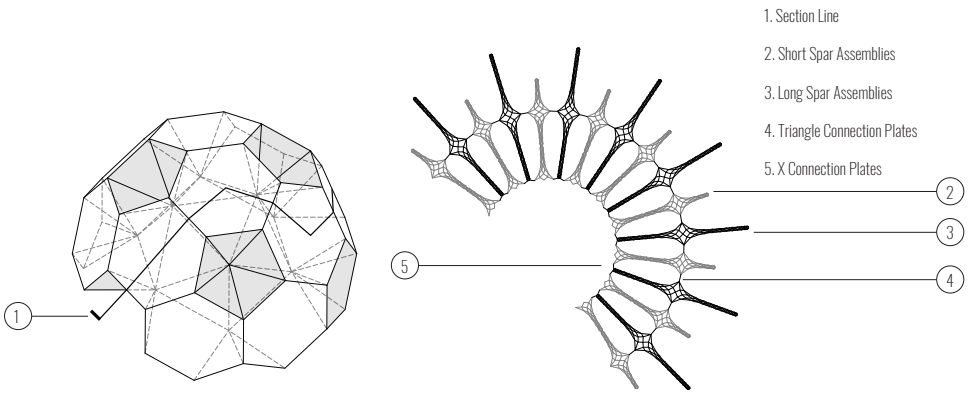

Figure 3-6: Left: Sphere unit composition, right: section of composition.

The geometry of the baseline system is based on the design of the Beauty installation by the LAS. The structure is composed of two single-shell full sphere units, flanking a half double shell unit. There is also a partial single shell appended to the small full single shell. The partial single shell also has a full single shell sphere attached solely to it.

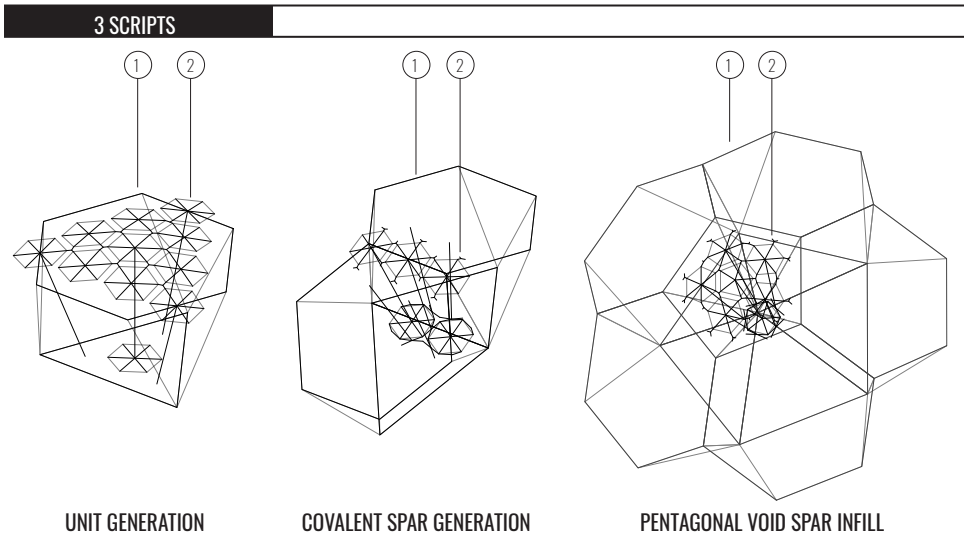

Figure 3-7: Illustration of the inputs and outputs of the three parametric scripts which generate the spar frame centerline curves.

The parametric script was divided into 3 parts in order to make the application robust and user friendly. The first part is the generation of the geometry within individual sphere units. For the purposes of analysis, each spar was approximated as a central beam element, with six radial beam elements to maintain proper connectivity. The input of this script is two curves, which can be generated by duplicating the hexagonal and triangular faces of the low-poly model. The script works by starting with the pentagonal curve input. It takes the center point and then draws radial lines to the vertices and midpoints of the pentagon. Next, it divides these segments based on figure 3-10; these ratios were derived from the design of previous LAS installations. A central hexagon is generated so that it intersects the correct point, then a polar array of same sized units are created.

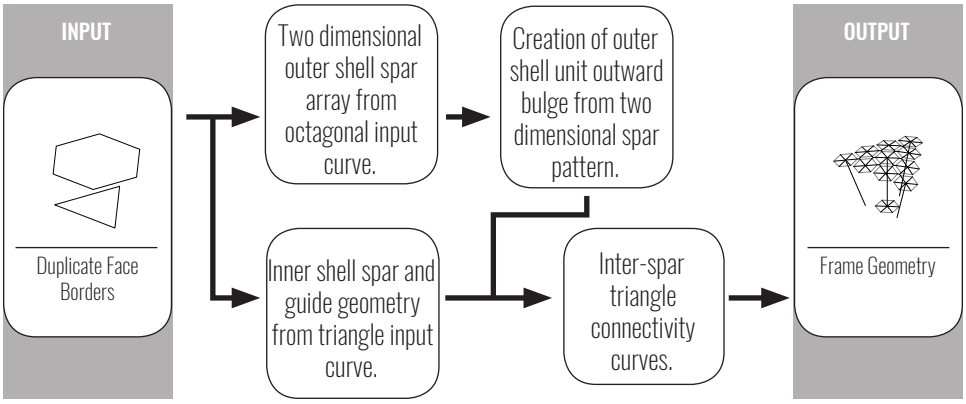

Figure 3-8: Concept diagram the spar unit generation script.

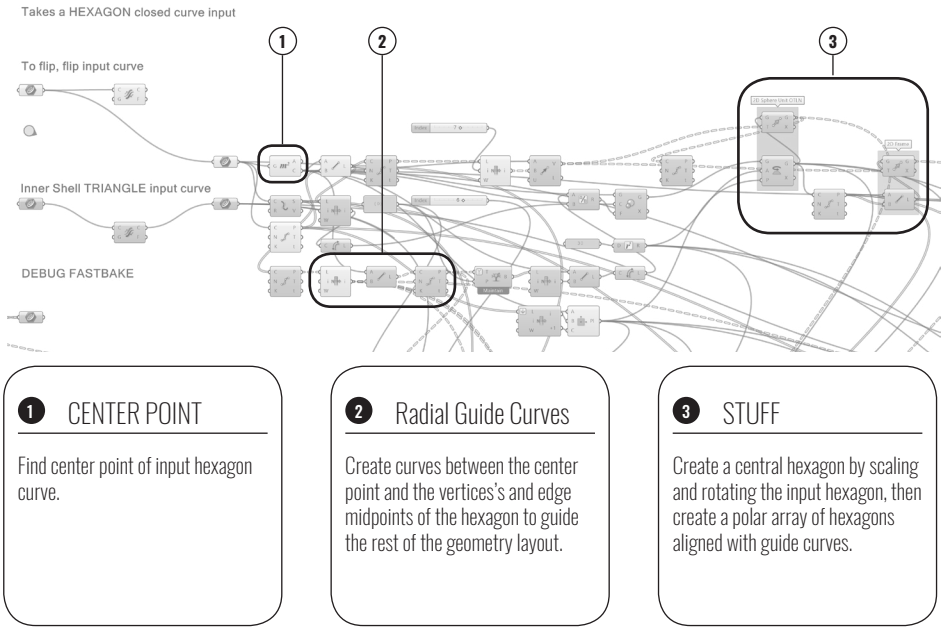

Figure 3-9: Spar unit generation: creation of outer shell spar outline array.

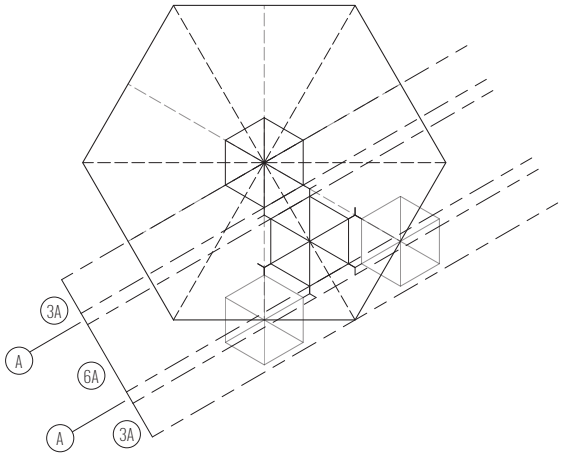

Figure 3-10: Proportions used to distribute spars within each unit.

A calculation is performed to create a slope, which is used to create the bulge of each unit. The polar spars are rotated by the slope, each pair utilize the nearest edge of the hexagon as the axis of rotation. If there were no bulge, the overall geometry would remain a truncated icosahedron, rather than an ellipsoid.

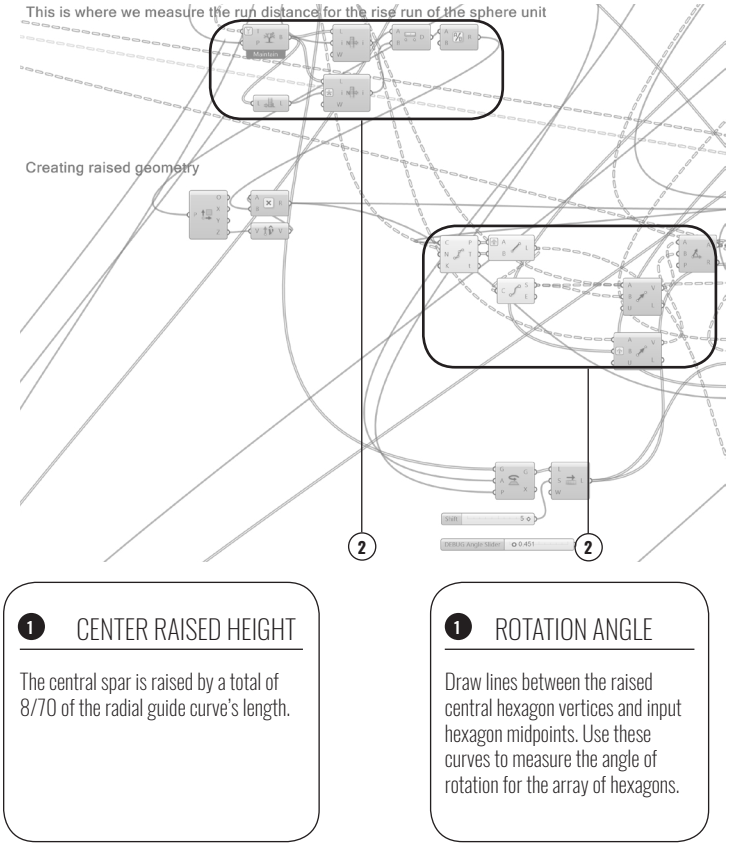

Figure 3-11: Spar unit generation: measuring of slope and creation of unit bulge.

Simultaneously, the triangle input curve is used to create a matching polar array of curves to the ones created by the hexagonal curve. The curves are divided in accordance to the ratio in figure 3-10, which is also derived from previous installations. The central hexagonal curve is brought down to meet this point.

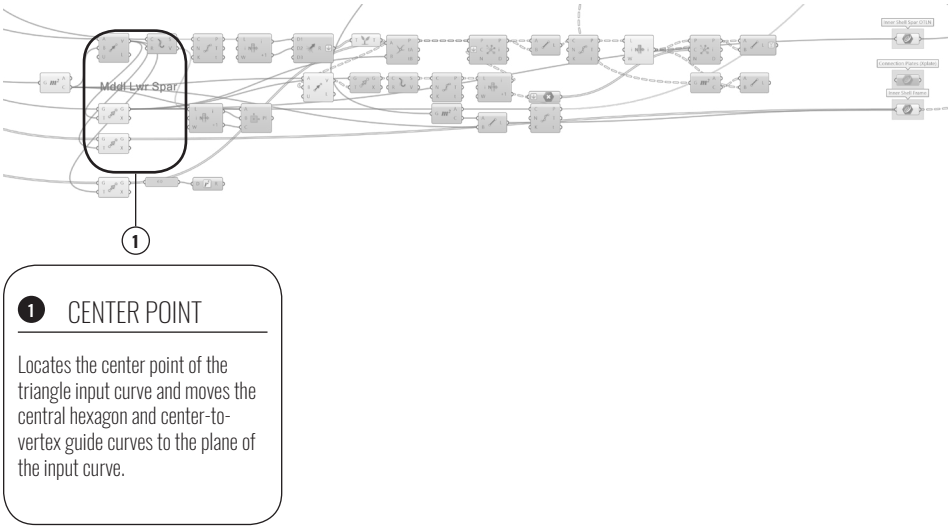

Figure 3-12: Spar unit generation: creation of the inner shell spar outline array.

Next, the edge spars are made by taking three non-adjacent hexagon side midpoints and creating a similar sized hexagon, rotated on its adjacent axis by the previously determined slope. The centerlines of each of these units are connected to specific ratio points on the inner shell. The radial connectivity beam elements of each spar are created by taking the center point of the derived hexagons, then connecting this point with each of that hexagon's vertices. Triangle plates were modeled by three beam elements. These plates were generated by locating all the hexagonal vertices adjacent to where the plate would be. The way this is achieved is by creating a general list of all polar hexagonal curve vertices, then selecting pairs that are closest to the central hexagons vertices. These points are grouped into threes, then used to create a three-point planar surface. The center of that surface is found, then connected radially to all that surface's vertices, thus forming the triplate approximation.

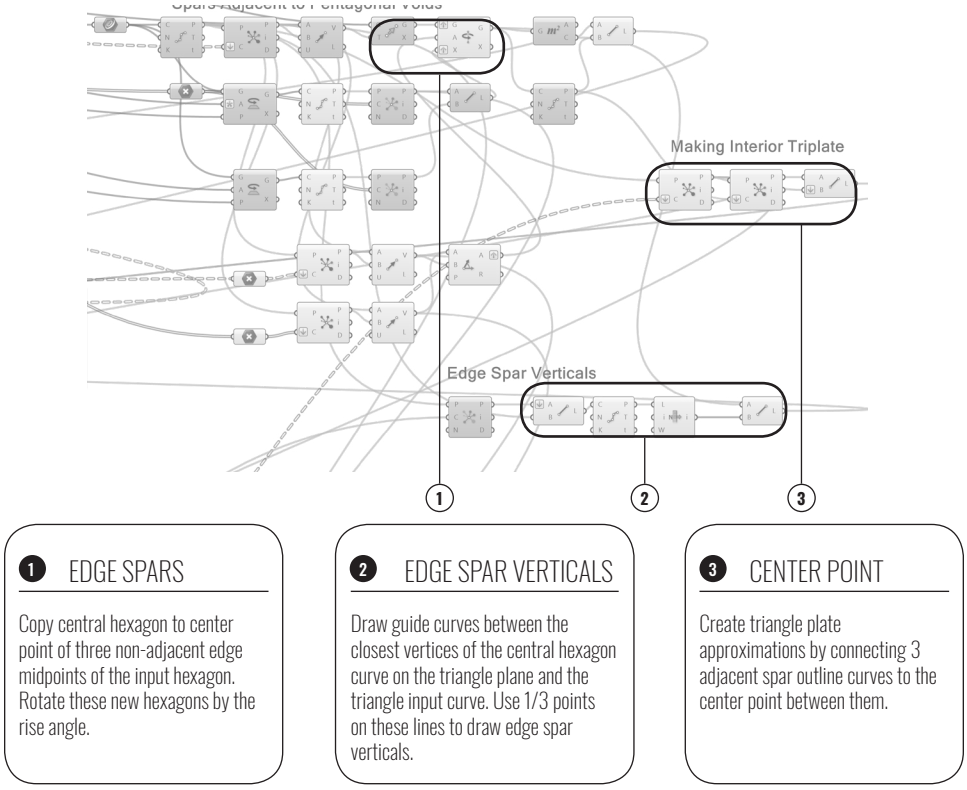

Figure 3-13: Spar unit generation: creation of triangle-plate inter-spar connection.

The second script creates the spars between sphere units, this was created as a separate script because these spars are shared between adjacent units. The input for this script is the set of adjacent outer hexagonal curves and inner triangular curves. The first part of the script is to divide all hexagon curve edges into thirds. Next, the 3 points, drawn from the list of all third points of the hexagon edge curves, closest to the coincident vertices of the shared hexagon edge are selected. These three points are used to define a plane. Next, a spar outline, the same size as those used in the sphere units, is generated on each of these two planes.

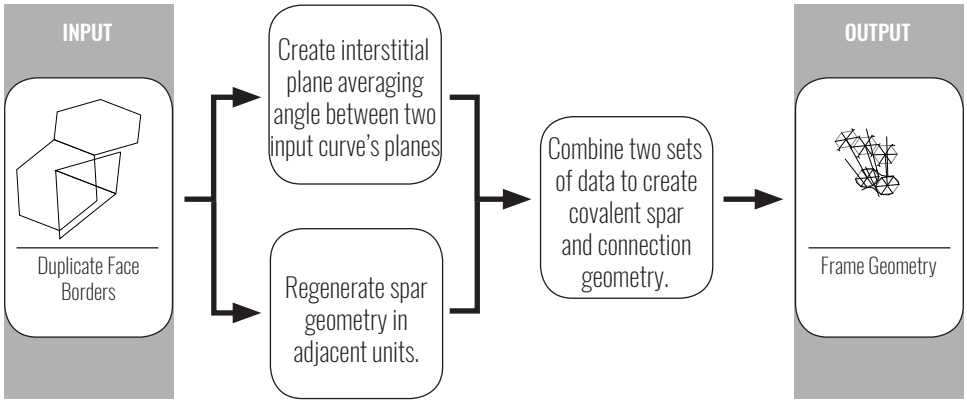

Figure 3-14: Concept diagram of covalent spar generation script.

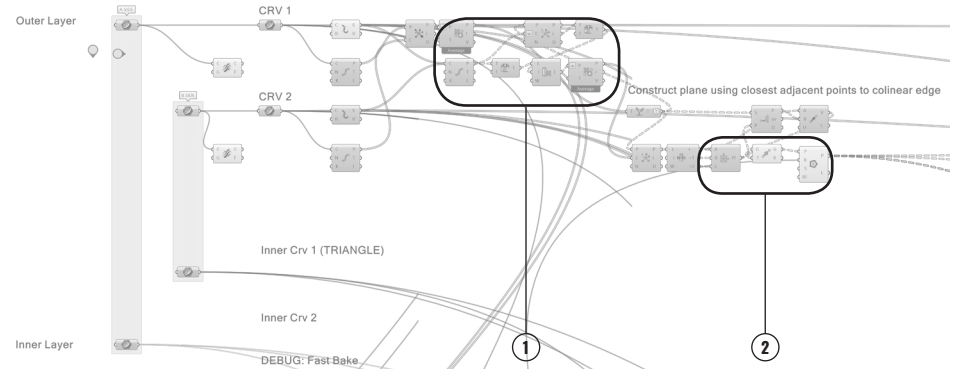

1 POINT CLUSTERS

Divide each hexagon input curve edge into thirds then isolate the 3 closest points to each overlapping vertex between the two inputs.

2 CONSTRUCT PLANE

Use the three points to define a new plane and create a hexagon curve on each.

Figure 3-15: Covalent Spar Generation Script: creation of covalent base planes.

The next part of the script is to generate the central spar outline, located on the midpoint of the shared edge of the two input hexagons. The central spar has its own plane, which is generated so that the angle between this plane and the respective planes of the two input curves is the same.

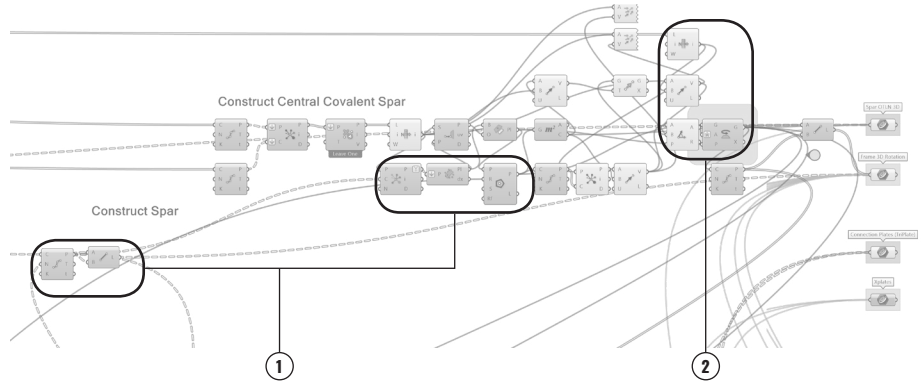

1 CENTRAL SPAR

Take the set vertices of the two hexagons previously created and isolate the 4 points closest to the center. Use these points to create a new plane to generate a hexagon upon.

2 ROTATION CORRECTION

Rotation of the newly generated central hexagon spar outline is corrected so that the midpoint of one of its edges aligns with the overlapping edge of the two input hexagon curves.

Figure 3-16: Covalent Spar Generation Script: creation of central covalent spar outline and base plane.

This script actually regenerates partial geometry of the adjacent spar units to get placements and measurements used in the rest of the script. This is inefficient, and should be phased out in further refinement.

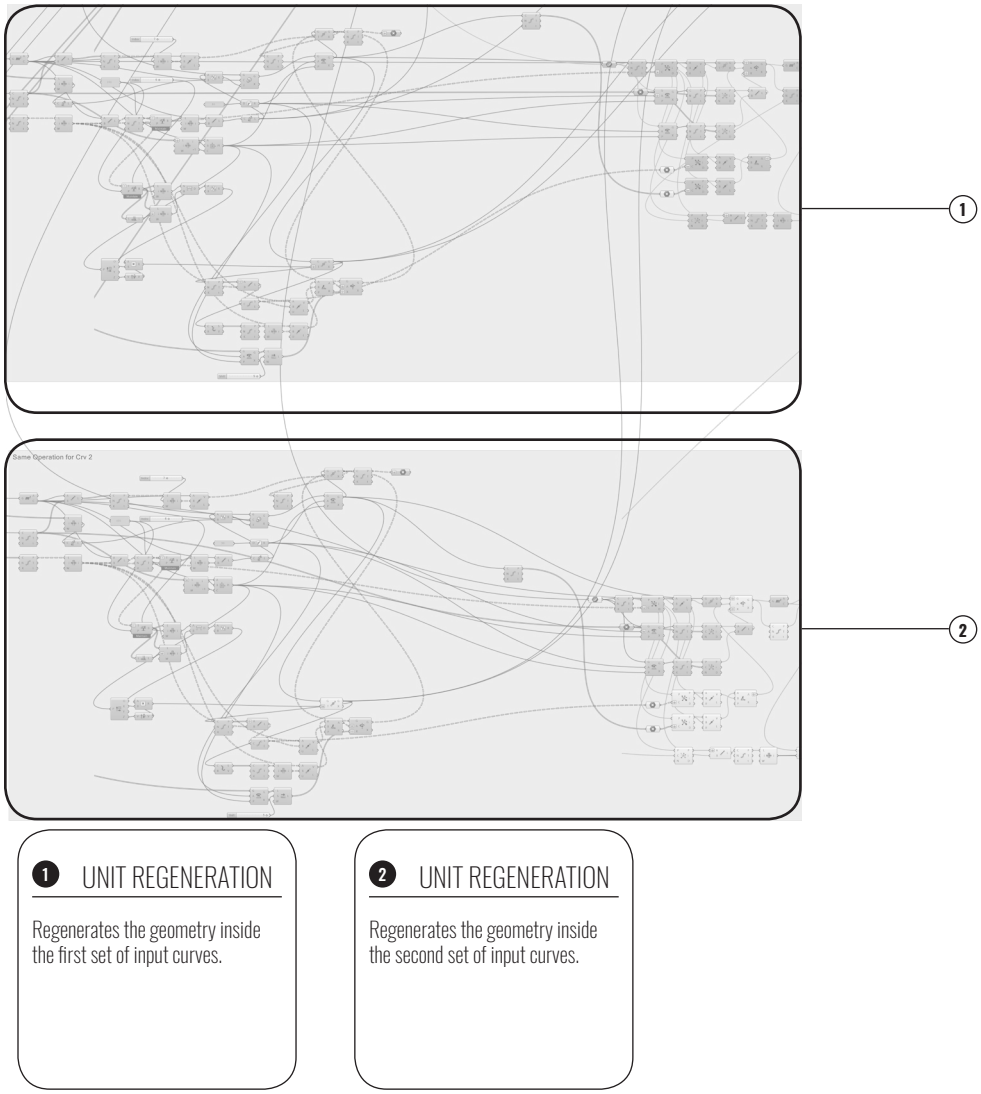

Figure 3-17: Covalent Spar Generation Script: regeneration of adjacent spar geometry.

The inner shell triangle curves are used to generate the lower spar outlines. The outline curves are located at third points of the shared edge of the triangle input curves, and the plane they rest on is projected from the outer shell center spar outline's plane. In order to generate accurate connectivity, the set of spar outlines adjacent to the set of edge spars, generated in this script, had to be made into an additional input. Originally, these curves were regenerated within this script; however, this led to minor inaccuracies, due to the local numbering of curves and vertices, causing defects in connectivity, rendering the analysis model unable to converge on a solution. Vertex points from the set of curves, surrounding the outer shared spars, are grouped into sets of three. These three points are used to create a triangular plane, whose centroid forms the center of the triangle plate connections. A similar method is used on the inner shell, but this time, the points are grouped into fours so that quadrilateral surfaces can be made. The centroid of these quadrilaterals form the center of the x-plate connectors. The set of output curves are grouped into: spar outline, frame, triangle plate, and x-plate elements.

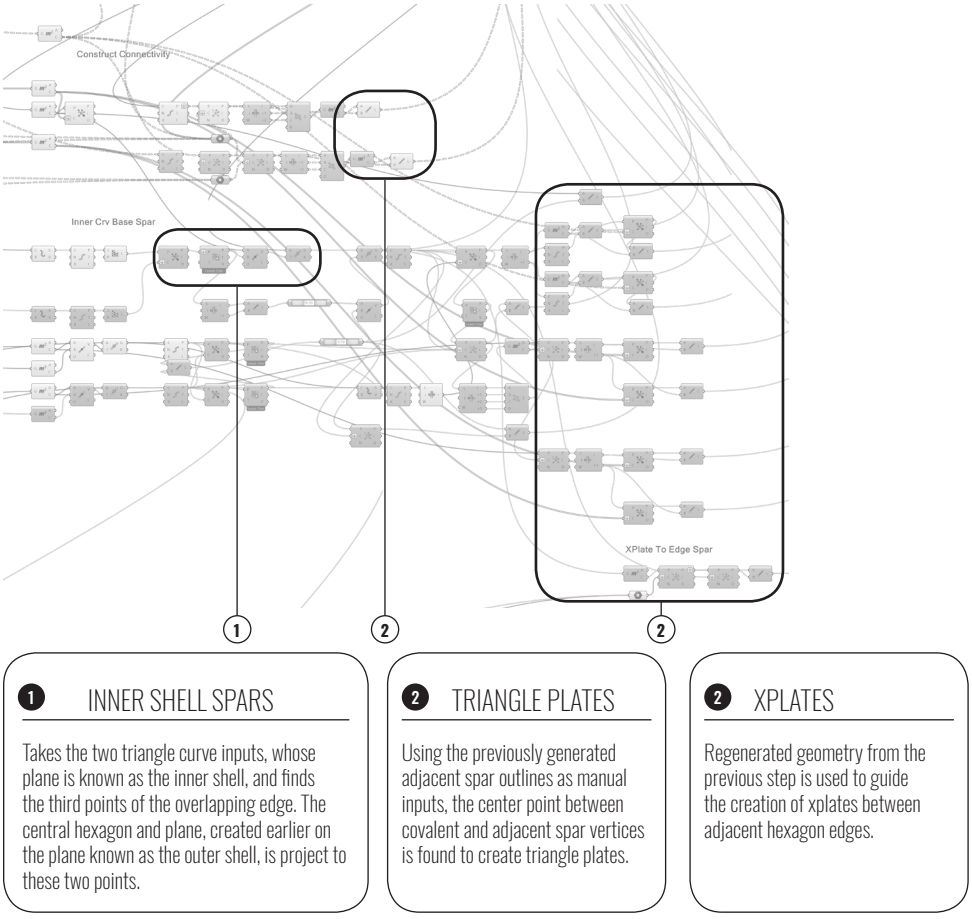

Figure 3-18: Covalent Spar Generation Script: creation of: inner shell, triangle plate and x-plate geometry.

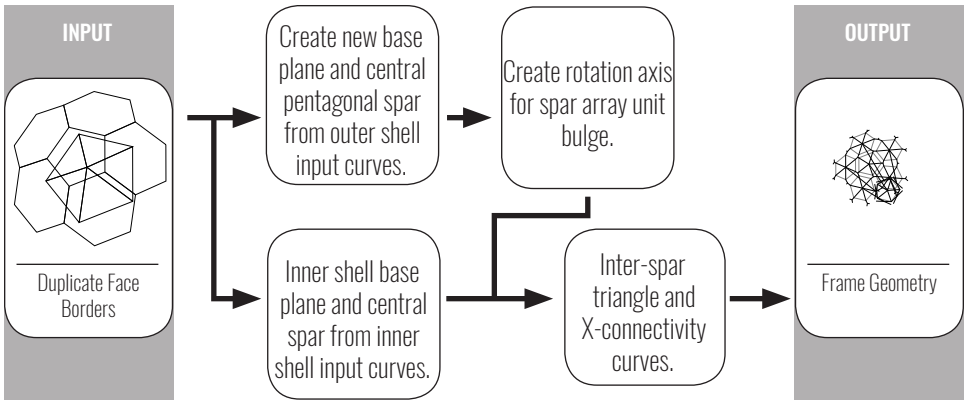

Figure 3-19: Concept diagram of pentagonal void infill generation script.

The third script generates the spars within the pentagonal voids. The first part takes the 5 hexagonal curves that surrounds each pentagonal void as input in order to generate a pentagon boundary curve. This curve is used to generate a base plane for the spar array, then a central pentagonal spar outline is created at the center of this curve.

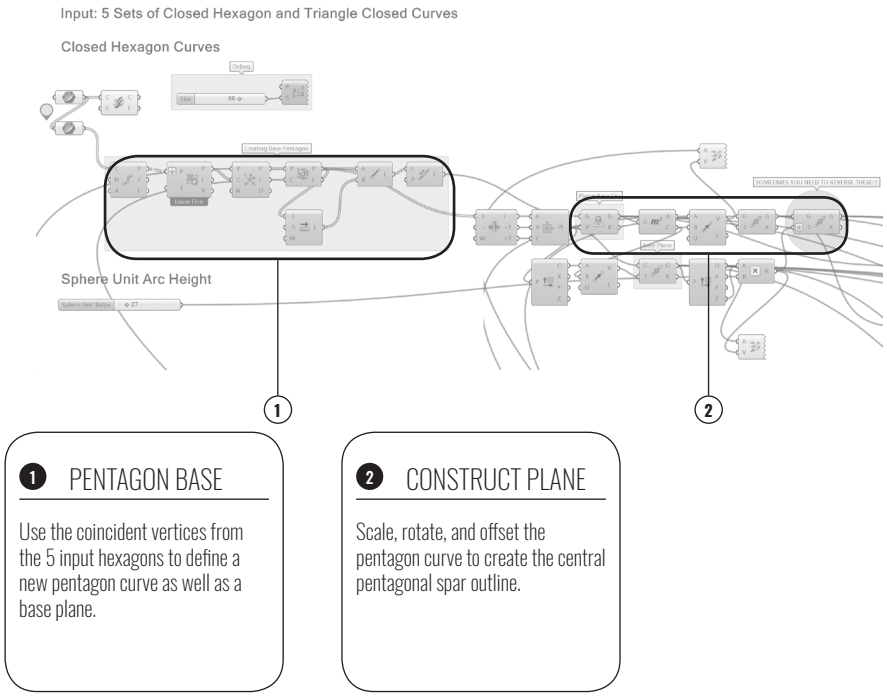

Figure 3-20: Pentagonal Unit Generation Script: outline curve and base plane generation.

This outline curve is offset from the base plane in order to create the bulge of the pentagonal unit. Lines connecting the vertices and midpoints of the central spar and outline hexagonal curve were made to guide the location of the arrayed spars. Constructing the rotational axis of the radial hexagonal spars within the hexagonal void proposed a challenge because the axis of rotation for each spar outline was aligned with a curve perpendicular to the line from the boundary pentagon's vertices to center. To solve this problem, the boundary hexagon was rotated and scaled so that it would create the correct rotation axes.

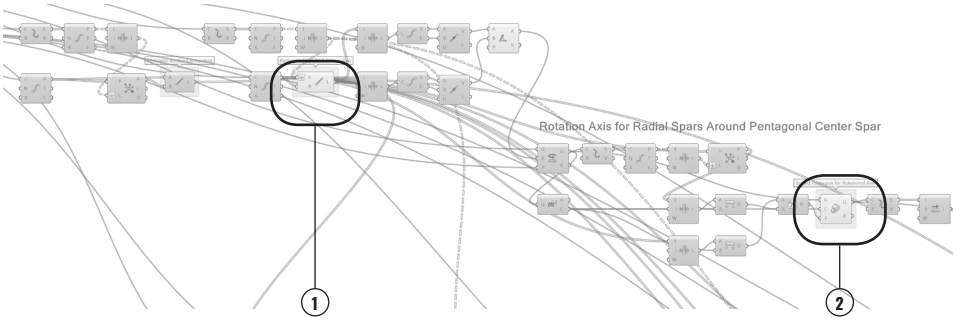

1 RADIAL GUIDES

Create guide curves for the future spar array by connecting the vertices of the pentagon base curve to the edge midpoints of the central pentagon.

2 ROTATION AXIS

Scale and rotate pentagon so that the edge midpoints of the new curve are coincident with the original pentagon vertices. This curve serves as the rotation axis for the future spar array bulge.

Figure 3-21: Pentagonal Unit Generation Script: rotation axis generation.

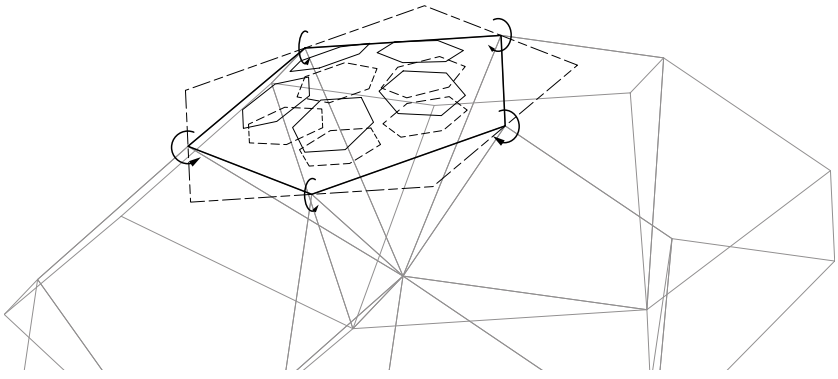

Figure 3-22: Rotation axis orientation orthogonal to radial curves connecting center to vertices.

The next part of the script generates the radial hexagonal spars, then rotates them along the previously generated rotation axes.

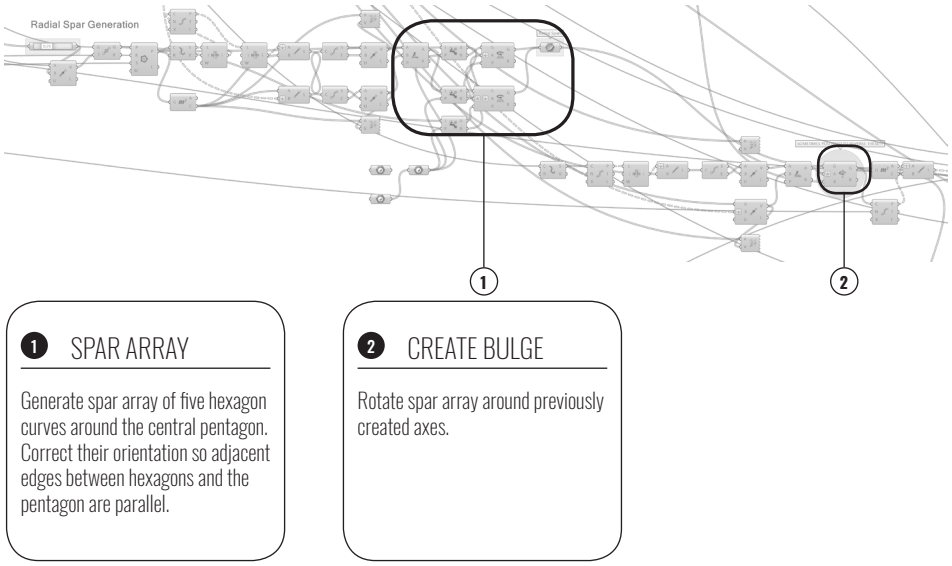

Figure 3-23: Pentagonal Unit Generation Script: generation and rotation of radial hexagonal spar outlines.

Simultaneously, the inner shell plane is created by accepting five straight edges of the pentagonal-based pyramid that surround the inner shell of the pentagonal void unit. The outline of the pentagonal inner shell spar is offset so that it has minimal distance from the surrounding inner shell hexagonal spars.

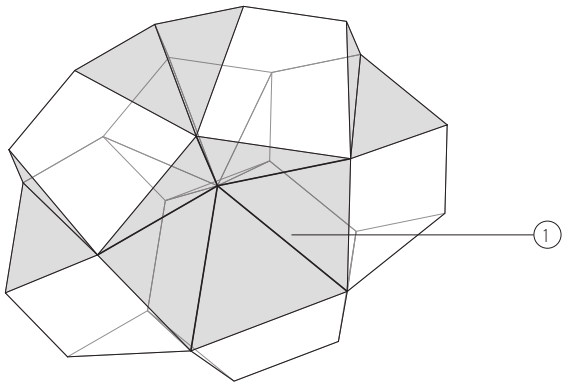

Figure 3-24: Five straight line inputs outlining the intersecting boarders around the inner shell pentagon arrangement of polygon primitives.

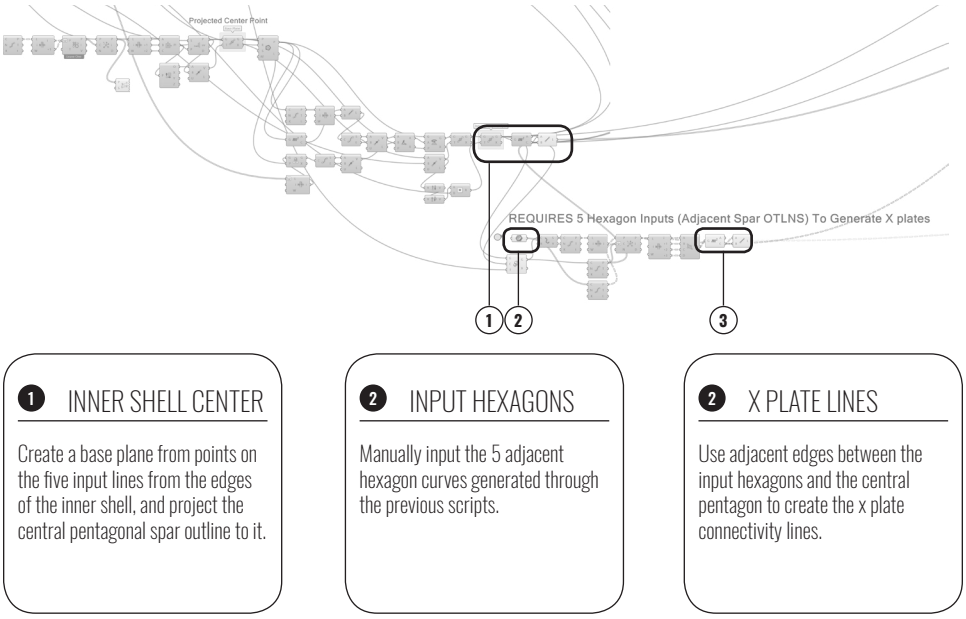

Figure 3-25: Pentagonal Unit Generation Script: creation of inner shell base plane, spar outline, and x-plate connectivity.

The five hexagonal spar outlines surrounding the inner shell pentagonal spar outline are used as inputs to create the x-plate beam element centerlines. Similarly, on the outer shell, the hexagonal spar outlines surrounding the unit are used as input to generate the triangle plate beam elements.

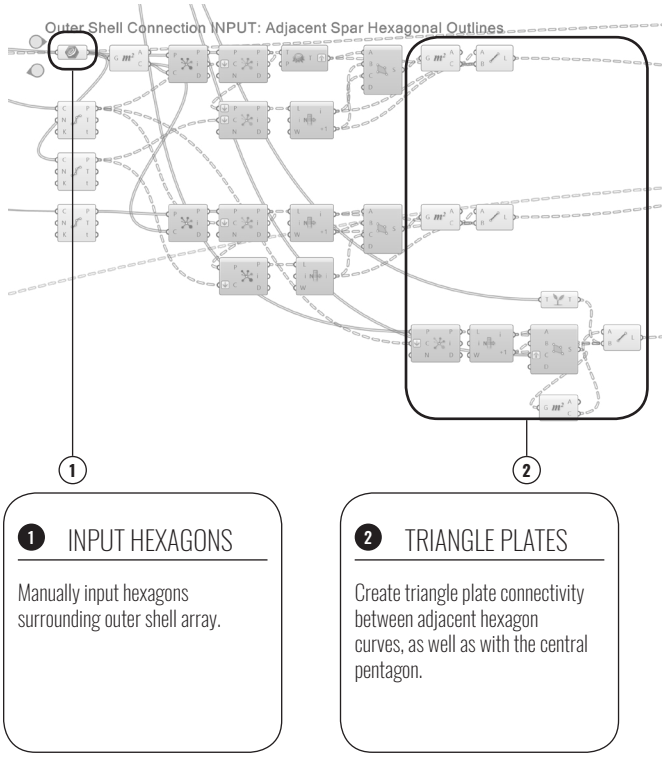

Figure 3-26: Pentagonal Unit Generation Script: creation of outer shell triangle plate elements.

3.2 INDIVIDUAL SPAR PARAMETRIC MODELING AND ANALYSIS

Before an overall model can be constructed, the equivalent stiffness of the individual elements should be determined. Since the overall model will be constructed of beam elements, a single stiffness value for each is required. This value is an approximation, since the actual elements are composed of many parts, rather than a single solid beam.

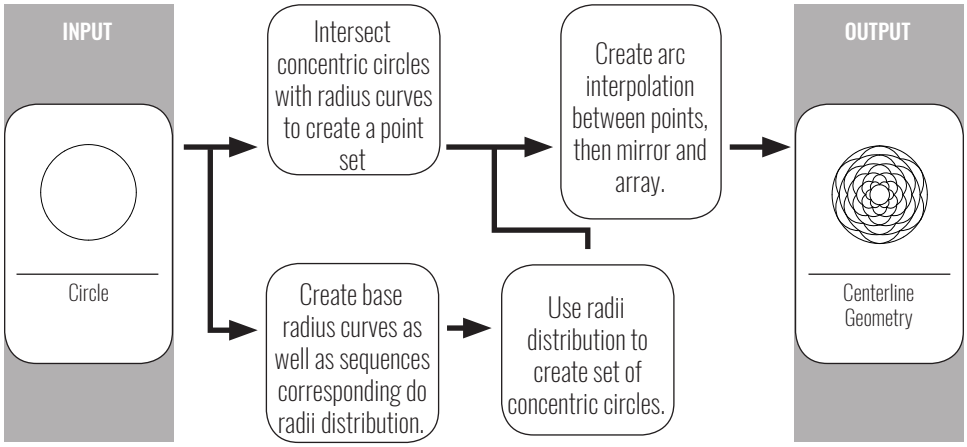

Figure 3-27: Conceptual overview of spar generation script.

The generation script for the two dimensional spar cut pattern is modified from a script written by Jonathan Gotfried of Philip Beesley Architect. The script accepts a circle curve as input which represents the boundary of the entire spar pattern. The first part of the script constructs a base plane and center point from the input curve, then create a radial lines within the input circle. The number of arc segments within the spar is set with an input integer.

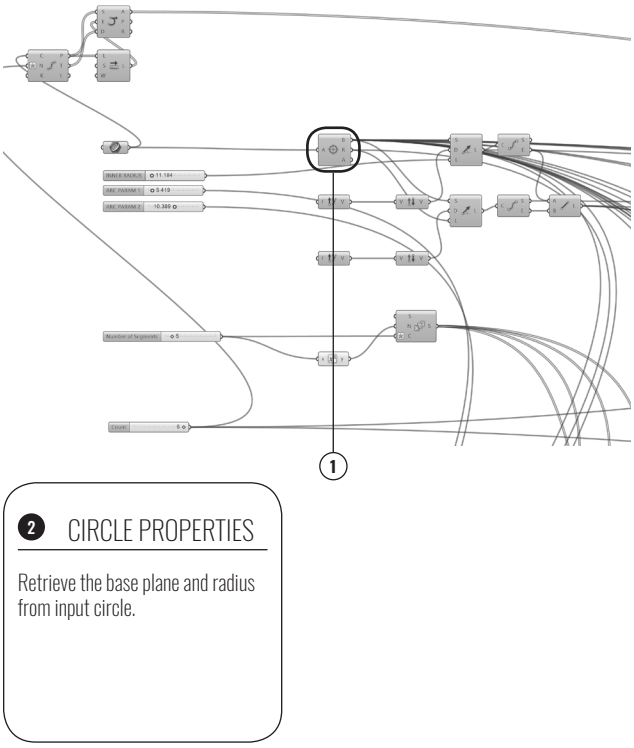

Figure 3-28: Two dimension spar pattern generation script: creation of base plane, centerpoint, and radial curve.

The number of segment is used in conjunction with a graph mapper to output a series of numbers within a set range. The graph mapper is a function mapped within a range that will output the dependent variable, or y-axis variable, based on an independent variable, or x-axis variable.

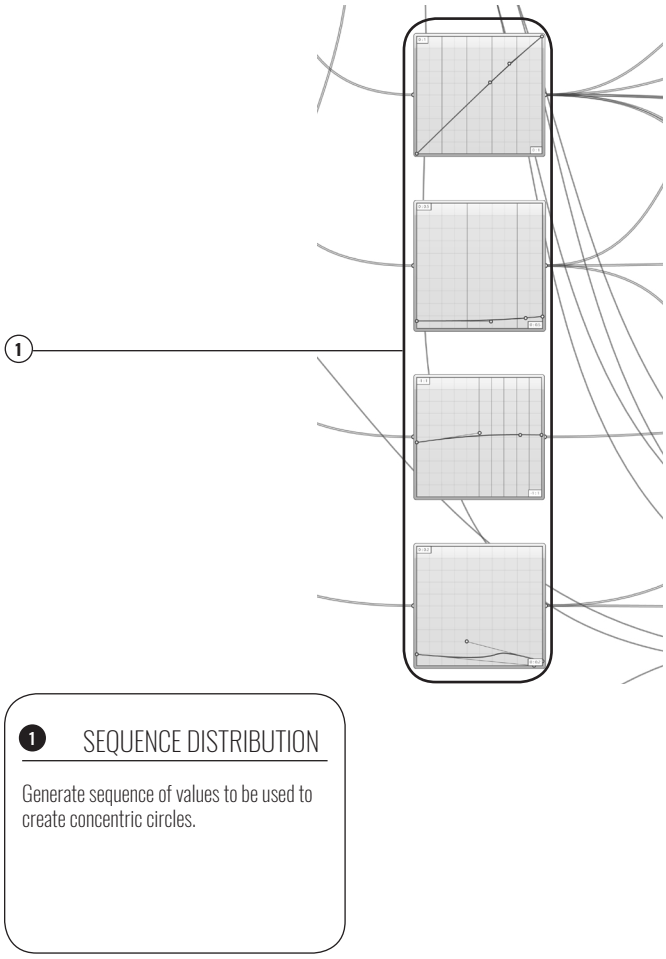

Figure 3-29: Two dimension spar pattern generation script: points are generated by four graph mappers.

The next section of the script generates a number of arc segments and tangents, equal to the number of arc sections, with radii varying by a combination of the graph mapper outputs. The next segment of the script creates a different set of arc segments and tangents that terminate at an angle derived from the number of desired radial segments.

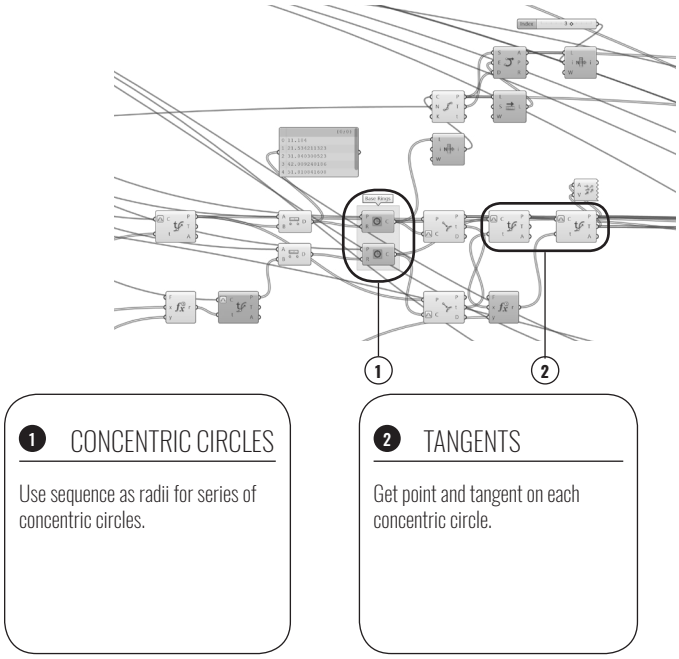

Figure 3-30: Two dimension spar pattern generation script: creation of arc segments and tangents.

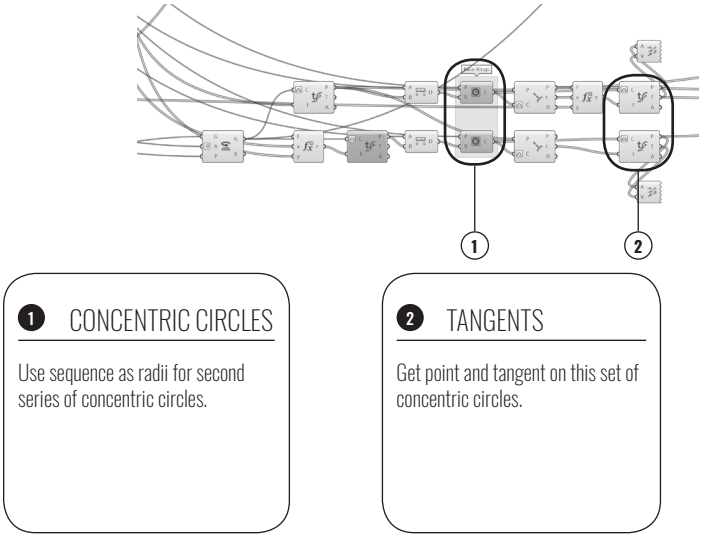

Figure 3-31: Two dimension spar pattern generation script: arc segments and tangents rotated at an angle based on desired radial segments.

The next portion of the script takes the points on both sets of arc segments and combines them into a list of points that can be connected by a continuous non-self-intersecting curve. Afterwards, the points are connected by arc segments that follow the tangents generated earlier.

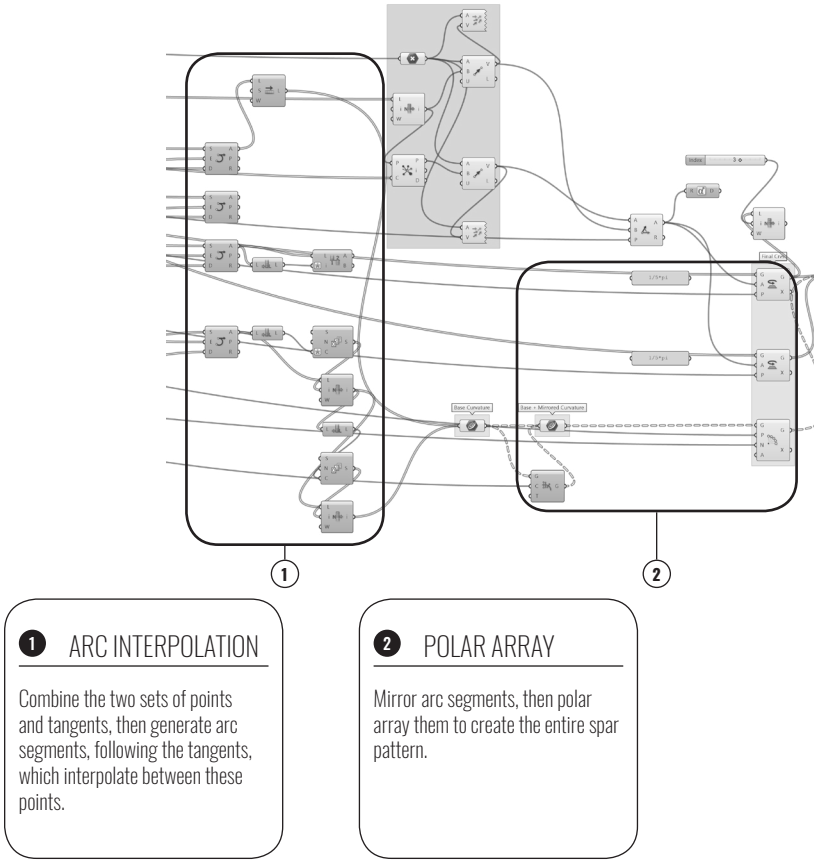

Figure 3-32: Two dimension spar pattern generation script: points are connected with arc segments then polar arrayed.

The last part of the script connects the points by arc segments, that follow the tangents generated earlier, then arrays these segments to create the entire spar pattern.

The first step in modelling a spar is deriving it's expanded form geometry from its two dimensional cut pattern. Unfortunately, since this brings steel out of it's linear elastic zone, it is a process requiring non linear analysis. The scope of this thesis is largely focused on frame composition, therefore

it was decided that this would not be a major topic of research. Karamba's large deformation solver was used to approximate these expanded forms. This solver uses linear analysis in load steps in order to approximate nonlinear modeling. The following is a comparison between an ANSYS large deformation finite element analysis and a Karamba beam element large deformation analysis.

The material is assumed to be T 300 stainless steel[1]:

Material Property	Value	Units
Young's Modulus	200	GPa
Shear Modulus	86	GPa
Specific Weight	8	g/cm^3
Yield Stress	215	MPa

Figure 3-33: T 300 Stainless steel mechanical properties.

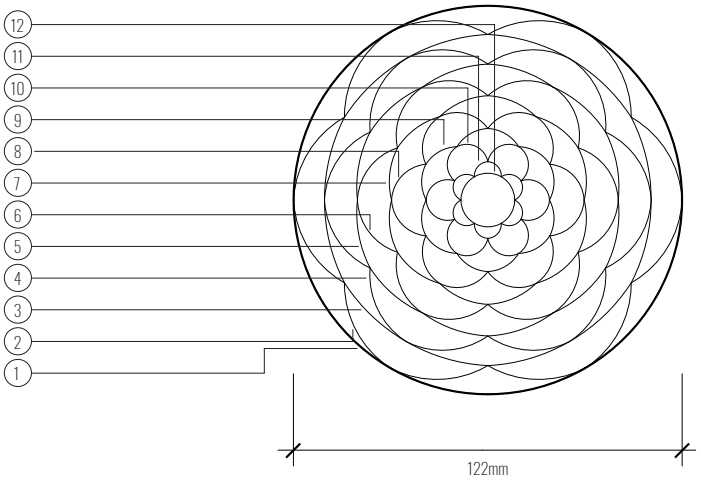

Figure 3-34: Number of sections and overall dimensions of two dimensional spar pattern used for formfinding tests. Annotation denotes section numbers.

Section	Width (in cm)
1	0.7
2	0.62
3	0.55
4	0.49
5	0.44
6	0.40
7	0.36
8	0.33
9	0.30
10	0.28
11	0.26
12	0.25

Figure 3-35: Test spar section widths (material thickness is 0.11 cm)

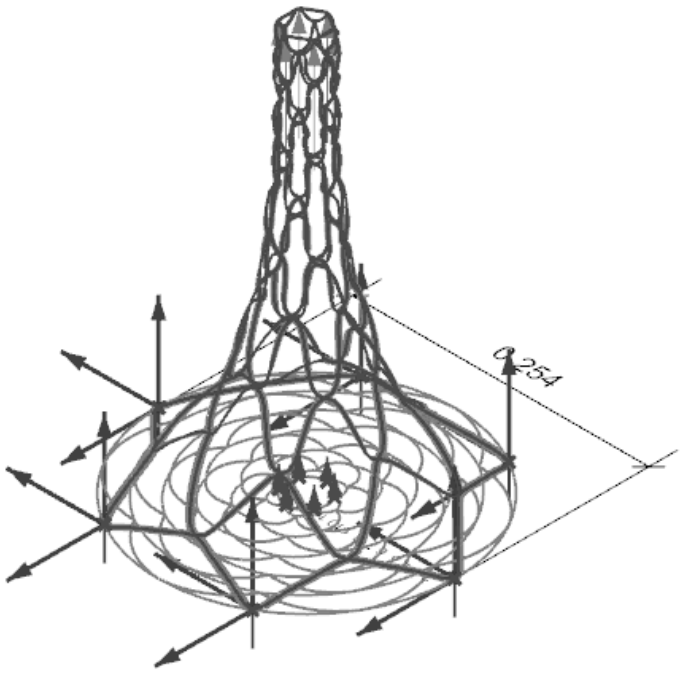

Figure 3-36: Setup of large deformation formfinding beam element convergence test. The 6 essential boundary conditions at the base where all translation is fixed. 6 loads placed at the center of the spar with values of 6kN (1238.4 lbf) each, for a total of 36 kN (8090 lbf).

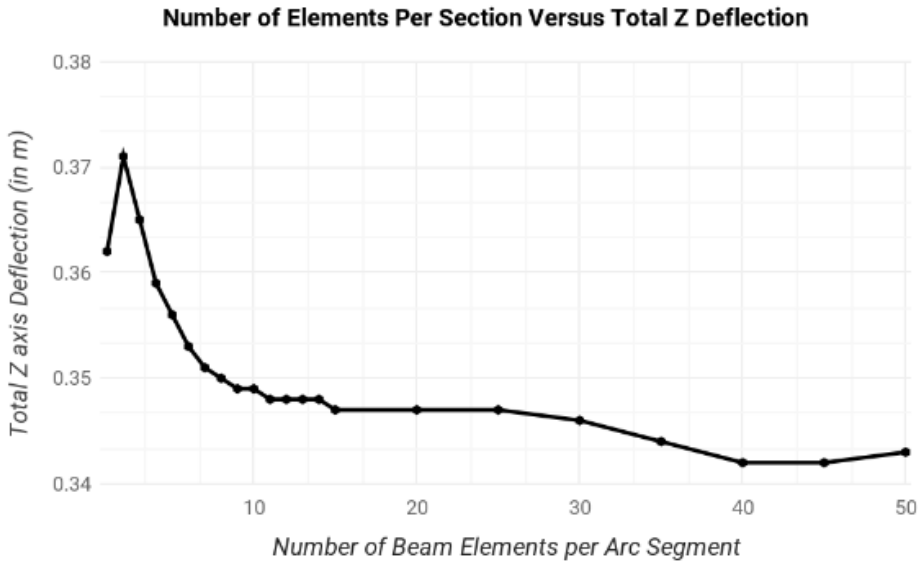

Figure 3-37: Test spar convergence of total deflection and number of elements. Tested with 100 load increments.

The solution seems convergent between 15-25 elements, where past that point the answer seems to deviate.

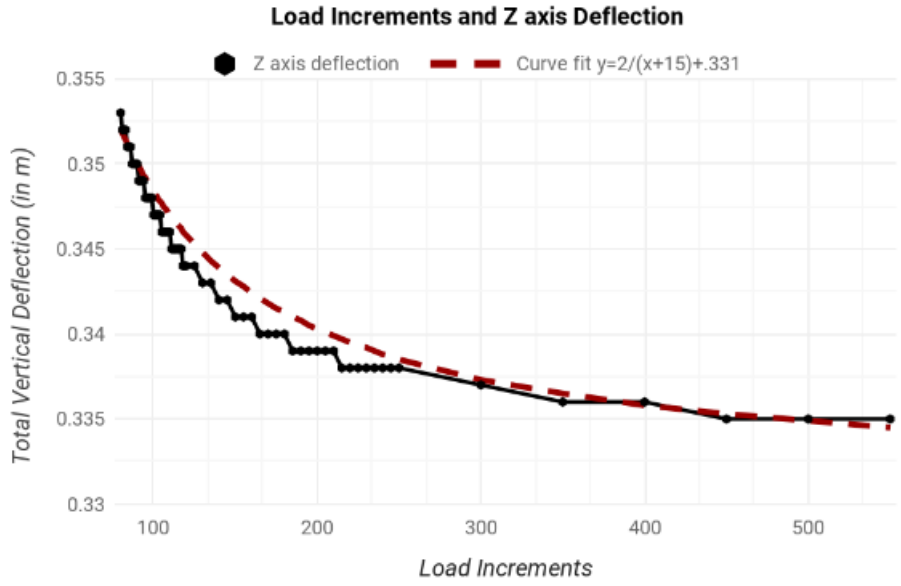

Figure 3-38: Test spar convergence of total deflection and number of load increments for large deformation analysis. 15 beam elements were used per arc segment and the model was setup as per figure 3-36..

Curve fitting was used to map to create a rational function approximation of the form:

$$\delta = \frac{2}{x + 15} + 0.331$$

If we take the lim: $x \to \infty; \delta = 0.331$

Therefore the deflection is approximated to be 0.331. The issue is that increasing the load increments exponentially increases computation time. If we use 300 increments, the error is less than 2%, so it should be acceptable for the purposes of this exploration. Therefore, the following simulations will be undertaken with 15 beam elements per arc segments and 300 load increments.

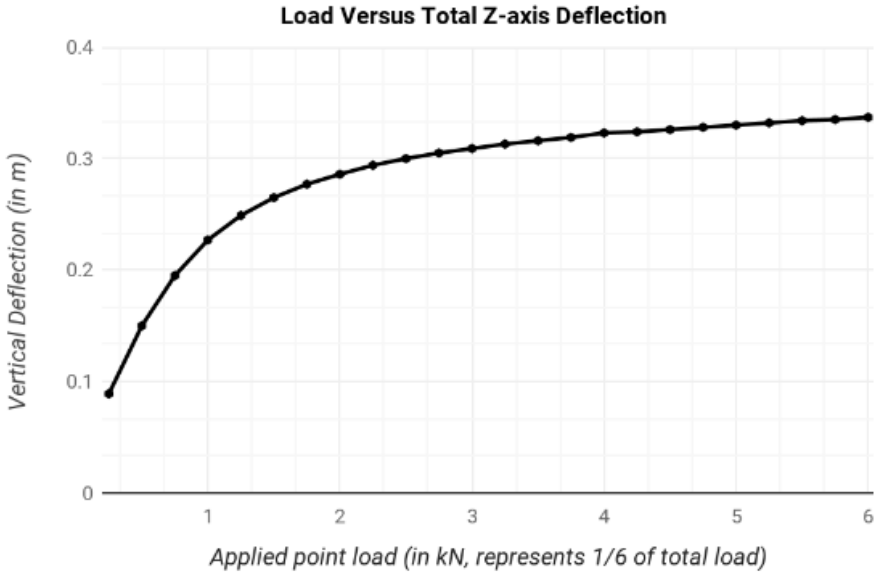

Figure 3-39: Test spar large deformation load versus displacement with 15 elements per section and 300 load steps. The model was setup as per figure 3-36.

As can be noted from the curve, the large deformation solver approximates non linear behaviour.

Possible sources of error in this analysis stem from the typical limitations of FEA: error in the boundary approximation of the domain, error due to the approximation of the solution as a series of algebraic equations, the error in numerical computation such as numeric integration and round-off error. A further complication is the error that arises from these sources is very difficult to estimate, because there would be no point in the FEA modelling if the exact solution was readily available[2]. Verification of a FEA

software can be achieved through the patch test, which is solving a problem for which the exact solution is already known, or comparing results with physical experiments[3]. Another source of error could be with the input data, it is impossible to know the exact loading conditions any frame will experience throughout its service life, therefore it is important to be able to predict the effect of these errors on the analysis model. For a linear model, the input error is directly related to the output error. If there is a 20% error in one input variable, the output would have an error of up to 20%[4]. In addition, in linear analysis, the only errors could be in the source data, boundary conditions, and material properties. All of these do not hold true for nonlinear analysis, thus making prediction of error much more difficult.

Of course if the exact solution to the problem at hand was available, there would be no point in using the finite element method. What can be observed; however, is the convergence of the model. By running the model in steps of increasing element mesh density, we can observe how the solution is changing. Once the solution is converged, meaning when there is no longer any meaningful change between mesh densities, we can consider the solution acceptable for the specific problem we have modeled.

The next study is a comparison between a spar modeled in beam elements and 3D 8 node brick elements. The boundary conditions are detailed in the chart below. The plot shows a comparison between the two models in

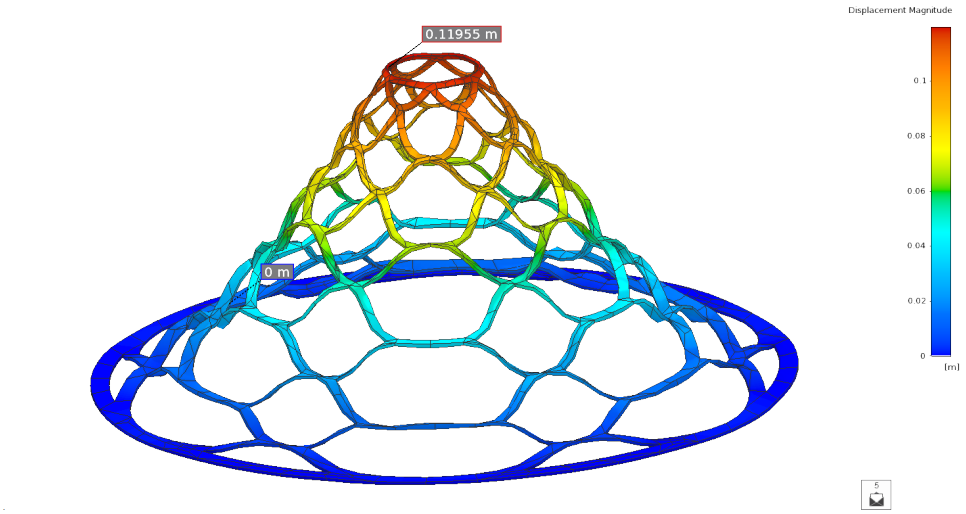

Figure 3-40: FEA of spar with elements fixed around its outer ring. Spar was subjected to a 26kN load applied along the inner edge of the inner most ring of the pattern.

Figure 3-41: Image of a sphere unit assembly installed at the University of Indiana.

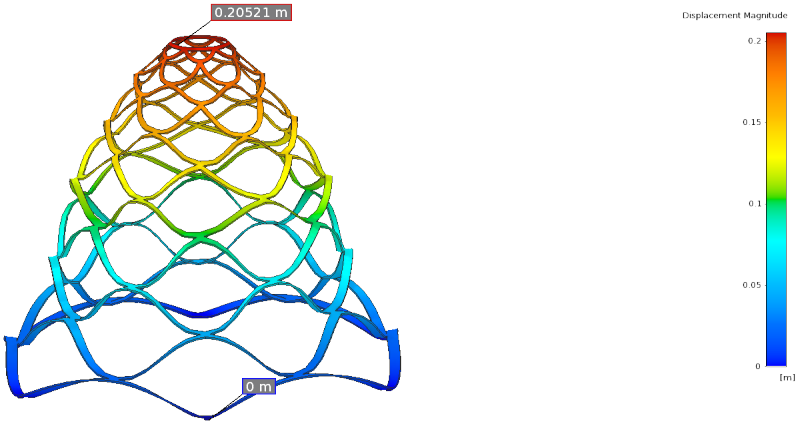

Figure 3-42: Setup of large deformation FEA spar model using 6 discrete locations for fixity. Model was subjected to a 36 kN load applied along the inside face of interior ring.

terms of x-direction deformation at the tip of the spar, versus the load. Comparison of the two techniques shows that the beam approximation yields results visually more similar to what has been achieved through physical tests. Furthermore, the resultant form from the beam model closely matches with actual Spar derived from physical testing; a 254mm wide 11 segment test spar yielded a 331mm pull, while a physical test with a 260mm wide 11 segment spar yielded a 330 mm pull. The relationship is linear, as to be expected with linear analysis; however, the data is invalidated once the material reaches past its yield point. The data point at 0.28kN per point, totaling 1.68kN, is out of the material's elastic range. Utilization shows the stress as a percentage of the Von Mesis stress, a type of failure criteria that predicts the behavior of steel. The steel, under these boundary conditions, reaches yield at approximately 0.1kN.

The following model was set up to explore the relationship between applied load and deflection on a single spar, while the material is within the linear elastic range:

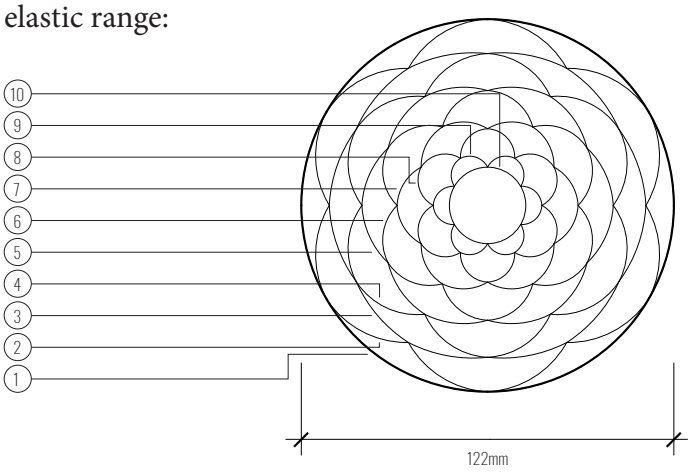

Figure 3-43: Overall dimensions and number of sections of spar pattern used for determining the ratio between load and deformation.

Section	Width (in cm)
1	0.55
2	0.49
3	0.44
4	0.40
5	0.36
6	0.33
7	0.30
8	0.28
9	0.26
10	0.25

Figure 3-44: Load-deformation test spar section widths.

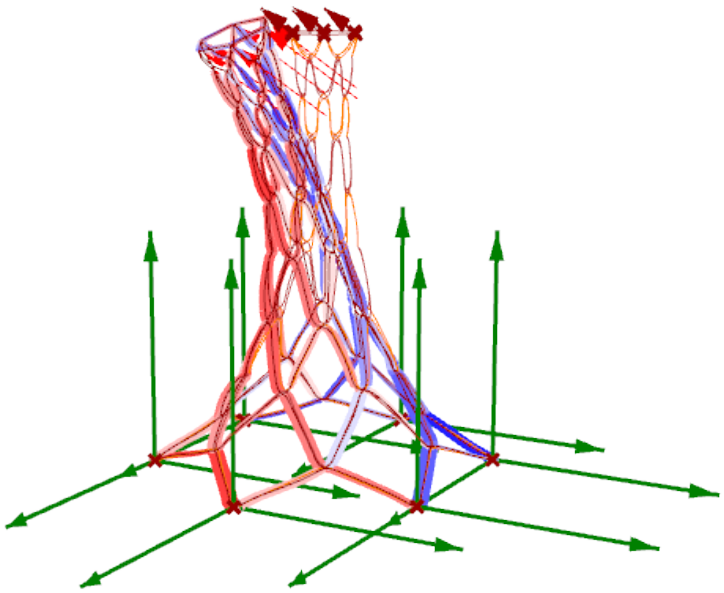

Figure 3-45: Image of deformed spar model with magnified deformations.

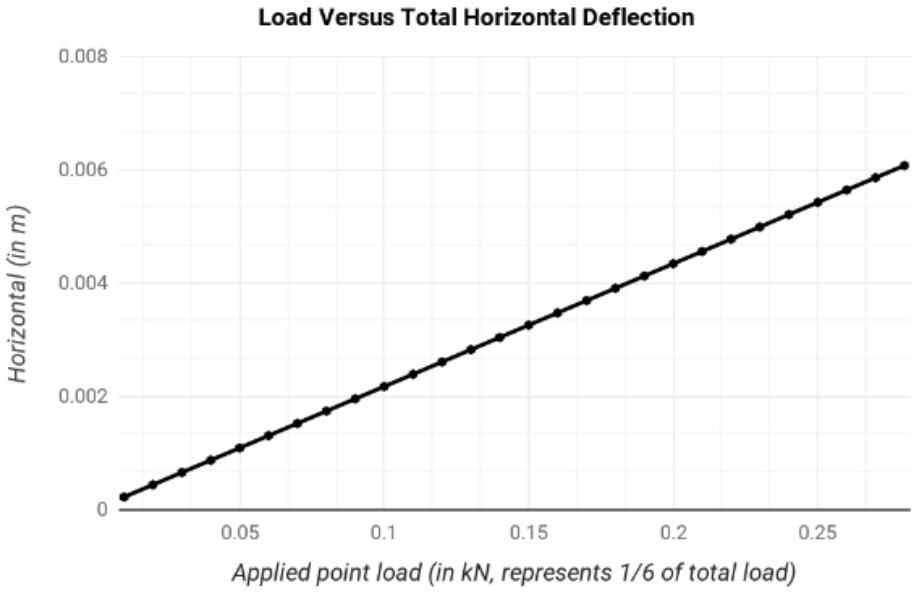

Figure 3-46: Load versus total horizontal deformation curve measured from the tip of the spar.

$$EI\frac{d^2u_y}{dx^4} - c = 0 \tag{2.6}$$

$$\int_\Omega \frac{d^2w}{dx^2} EI \frac{d_y^{2u}}{dx^2} dx = \int_\Omega wpdx + \left(\frac{dw}{dx}\,\bar{m}\right)\Big|_{\Gamma_m} + (w\bar{s})|_{\Gamma_s}\ for\ \forall w \in\ U_0 \tag{2.7}$$

We know from equation (2.6), and subsequently its weak form (2.7), that the displacement is related to force by the product of Young's Modulus E and the Moment of inertia I:

As we know, the force is a product of the displacement and the stiffness matrix. We can derive the effective stiffness from the slope of the force displacement curve from figure 3-46. This slope was determined to be 0.0215 for 1/6th the load or 0.003515557 m/kn

Assuming that solving the individual deformation of frame elements is equivalent and summing them together, and enforcing continuity, will

result in the total deformation of an entire frame:

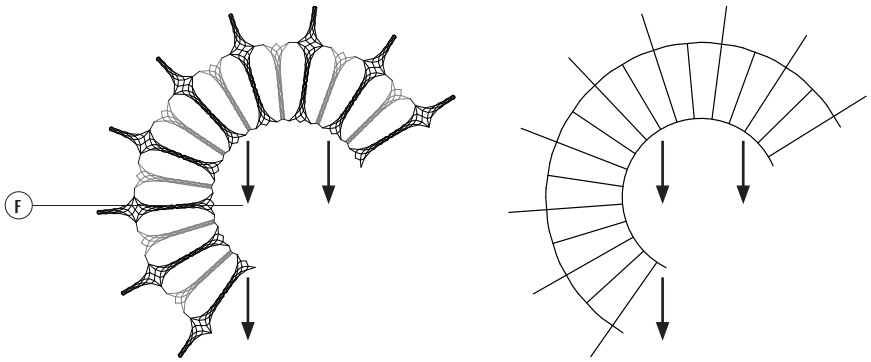

Figure 3-47: Left: detailed beam element model of a frame comprised of sphere units, right: simplified model of the same structure.

The left hand side represents a frame model (Model $M\boldsymbol{\alpha}$) consisting of beam elements, and the right hand side is an approximation of the same frame with less elements (Model $M\boldsymbol{\beta}$). Both models are subjected to some set of forces $\boldsymbol{F}$. The support conditions, or essential boundary conditions, are the same and not shown on these diagrams.

$M\boldsymbol{\beta}$ is an approximation of $M\boldsymbol{\alpha}$

$M\boldsymbol{\alpha}(\boldsymbol{F}) = \Delta_{\boldsymbol{\alpha}}$ and $M\boldsymbol{\beta}(\boldsymbol{F}) = \Delta_{\boldsymbol{\beta}}$

We want to make $M\boldsymbol{\beta} \approx M\boldsymbol{\alpha}$, so that $\Delta_{\boldsymbol{\beta}} \approx \Delta_{\boldsymbol{\alpha}}$

From the theory of finite elements we can propose that $M\boldsymbol{\alpha} = \sum m_{\alpha}^{c}$,

where m_{α}^{c} is a repetitive component module of $M\boldsymbol{\alpha}$. A similar statement can be made for $M\boldsymbol{\beta}$

At the component level we have:

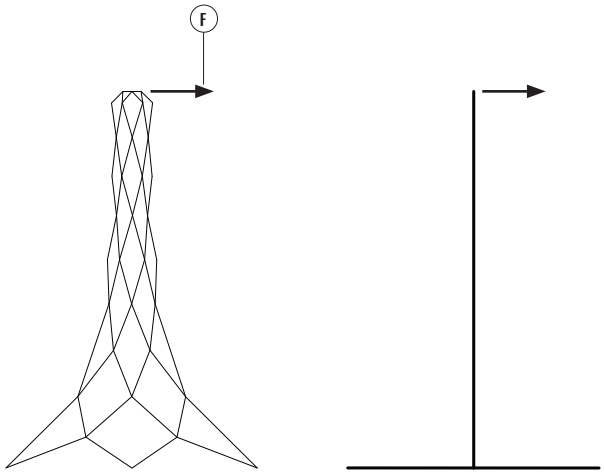

Figure 3-48: Left: detailed model of a spar, right simplified model of the same spar.

The left side diagram represents a component module of the frame model , and the right side represents an approximation with three beam elements m_{β}^{c}. Both models are subjected to the force *f* and have the same un-shown support conditions.

Much like the overal model:

$$m_{\alpha}^{c}(f) = \delta_{\alpha} \text{ and } m_{\beta}^{c}(f) = \delta_{\beta}$$

We can plot the force vs displacement of each model:

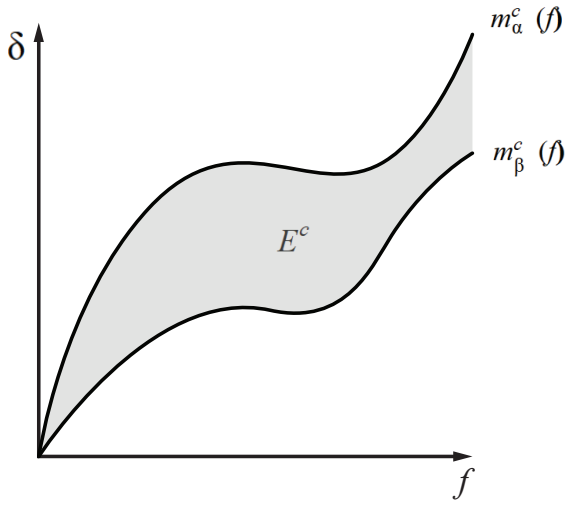

Figure 3-49: Error function between the deformation-force curves of the detailed and simplified spar models.

Where E^C is the function of error.

$$E^C = \int_0^f \left[m_\alpha^c - m_\beta^c\right]^2 df$$

We want to find m_β^c such that E^C is minimized.

Since $m_\beta^c(I_1, I_2)$, $E^C(I_1, I_2)$

We shall find $\frac{\partial E^x}{\partial \mathrm{I}_1} = 0, \qquad \frac{\partial E^x}{\partial \mathrm{I}_2} = 0$.

Since our analysis is linear elastic, the relationship between f and δ is linear for both models.

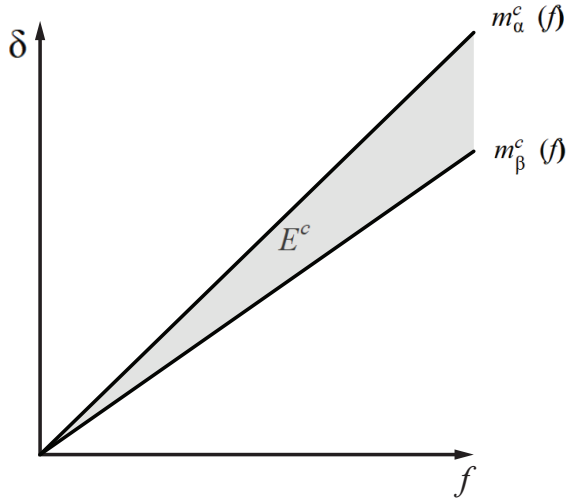

Figure 3-50: Load-deformation functions of each model become linear when considering small deformations only.

Therefore $E^C = \frac{f}{2}\left[m_\alpha^c(f) - m_\beta^c(f)\right]$

Since $\frac{f}{2} \neq 0 \; \forall \, f, \qquad m_\alpha^c(f) = m_\beta^c(f)$

$$m_\beta^c(f) = (f + r)\mathbf{k}^{-1}$$

$\mathbf{k} = \int_0^L EI \; \boldsymbol{B}^T \boldsymbol{B} \; dx$,but $\boldsymbol{B}^T$ and $\boldsymbol{B}$ are defined.

Therefore $\mathbf{k} \propto$ EI, and since $m_\beta^c \propto \mathbf{k}$, $m_\beta^c \propto$ EI

Therefore we find EI such that E^C is minimized.

If E^C is minimized, $m_\alpha^c(f) \approx m_\beta^c(f)$

Then by our initial assumption, $M\boldsymbol{\beta} \approx M\boldsymbol{\alpha}$

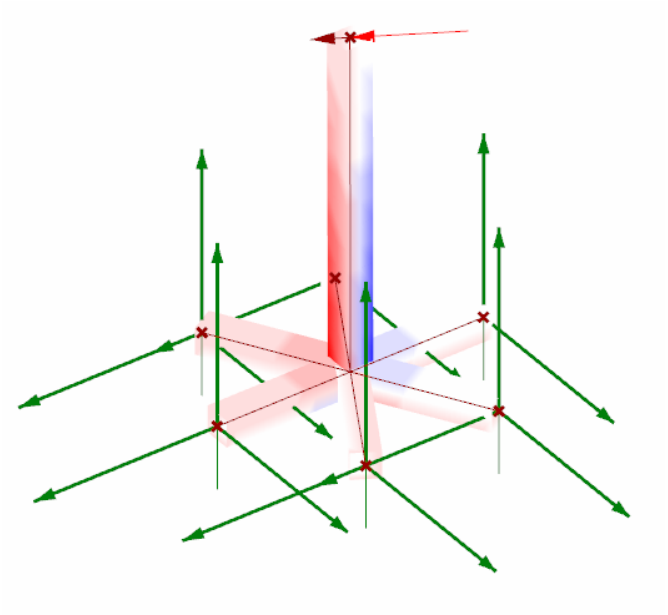

Figure 3-51: Simplified model of the spar from figure 3-45.

If :

The approximation model was set up 7 sections with 15 beam elements each. The E = 20000 kN/cm2, and I = 3765.39577cm4. Input is the h, which physically represents an elements length, width and height, in this case h_s=1.226cm.

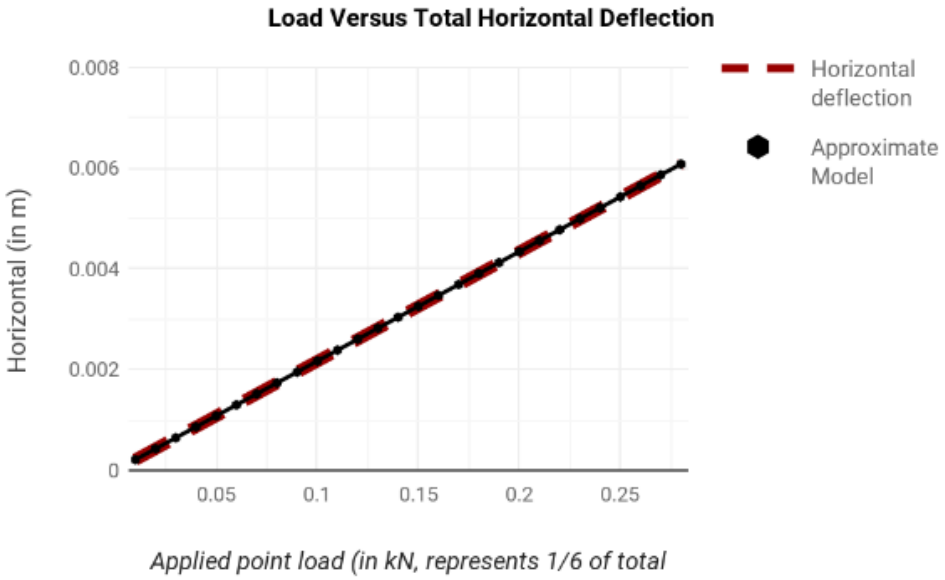

Figure 3-52: Overlay of the load-deformation curves of the simplified and detailed horizontal deformation spar models. This figure concludes that these models return the same result.

In order to increase the accuracy of the model an effective stiffness should be prescribed for the bending as well as the torsion of each spar; however, the current program does not allow for this to happen. In future research, it would be highly beneficial to use a custom finite element program. The best way to integrate this would probably to interface grasshopper with Matlab.

3.3 CONNECTION MODELING

Since the overall frame model will use the Direct Stiffness method, the connections also have to be approximated as beam elements. The triangle plates and x-plates were split into three and four beam elements respectively, and, in a similar manner to the spars, an equivalent stiffness was determined for each beam element. The X-plate was modeled using beam elements and three dimensional four node tetrahedral elements. The boundary conditions was kept as similar as possible, and details are in the chart below. The plot shows a comparison of the two models' x-direction deformation at the center of the connection, versus the load.

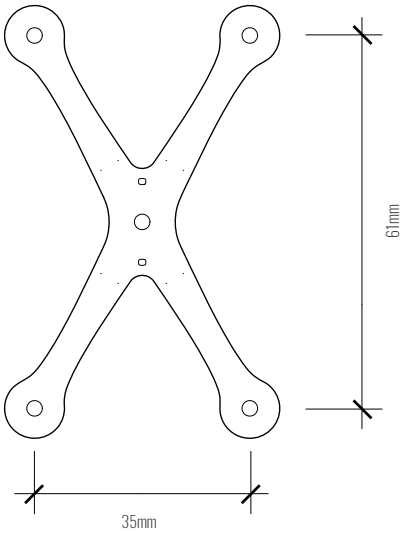

Figure 3-53: The Xplate FEA model was set up as follows.

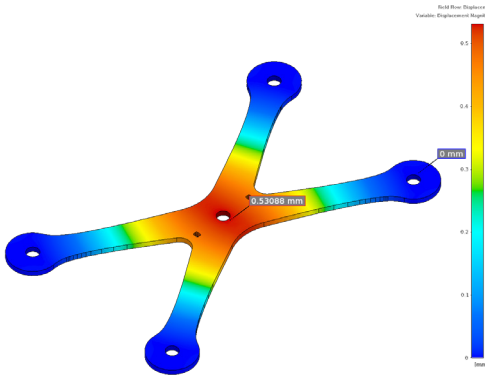

Figure 3-54: The plate was simulated with three dimensional elasticity with 4980 hexahedral elements. The support conditions fix translation on the inside surface of the four arm's bolt holes.

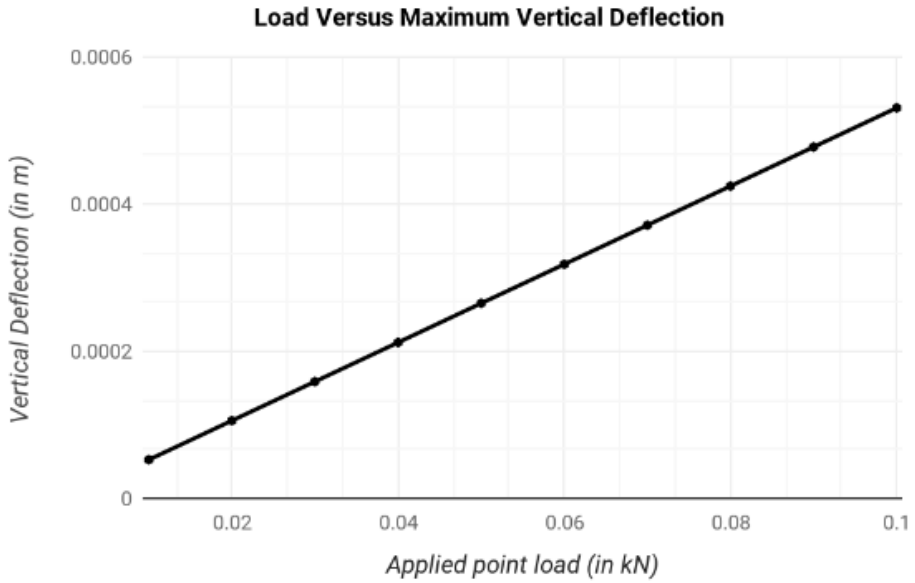

Figure 3-55: This plot reports the load deformation curve of the detailed model.

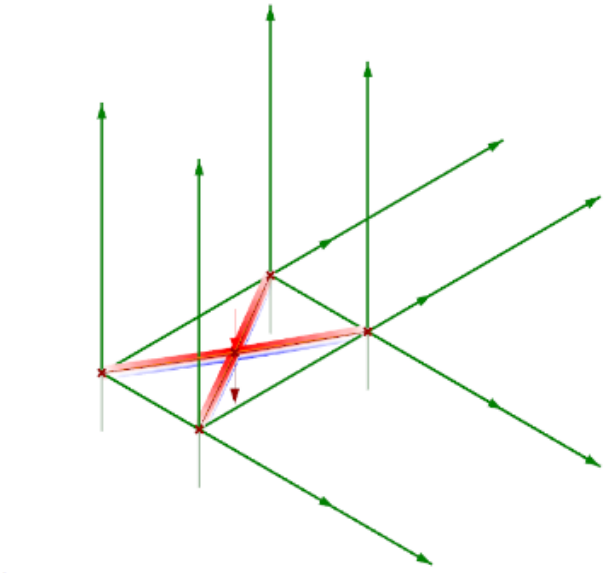

Figure 3-56: Simplified model of the X-plate.

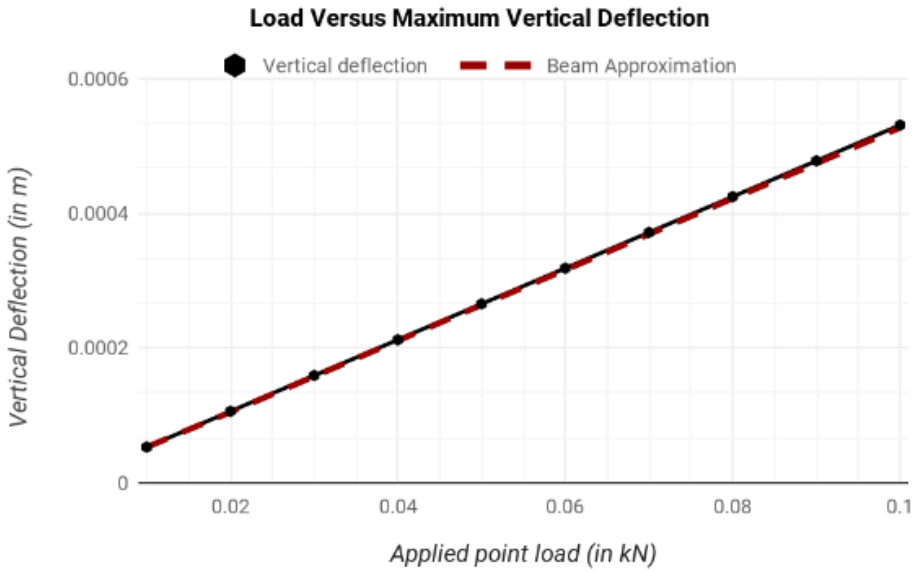

Figure 3-57: Overlay of the load-deformation curves of detailed and simplified x-plate models. These models return the same quantities.

A similar study was conducted for triangle plates. The plates were modeled in beam elements and tetrahedral elements, for which details are given below, and the deformations predicted by each model are compared in the following chart. h_x=0.251cm

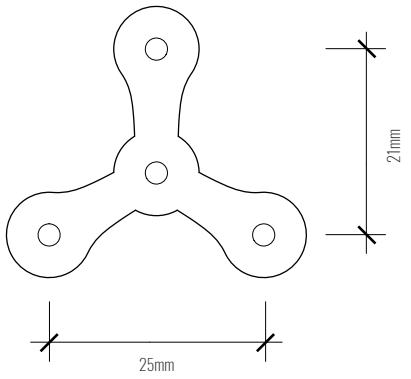

Figure 3-58: The Triangle Plate FEA model was set up as follows.

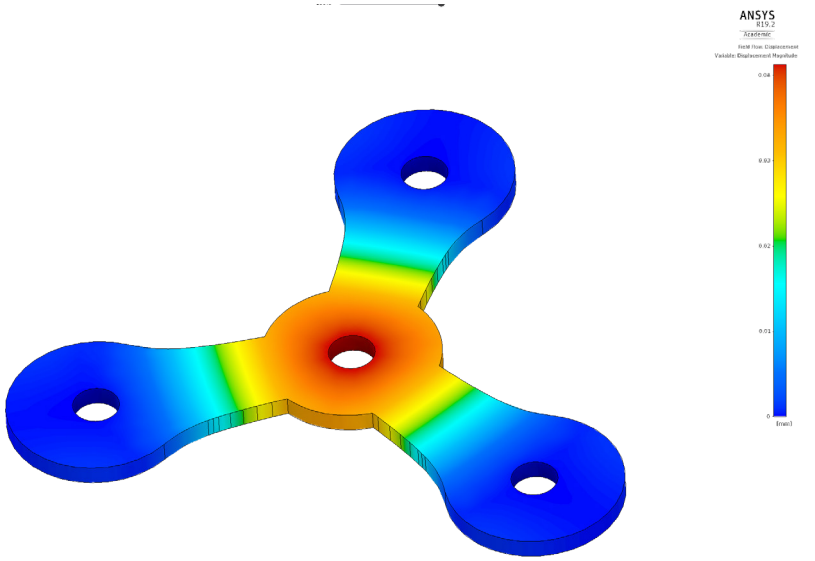

Figure 3-59: The plate was simulated with three dimensional elasticity with 2489 hexahedral elements. The support conditions fix translation on the inside surface of the three arm's bolt holes.

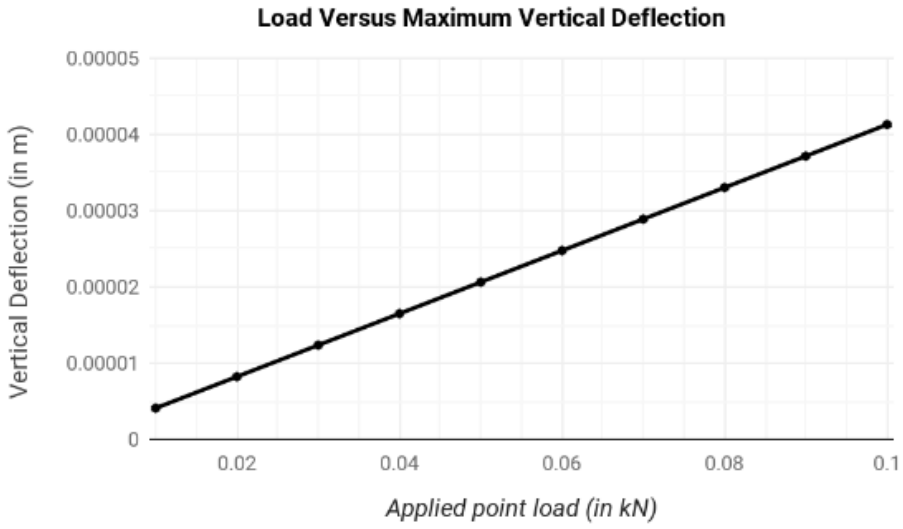

Figure 3-60: Load-deformation curve of the detailed tri-plate model.

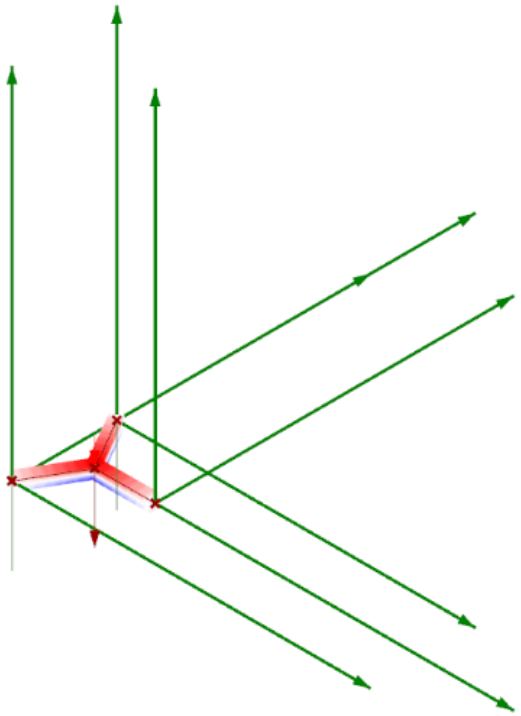

Figure 3-61: Approximation model utilizes 15 beam elements per leg of the tri-plate.

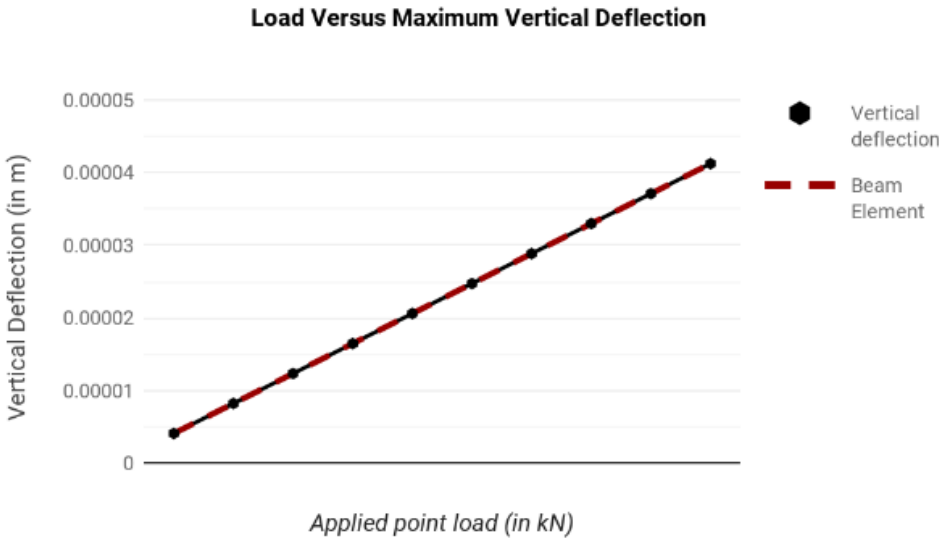

Figure 3-62: Overlay of the load-deformation curves of detailed and simplified tri-plate models. These models return the same quantities.

3.4 OVERALL FRAME ANALYSIS

The following frame parameters were tested in order to gain insight on effective material distribution: effects of individual components on maximum model displacement and energy, effects of hanging points, and topology of the frame. The baseline model described in section 3.1 is used to explore the first two sets of parameters; while a set of boundary conditions, fixed loads and supports, are used to explore the last set of parameters.

The following model explores the effect of strengthening the three major components of the spar frame: Spars, triangle plates and x-plates. Increasing the strength in this model was achieved by changing the stiffness of these beam elements. It should be noted that, because this model is based on equivalent stiffness, the stiffness does not represent the exact material stiffness. These equivalent stiffnesses can be achieved by increasing the material thickness and, in the case of the spars, material distribution.

The model uses the following physical properties:

Physical Property	Value	Units
E modulus of elasticity	200	GPa
I_{SPAR}	$1.226^4/12 = 0.1883$	cm^4
$I_{TriPlate}$	$0.26222^4/12 = 0.000394$	cm^4
I_{Xplate}	$0.251^4/12 = 0.000331$	cm^4
W (Overall Structure Weight)	370*1.5 = 555	kg
P (Superimposed Point Load)	W x 9.81/1000 = 5.444	kN

Figure 3-63: Model properties of the overall frame analysis model.

The connections between sphere units were not considered for this studied, therefore they were modeled with significantly higher stiffness so that they would not impact the overall deflection.

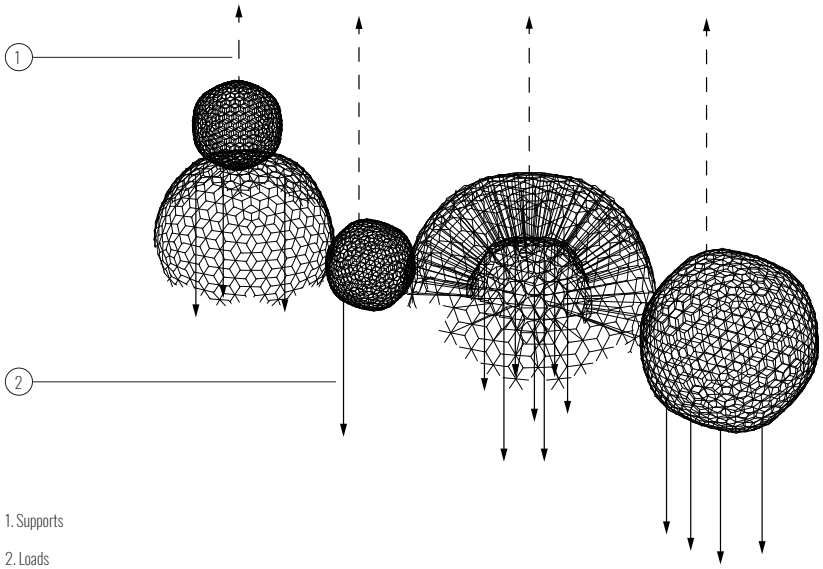

Figure 3-64: Model setup. Model was constructed from simplified spar, tri-plate, and x-plate models.

The supports were set up in the same positions as they were for the LAS beauty installation for which this model was created after. The loads were modeled as 15 point loads at P/15 = 0.3629 kN each. Distribution of these point loads to find the worst case scenario was not studied, and would be an important topic for future research.

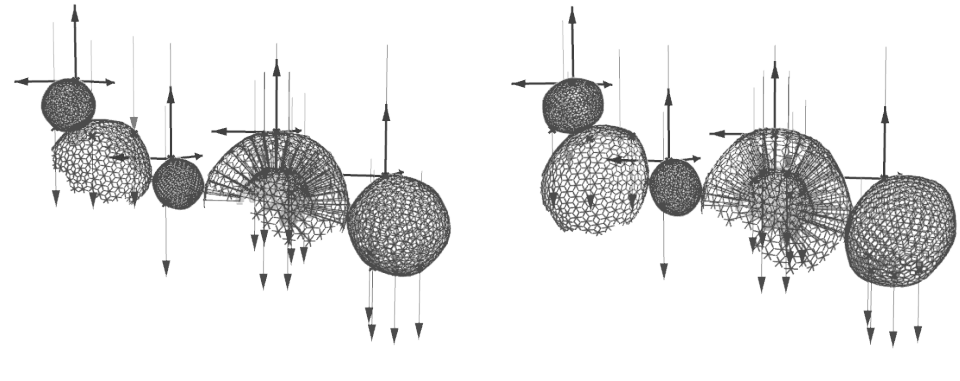

Figure 3-65: Left: Model setup, Right: deformed model with displacements magnified by 10 times.

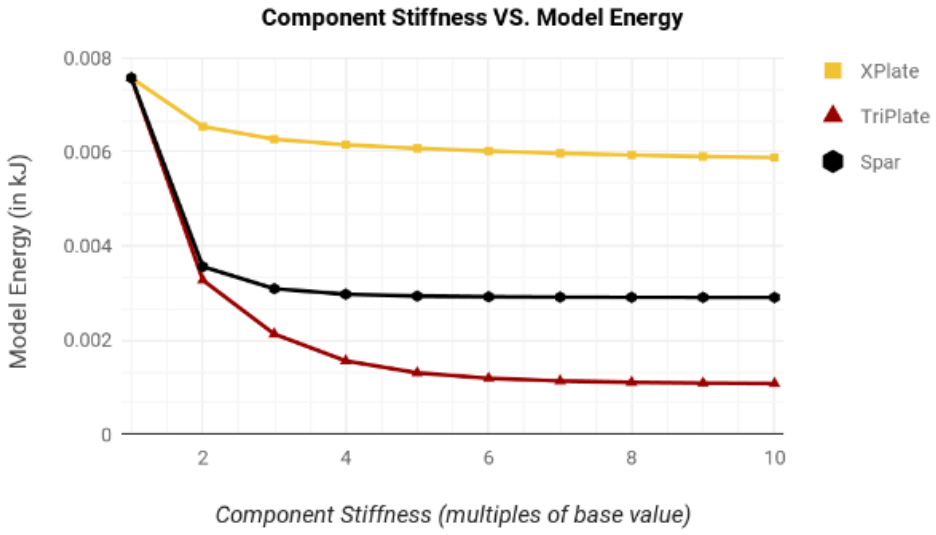

Figure 3-66: Component equivalent stiffness in multiples of $I_{TriPlate}$, I_{Xplate} , $I_{SPAR,}$ and their relative effect on the total model deformation energy.

When loaded in this particular fashion, which approximates gravity loading, the model shows that increasing the stiffness of the Triangle Plates as most effective at reducing the overall model energy. A lower model energy means that the structure is deforming less under the same load. This result is expected because this model uses fairly few Xplate components. It is important to note that this refers to the effective stiffness of the components, achieving these effective stiffnesses can be done in a variety of ways, for example: increasing material thickness, changing the cross section shapes.

Endnotes

1 "AISI Type 304 Stainless Steel," *ASM Aerospace Specification Metals*, accessed March 20, 2018, http://asm.matweb.com/search/SpecificMaterial.asp?bassnum=mq304a.

2 Reddy, J. N. *Introduction to the Finite Element Method*, 22.

3 Fish, Jacob, and Ted Belytschko. *A First Course in Finite Elements*, 203.

4 Fish, Jacob, and Ted Belytschko. *A First Course in Finite Elements*, 204.

part 4

IMPLEMENTATION

4.1 LUDDY HALL

4.1.1 DESIGN CONSTRAINTS

Utilizing the modular hexapod spar in configurations known as sphere units the LAS created Amatria, an installation for Luddy Hall at the University of Indiana. The dimensional constraints of the system for Luddy hall are that it must have a symmetrical hexapod unit which, including the dimensions of the connection plates, creates a matrix of tessellating hexagons distanced 300 mm on center for any axis perpendicular to one of the hexagons faces. These units must be fabricated from sheet material of thickness no greater than what can be mechanically formed by a simple pulley and winch machine. The structure should not deflect significantly. The structure should also interface between the many mechatronic systems of sensors, actuators and microprocessors housed within the sculpture. Finally, since the structure will compose the largest percentage of the body of the sculpture, it should be aesthetically and symbolically evocative of the dissipative forms Beesley and the LAS are interested in.

The geometry of the overall structure makes it very difficult to perform analysis on because there are so many members which are in themselves composed of smaller members.

Another important issue is the predictability of failure, because the structure is not directly inhabited, to what degree of deformation is the structure considered to be failed?

The structure is also difficult to test because of the three dimensional nature of its displacement. String potentiometers,or string pots can be used to measure displacements of nodes; however, it would require three string pots per node to extract three dimensional movements. Furthermore, as the spar deforms during the test, the strings of the string pots will be pulled at angles not collinear to their initial positions and thus introducing significant error into the method. Digital image correlation or DIC is seemingly the best options; however, due to the small size of the spar's composite elements, the position tracking balls will be so closely spaced to one another that the computer may confuse which displacements correlate with which tracking ball. This issue is typically combated by utilizing a randomized speckled paint pattern; however, this technique is usually used for two dimensional measurements. DIC software looks for distortions in the contrast ratio of the pattern in order to interpolate strain, but if you were to apply this paint to a three dimensional surface, shadows cast on or by the surface may be falsely interpreted by the computer as strain. The analytical modeling was created using Solidworks Simulation and SAP2000.

4.1.2 PROCESS

Failure modes are difficult to predict, there exists a variety of different failure theories which have been discovered through historic scientific endeavour like the Von Mesis theory of maximum energy of distortion. The validity of these theories depends on the materials used.

Four categories of critical parameters were identified: architectural, structural, economy, and fabrication. Parameters from these categories were organized on a chart that looked at the relative importance of each parameter versus its effect on other parameters. For instance, transparency affects the structural strength and stiffness of the sculpture as well as the cost and ease of installation. For the sculpture to be transparent, it would have to be made of polymer rather than steel. Polymer is much less strong and stiff then steel. Particularly because it is less stiff, a mostly plastic frame would be harder to install because it would deform out of shape whilst it is being positioned on site. On the other hand, a steel frame would be more expensive for several reasons: The first is that steel is more expensive than polymer. Second, it is more difficult to cut because it requires expensive machinery. Finally it is more difficult to form because of the amount of force required to pull it into shape.

When I asked engineers how they would frame the installation, the unanimous response was to use an interior steel frame to mount the plastic spars onto. This framing option would maximize the strength, stiffness and predictability of the structure which was why it was the obvious choice from an engineering perspective. The option may seem like the best choice when looking at engineering performance criteria alone; however, when looking at all the performance criteria; we can see that it causes the sculpture to lose transparency because of the solid steel interior frame. Furthermore, this type of straight forward framing would betray the network complexity for which the sculpture is supposed to represent. Therefore, when looking at the global performance criteria, this option actually fairs quite poorly.

The chosen structural framing option was to use metal spars along the effective load paths. Although the resulting frame does not have the same stiffness as the interior frame option, the strength is similar. Cost and weight is reduced because of the reduction of redundancy, and more importantly the sculpture maintains its network complexity and a fair bit of transparency.

The preliminary analysis of the components was conducted in two dimensions. During use, the installation is only subjected to its own self

weight. The scenario that produces the most load on a single spar is during the installation process. Sphere units were to be set up in groups of 3, supported from a single cable, therefore the spar attached to this cable must be capable of taking the load of 3 units.

Extra elements were added to the typical spar representing the spider plate and the central rod.

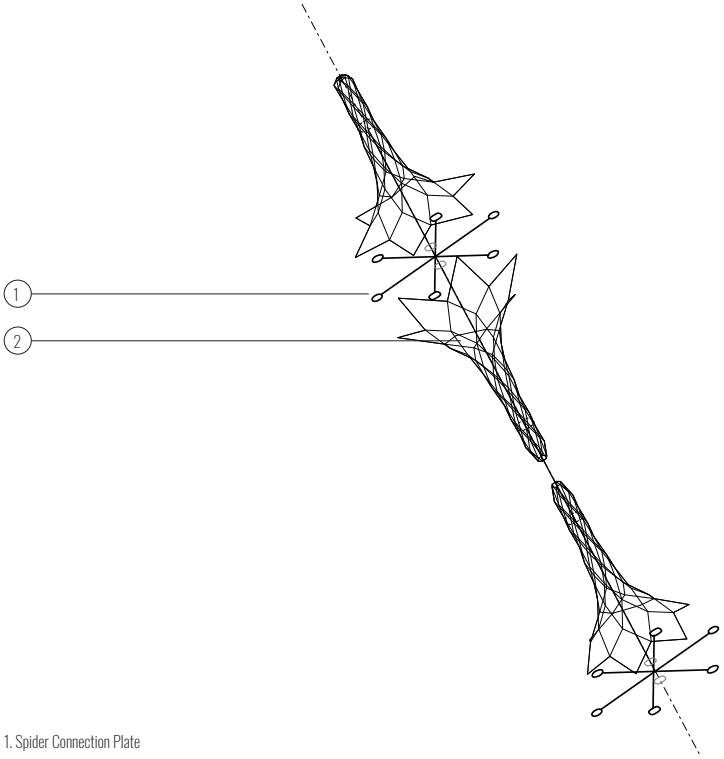

1. Spider Connection Plate

2. Central Rod

Figure 4-1: Additional Components added to critical assembly.

Physical Property	Value	Units
Installation Weight	4.448	kN
Sphere Unit Weight	4.448/10 = 0.4448	kN
SD factored superimposed dead load per sphere unit	1.4 x 0.4448 = 0.6227	kN
E Modulus of elasticity	200	GPa
U Poisson's Ratio	0.3	None
G Shear Modulus	76.9	MPa
Fy Yield Stress	345	MPa

Figure 4-2: Table of Assumptions

The maximum axial force in tension occurs in the central support rod at 1.47 kN, and the maximum compression occurs in the spider plate at 0.79kN. Failure criteria was checked using axial stress and Euler buckling. The maximum axial stress was 74.86kN, which is less then F_y and therefore acceptable. The Euler buckling load in the spider plate was calculated at 1.17kN which is greater then the maximum compression in the plate and permissible.

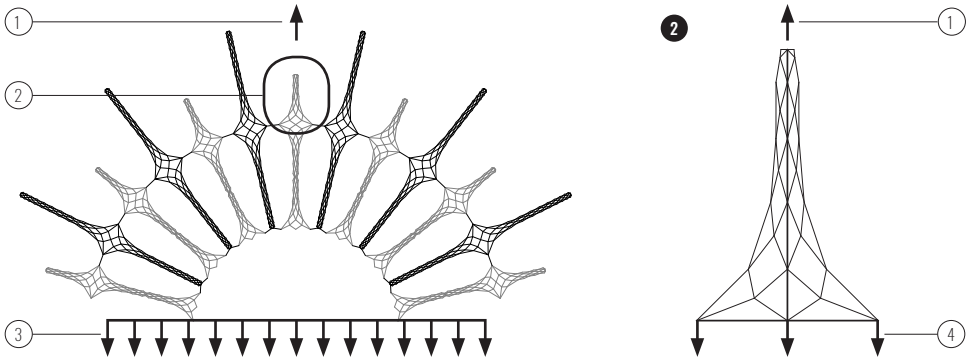

1. Reaction force from support cable
2. Critical spar
3. Gravity load
4. Superimposed point loads approximating weight of entire assembly

Figure 4-3: Loading Approximation of the Central Spar

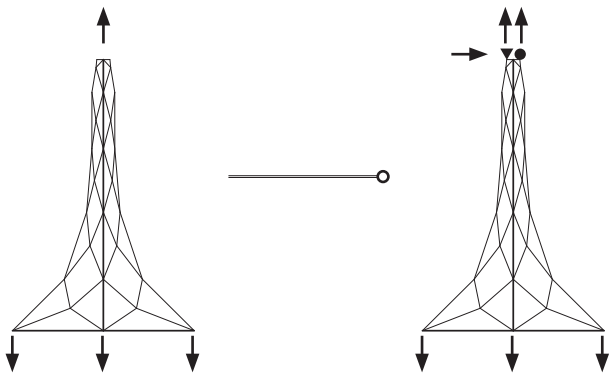

Figure 4-4: Critical Spar Boundary Modeling.

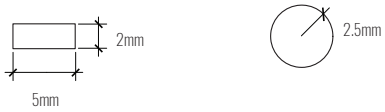

Figure 4-5: Left: spar cross section approximation, right: rod cross section approximation.

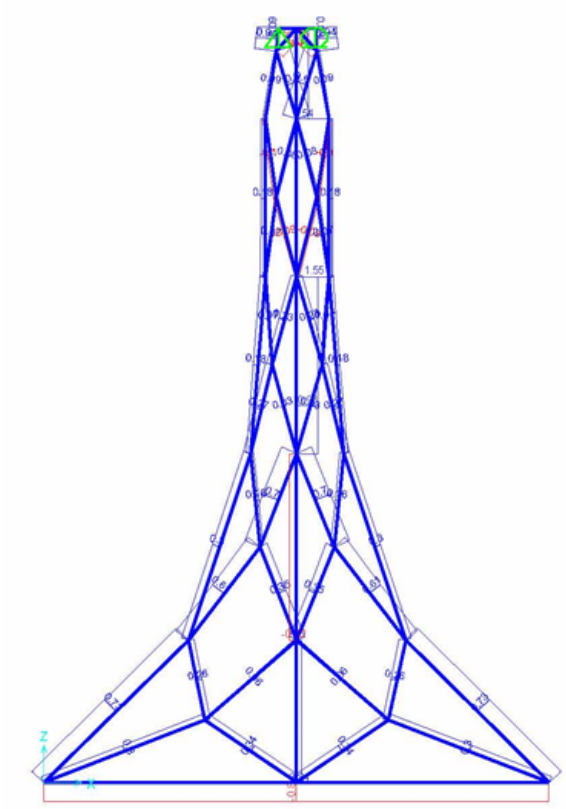

Figure 4-6: Frame Analysis Results from SAP 2000

Another loading scenario considered is when the cable does not project normal to the spar. This could happen at various times during the installation process. In the case of this study, theta was considered to be 30 degrees.

From these models: maximum tension is 1.61 kN in the spar midsection, maximum compression is 1.24 kN in the spar midsection, maximum shear is 0.12 kN in the central rod, and maximum moment is 0.005849 kNm in the central rod. The axial stress was permissible at 161 MPa. The

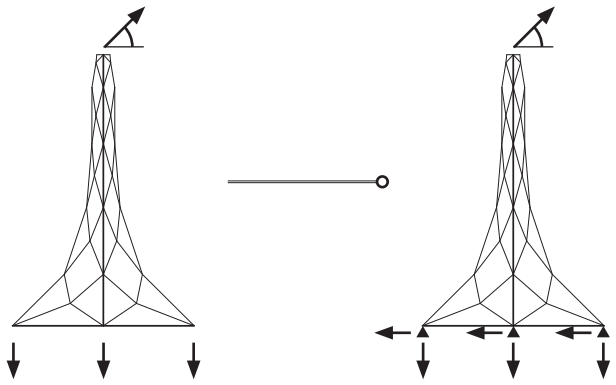

Figure 4-7: Angled loading scenario

critical buckling load at the spar midsection is 1.83 kN, therefore 1.24 kN is permissible. Allowable shear stress is half of F_y, and the calculated stress was only 18 MPa. The maximum bending stress is 476.6 MPa, this is greater than F_y, and therefore it was recommended that the internal rod be thickened to a radius of 2.8mm. Also it was recommended to avoid this loading situation if possible.

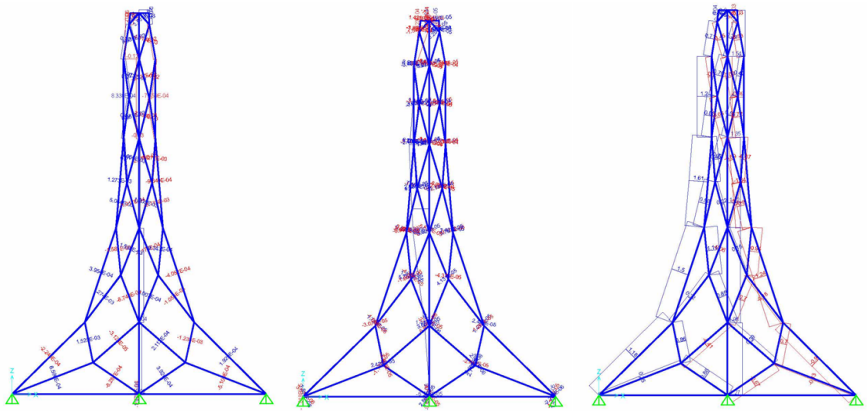

Figure 4-8: From left to right: Axial force results, shear force results, bending results.

Utilizing three dimensional analysis, it was shown that the interior rod and plate were still engaged and reduce the maximum stress in the critical unit. It is important to note that the two models shown above have been tested with a much higher load then what could be expected, and are both past their material yield points. Yet, the study still illustrates the former point.

The design of the X plate connections was revised considerably after FEA study pointed out areas of stress concentration at sharp angles.
Elastic 3 dimensional elements have and advantage over beam elements because they can show stress concentrations. While FEA has more general application. It was not possible to construct an FEA model of the entire

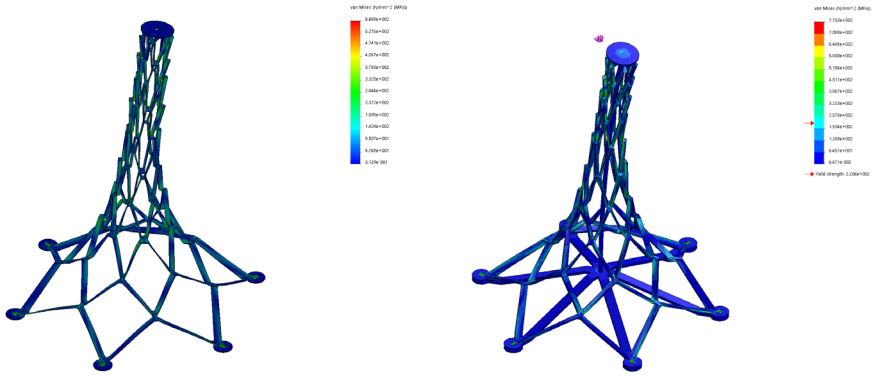

Figure 4-9: Linear elastic FEA models of the spar with and without the internal structure.

sculpture because the geometric model of the project was not perfect and therefore required the elastic flexibility of steel and plastic in order to be physically assembled. The numerous amounts of geometric discontinuities were not feasible to be rebuilt in the project's time-frame. Instead, the most critical members were analyzed under the worst loading conditions in order to determine the overall integrity of the structure. These members

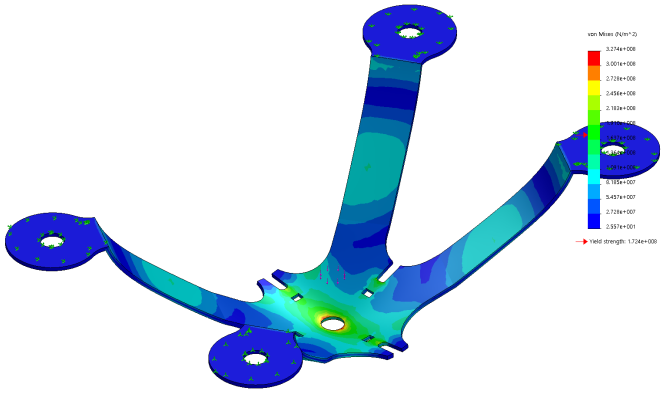

Figure 4-10: Comparison of Xplate designs.

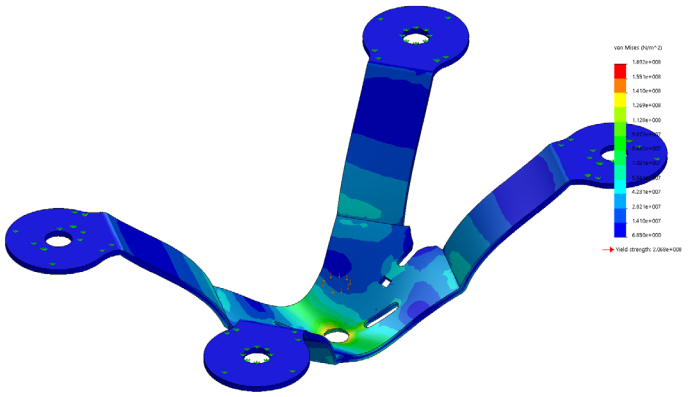

Figure 4-11: Comparison of Xplate designs.

were the central short spars which were directly connected to the support cables and the x-connection plates. The worst case was considered to be when four sphere units hung from a single spar with a large angle deviation from the normal of the spar.

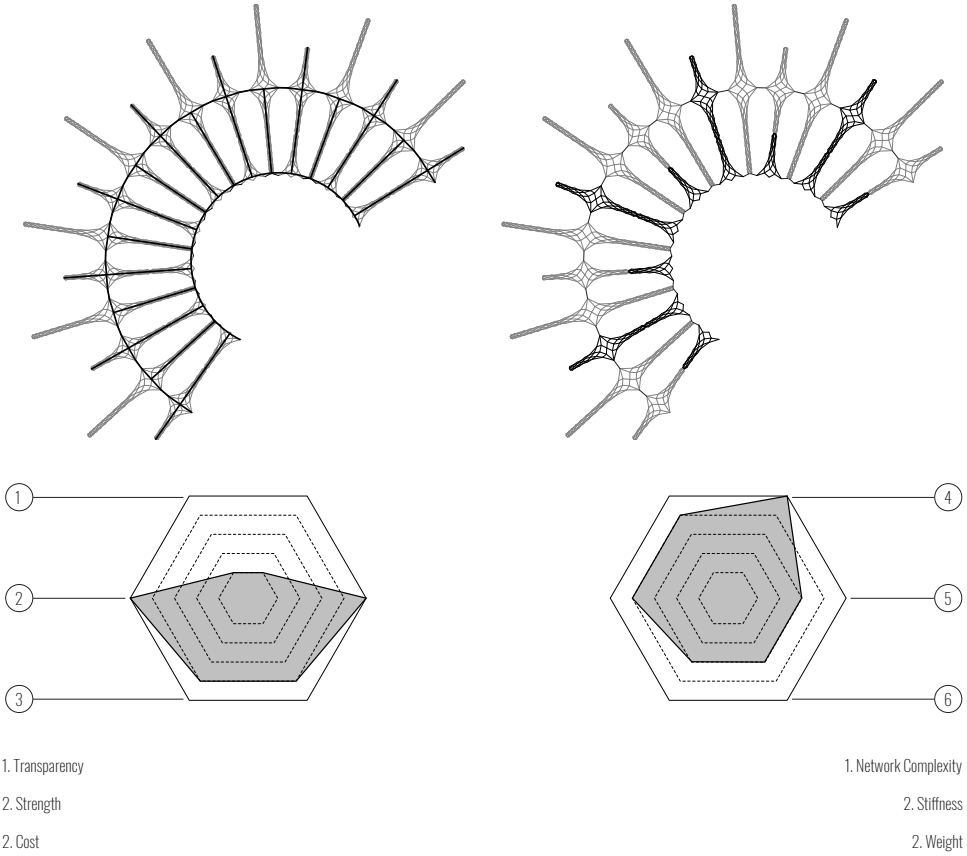

Figure 4-12: Comparison of Proposed Framing.

Figure 4-13: Image of the installation progress showing the angled cables.

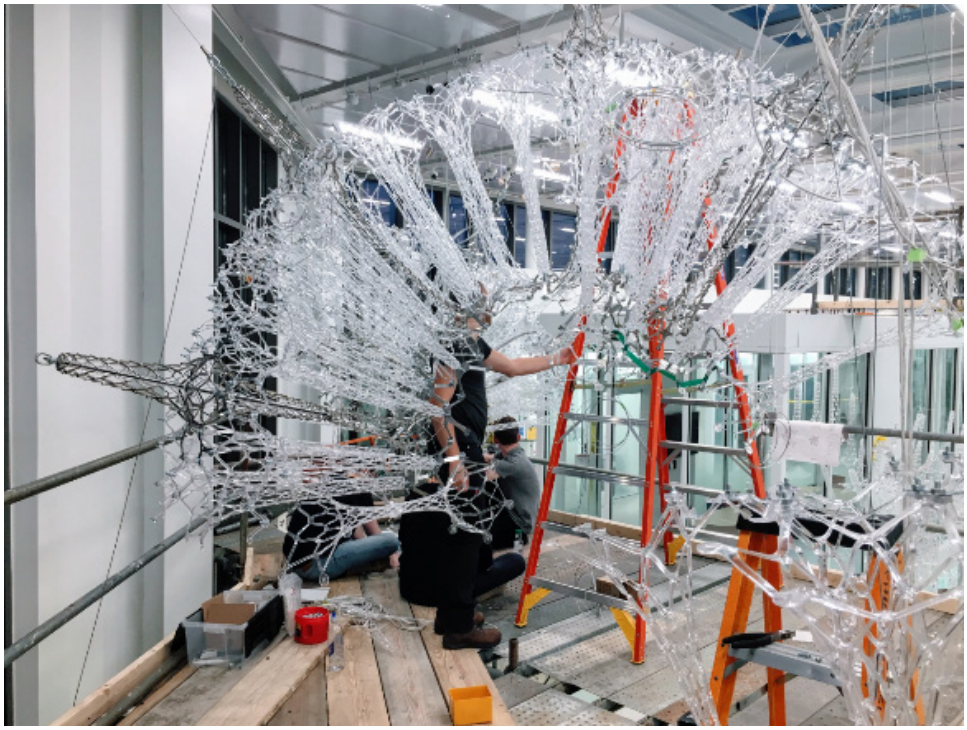

Figure 4-14: Further progress.

Figure 4-15: Main sphere units in place with cables adjusted to project from close to normal.

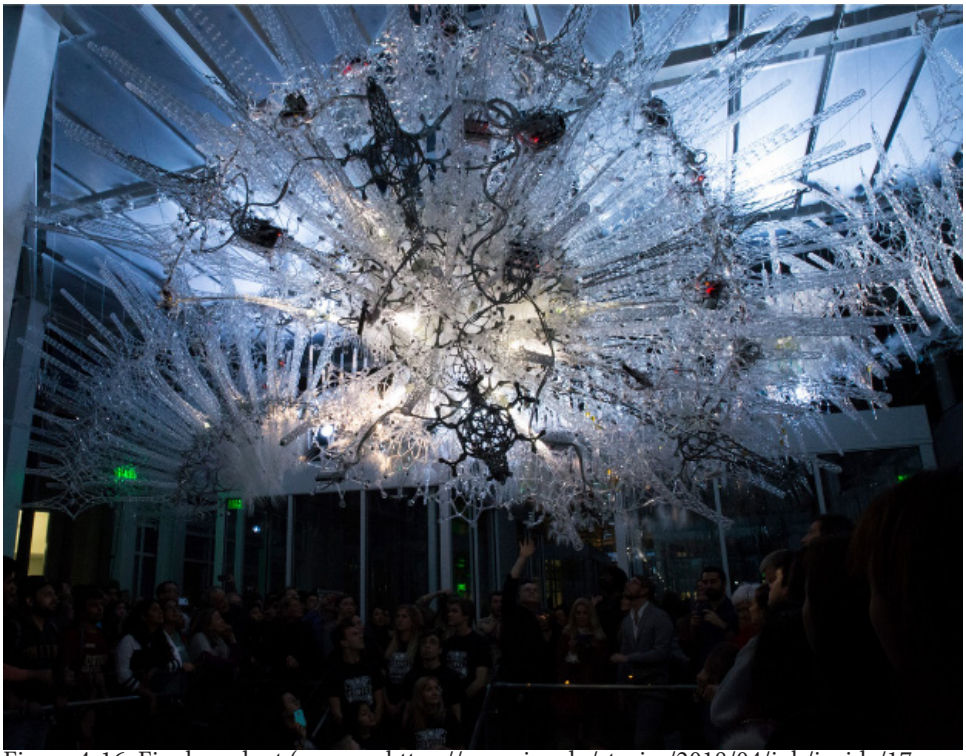

Figure 4-16: Final product.(source: https://news.iu.edu/stories/2018/04/iub/inside/17-sentient-art-unveiled-at-luddy-hall.html. Photo by Amelia Herrick and Chris Meyer).

The worst case for the x-plate was considered to be when the structure was loaded in the aforementioned scenario. In this load case, each of the x-plates attached to the central spar would have to carry one sixth of the overall load.

Physical testing was performed by cutting spars from sheet metal with an OMAX water jet cutter, mechanically forming them with a pulley, and, using the same pulley, loading the formed structure. Knowing that the pulley had a mechanical advantage of one to six, it was possible to load the spar with the approximate 1200lbs it was designed to take.

4.1.3 RESULTS AND DISCUSSION

The strength and stiffness of the new structure allowed the sculpture to be built in a much more logical and easy manner when compared with the previous installation. Since the sculpture was not loaded, the entire sphere could be supported from one hanging point and spun around. Also the design was rigid enough to move as one so it could not be tilted and maneuvered.

4.2 EVENT PAVILION DESIGN INVESTIGATION

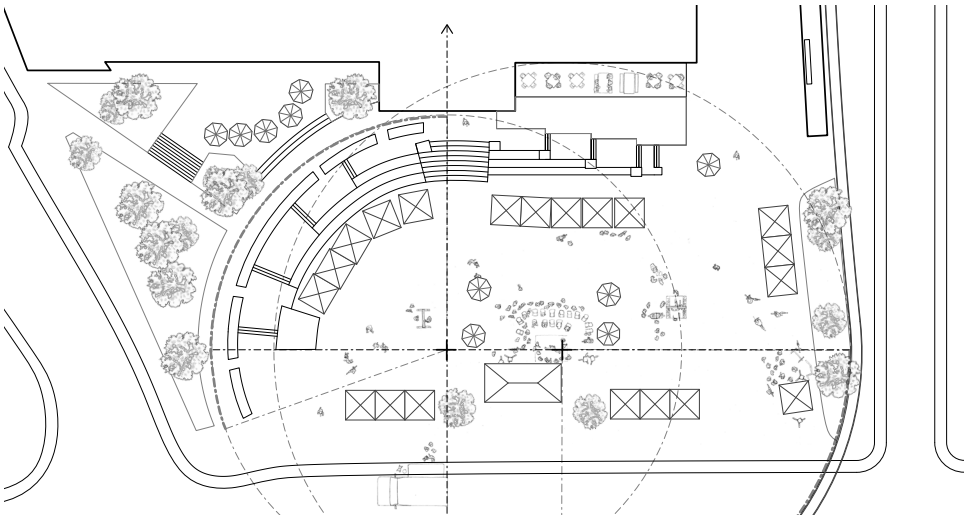

Figure 4-17: Waterloo Public Square Open Streets Event September 2017 site plan.

The site for the design experiments was the Waterloo Public Square Open Streets Event on September 17th 2017. Lightweight modular frame structures can contribute to outdoor events like Open Streets because they can be set up and taken down quickly. Furthermore, as an alternate to the typical telescopic tent structures used in outdoor events, lightweight frames can create a quality of space which extends beyond utility.

The event was held in the Uptown Waterloo Public square 75 King Street South in Waterloo, Ontario Canada. The square is flanked by King street, one of the major commercial streets in Waterloo, to the East, and a mid size shopping mall on the West. There is a grade change from the East side upward toward the West side of the site. There is a significant landscape feature that addresses this grade change which is composed of: an arched accessible slope, terraced steps with dispersed cafe seating and parasols, tiered seating, and steps up to the entrance of the mall. Towards the North end, there is a large planting feature that divides the public steps from a restaurant's, that is part of the mall, patio. The East side is flat and has a major transit spot. This edge of the square uses trees to separate the space of the square from the sidewalk.

The Open Streets event describes itself as an event that "Turns vehicular roads into family friendly community spaces four times a year[1]." The activities held in the square were as series of tents promoting community events, a speech area, a games area, and a breakdancing tournament. The dance tournament was the largest event; however, it was oddly placed at the East end of the site, rather than at the West end of the site where the raked seating landscape feature was located. Instead, the majority of the event

tents were located around the base of the steps and seating. These tents were oriented so that they faced the square, rendering the seating built into the site useless. One simple solution to this event planning problem would be to swap the location of these two events. Flipping the location of the tents will require them to function as an attractive frame for the entrance to the space from King street. The redesign of these tents in their new proposed position provides a suitable opportunity for architectural experimentation in expanded metal frame structures.

The hypothetical design problem here is to design a modular event pavilion that can be easily: transported, set up, and taken down. The pavilions should be able to function from at least two directions, furthermore, they should incorporate a significant degree of transparency so that other activities can be seen through them. The combination of these pavilions in rows should be able to create a welcoming frame, that helps to define the space of an event. The pavilion should shelter the event personale and event visitors from the sun and light rain. They should not have any permanent foundations, and also readily provide an armature for systems, such as screens and sound systems, to be integrated. There should be a variety of combinations that sufficiently cover several scales of pavilions. The system should also have options for geometrical manipulation that sufficiently deals with the following programs: initiative promotion, refreshment vending, speeches and performances. Finally, all pieces should be light enough that they can easily be lifted and manipulated by one person.

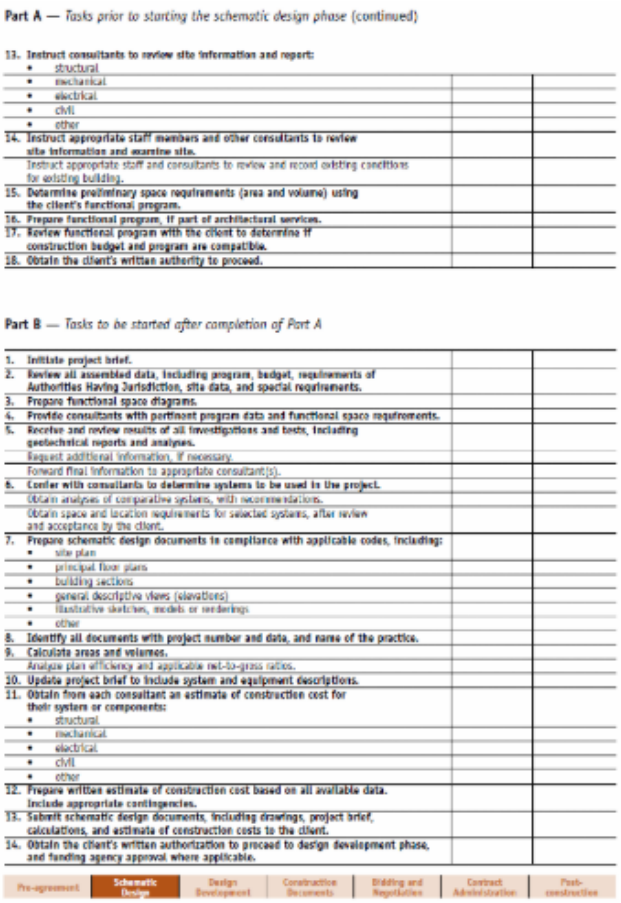

Part A — *Tasks prior to starting the schematic design phase* (continued)

13. Instruct consultants to review site information and report:		
• structural		
• mechanical		
• electrical		
• civil		
• other		
14. Instruct appropriate staff members and other consultants to review site information and examine site.		
Instruct appropriate staff and consultants to review and record existing conditions for existing building.		
15. Determine preliminary space requirements (area and volume) using the client's functional program.		
16. Prepare functional program, if part of architectural services.		
17. Review functional program with the client to determine if construction budget and program are compatible.		
18. Obtain the client's written authority to proceed.		

Part B — *Tasks to be started after completion of Part A*

1. Initiate project brief.		
2. Review all assembled data, including program, budget, requirements of Authorities Having Jurisdiction, site data, and special requirements.		
3. Prepare functional space diagrams.		
4. Provide consultants with pertinent program data and functional space requirements.		
5. Receive and review results of all investigations and tests, including geotechnical reports and analyses.		
Request additional information, if necessary.		
Forward final information to appropriate consultant(s).		
6. Confer with consultants to determine systems to be used in the project.		
Obtain analyses of comparative systems, with recommendations.		
Obtain space and location requirements for selected systems, after review and acceptance by the client.		
7. Prepare schematic design documents in compliance with applicable codes, including:		
• site plan		
• principal floor plans		
• building sections		
• general descriptive views (elevations)		
• illustrative sketches, models or renderings		
• other		
8. Identify all documents with project number and date, and name of the practice.		
9. Calculate areas and volumes.		
Analyze plan efficiency and applicable net-to-gross ratios.		
10. Update project brief to include system and equipment descriptions.		
11. Obtain from each consultant an estimate of construction cost for their system or components:		
• structural		
• mechanical		
• electrical		
• civil		
• other		
12. Prepare written estimate of construction cost based on all available data. Include appropriate contingencies.		
13. Submit schematic design documents, including drawings, project brief, calculations, and estimate of construction costs to the client.		
14. Obtain the client's written authorization to proceed to design development phase, and funding agency approval where applicable.		

Pre-agreement | Schematic Design | Design Development | Construction Documents | Bidding and Negotiation | Contract Administration | Post-construction

Figure 4-18: Schematic design project management checklist.

The process for schematic design is outlined in the Canadian handbook of Practice for Architects, the major points processes concerning the structural design of the project are summarized in figure 4-18. According to this process, engineers typically prepare schematic cost estimates without knowing the exact layout of the building. More concerning is that engineers have little to no input on the process of determining a buildings layout and massing. I propose a modified process where structural form finding is inserted at two points in the process: once before the meeting with the structural engineers, and once after. In this way, more value can be added to the meeting, and structural framing can be incorporated at the stage where changes are still easy to implement. The functional space diagrams can be used to derive the loads and boundary conditions necessary to run topology optimization. In this way, structure driven forms

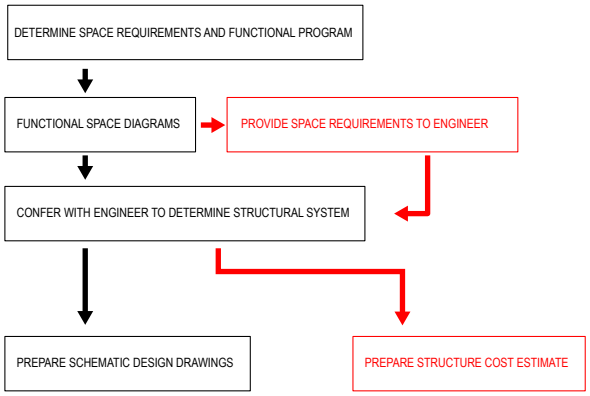

Figure 4-19: Workflow diagram of engineer's involvement in the schematic design process.

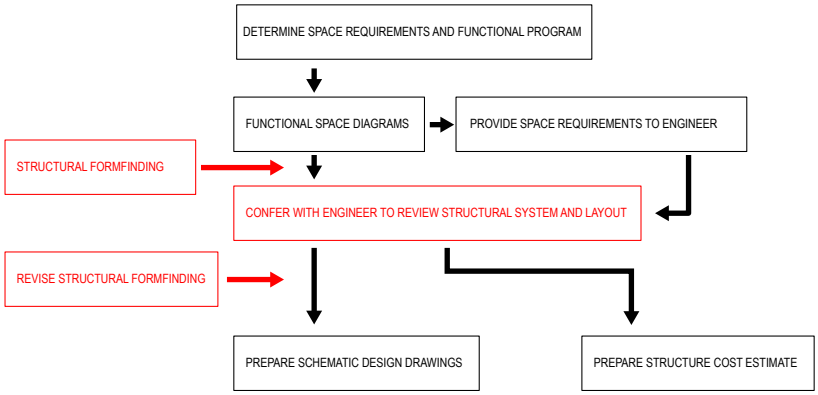

Figure 4-20: Proposed revision to the process.

can be quickly generated and evaluated against other architectural criteria. The potential of this technique shall be investigated through this pavilion design.

The program of shall be simple: a booth for vendors and or event personale. The following diagram shows the rationalization of the revisions to the site plan of the Open Streets event. From a structural design perspective, a pavillion can be simplified to a surface spanning between supports. The geometry of this surface plays a big roll in both the experience of the space and its structural efficiency. For this reason, a study of different surface geometries is a simultaneous architectural and

structural study. To this effect, three surfaces were explored representing the three types of spanning surfaces: flat, arched, and free form. Surfaces of these three types were approximated by tessellating the low-poly sphere unit element. Each cluster of polygons was then subjected to the parametric frame generation process to produce an analytical frame model.

For the sake of comparison, these surfaces where created so that they would have as similar span and loading conditions as possible; however, due to the nature of using discrete units for each pattern, these values could not be made exactly the same. Following the process laid out in chapter three, these models can be used to extract analytical results for direct comparison. It follows that these models can and should also be used for architectural massing studies; however, these are not explored in this thesis.

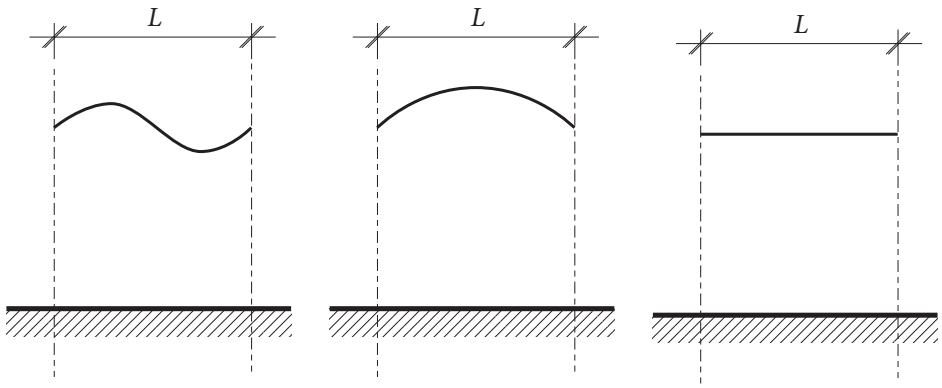

Figure 4-21: Shows the different forms to be considered within the same boundary conditions.

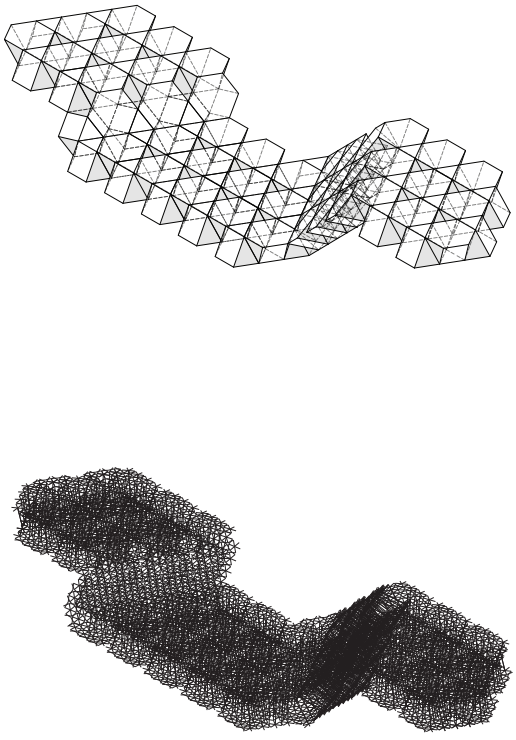

Figure 4-22: Top: frame composed of interlocking polygons, bottom: PTAF executed on xomposition.

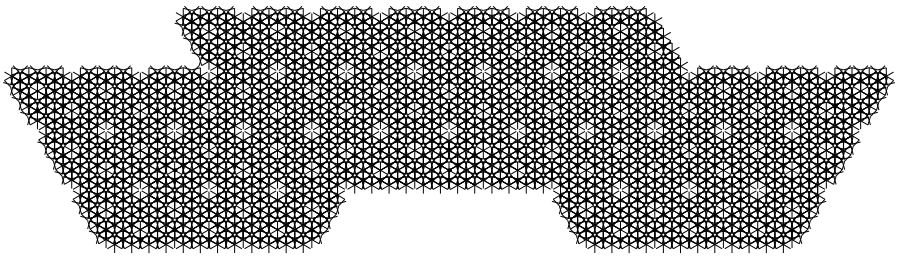

Figure 4-23: Plan of flat frame configuration.

The flat frame configuration is composed of low-poly sphere units in an alternating interlocking arrangement.

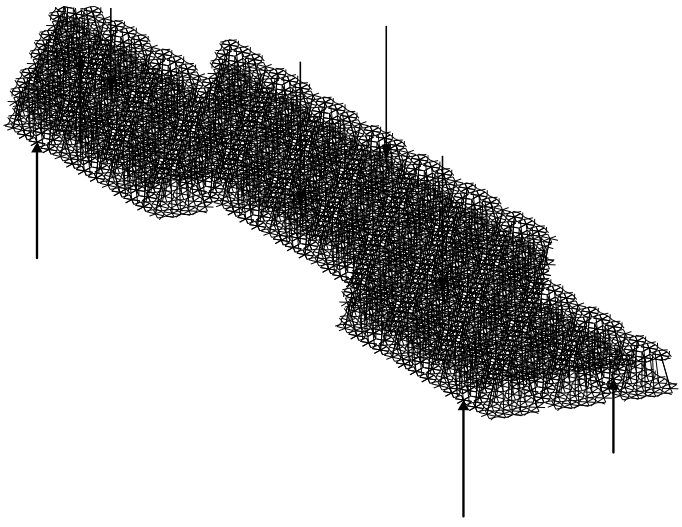

Figure 4-24: Axonometric view of flat frame configuration.

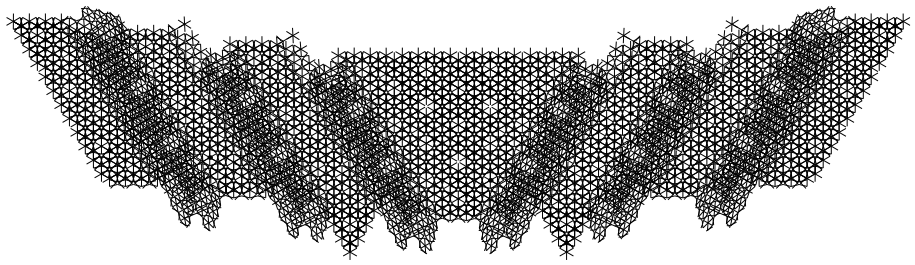

Figure 4-25: Plan of stepped arch configuration.

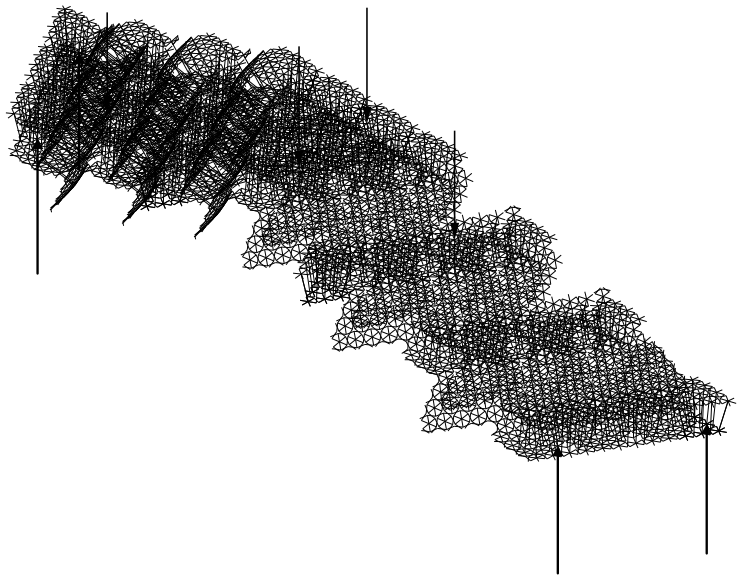

Figure 4-26: Axonometric view of stepped frame.

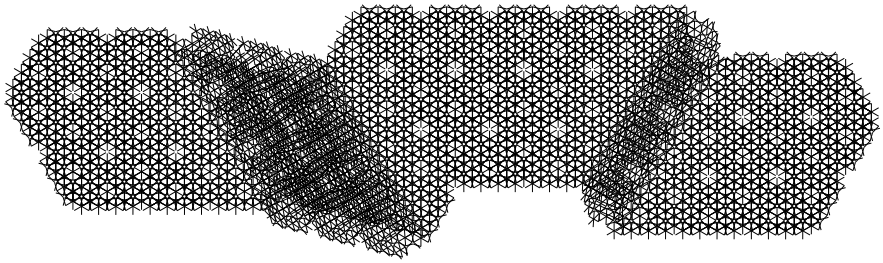

Figure 4-27: Plan view of undulating frame.

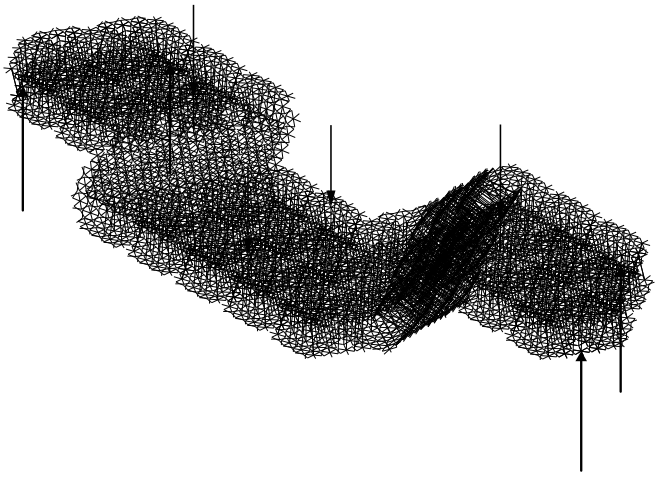

Figure 4-28: Axonometric view of undulating frame.

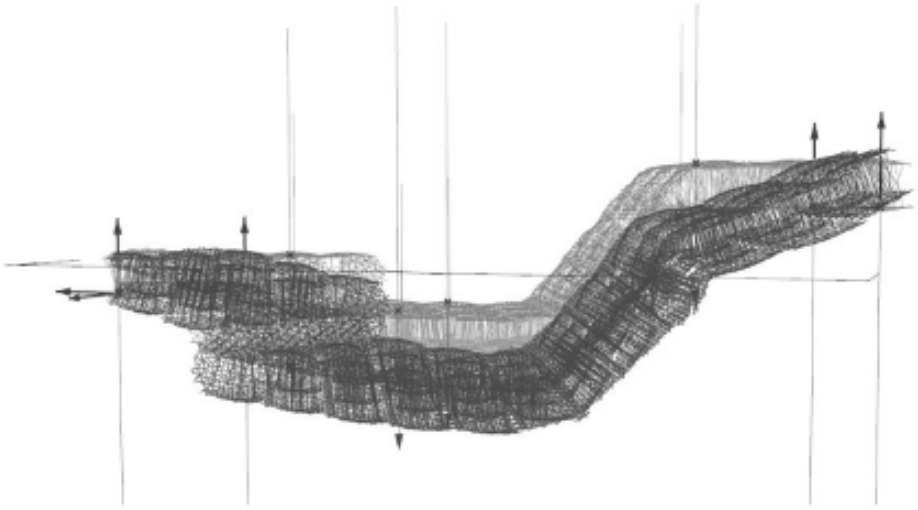

Figure 4-29: Deflected shape of loaded undulating frame model.

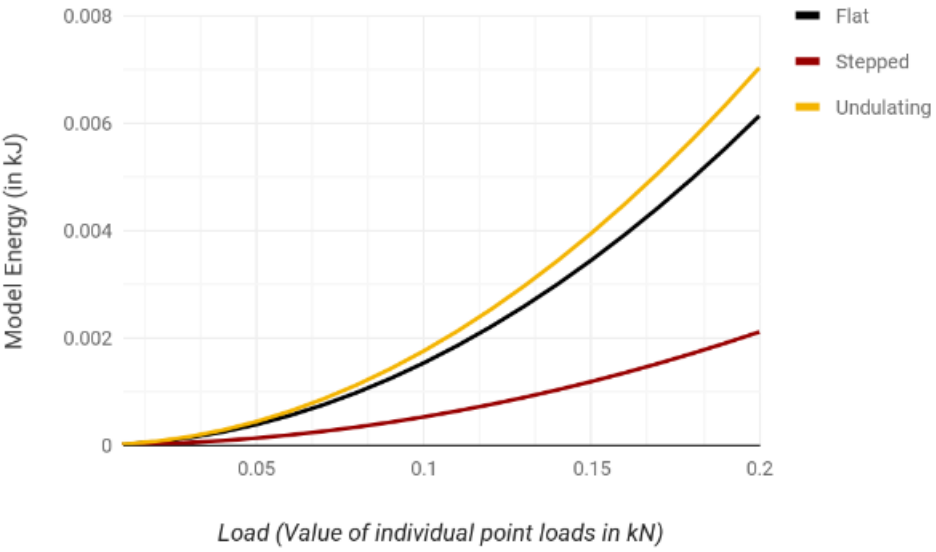

Figure 4-30: Component equivalent stiffness in multiples of ITriPlate , IXplate , ISPAR versus model energy.

From figure 4-30, it is clear that the stepped frame is superior in terms of structural efficiency when compared to the flat and the undulating options. What is interesting is that the flat and the undulating frames are similar in performance, this could very well mean that architectural criteria could easily take precedence over efficiency when deciding between these two types of frames. It is also important to note that model energy is only one type of structural analysis, furthermore these results only reflect a single load case. Throughout the pavilions use, it will undoubtedly experience several loading conditions such as: wind, rain, human interactions, etc. Rather than being conclusive, this exercise is meant to illustrate the types of information this analysis technique can generate to aid with early design decision making.

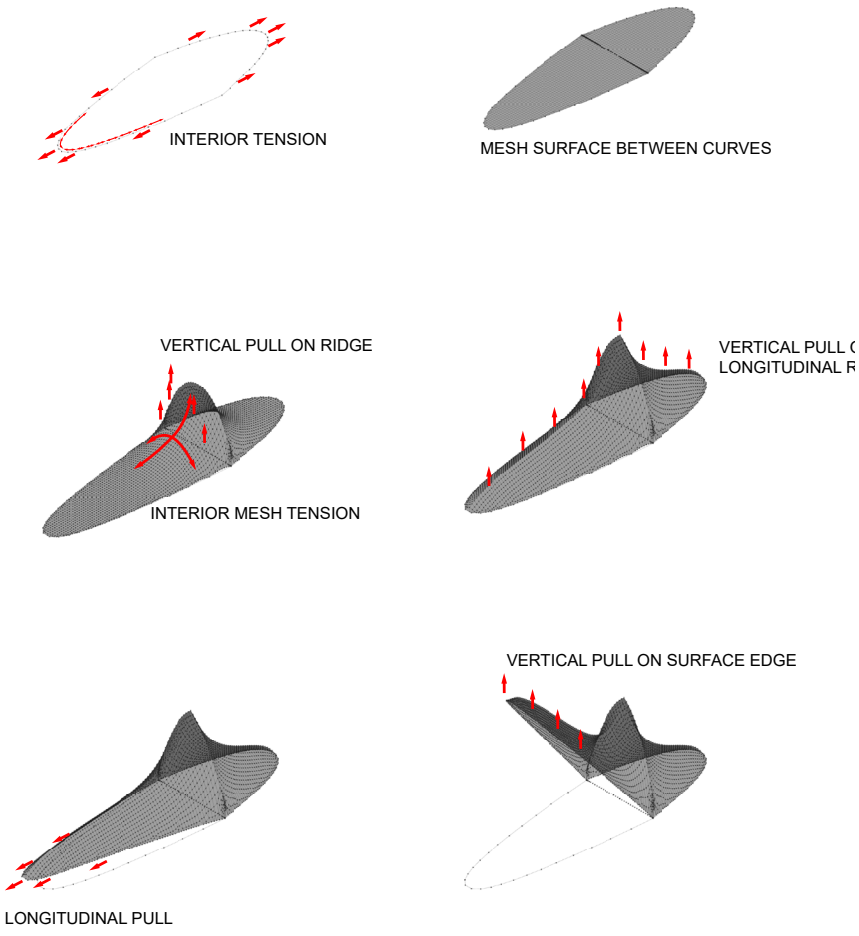

Figure 4-31: Catenary form finding process.

The next step in this hypothetical exercise is to take the knowledge learned about frame combinations learned in the previous study and apply them to the design space. Again, the findings in the previous study are in no way conclusive; however, with accurate input element stiffnesses and testing a robust range of load cases, reasonably reliable conclusions can be made. Hypothetically, from the last exercise it was learned that frames in arch formations perform better structurally than frames which are not. This aligns with the centuries of human experience building arch and shell structures. Since arches and shells behave in a similar manner, it can be assumed that a frame in a shell configuration would also perform well. In order to assist in the massing studies of this pavilion, catenary form finding can be employed because it will find, given a set of boundary forces, the ideal form of a shell between a set of points.

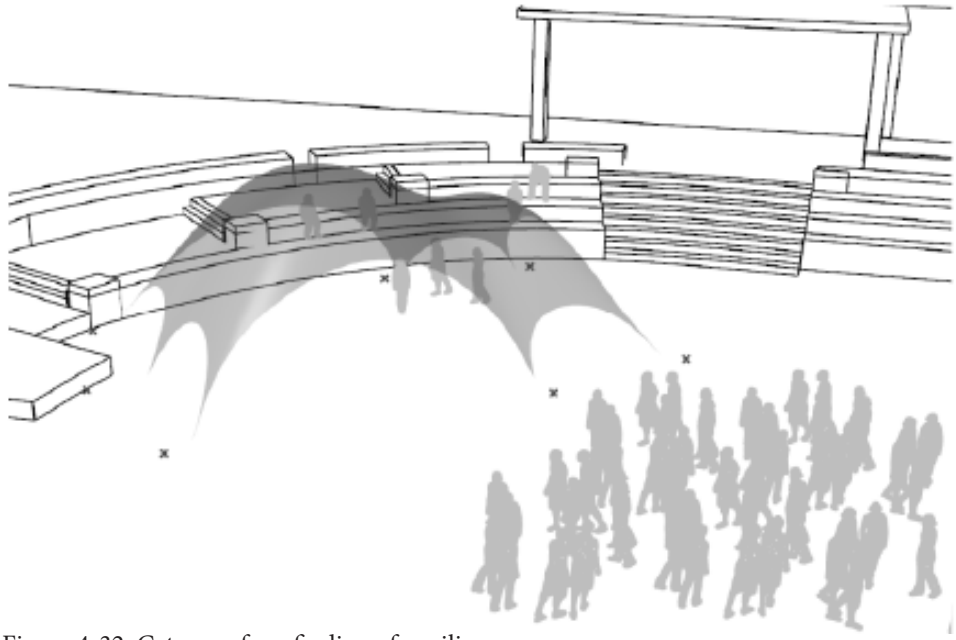

Figure 4-32: Catenary formfinding of pavilion.

Given that the structural analysis methods were developed for the Rhinoceros 3D modeling environment, it makes sense that the form finding process should be performed natively in the same environment as well. To this end, the Kangaroo physics plug-in for Rhino was employed. A script that uses a rectilinear surface and a set of points as input, was created. It takes the surface and meshes it, then it treats the mesh edges as springs which tighten, simulating the effect of a taut surface. The points

are used to anchor the surface, and an upward force is use to push this taut and anchored surface up into a catenary shell form.

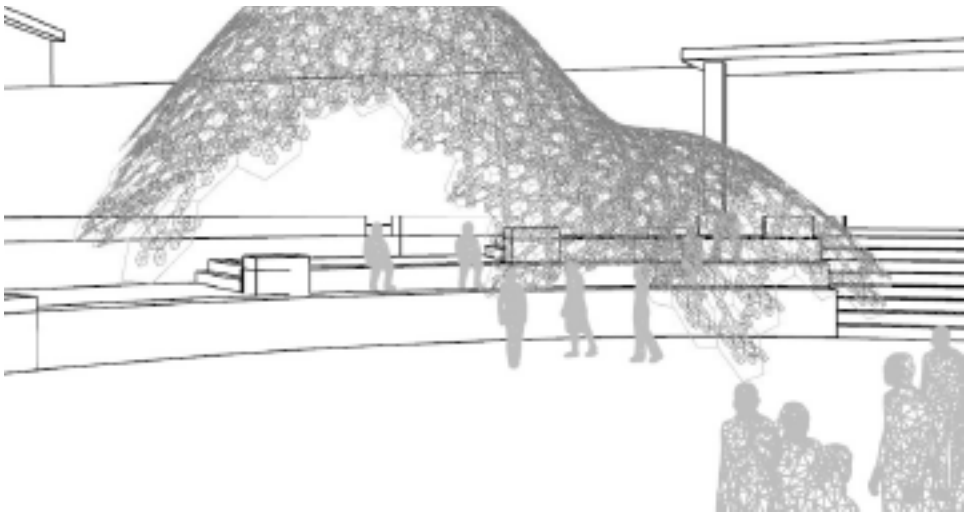

Figure 4-33: Parametric frame generation from input surface.

The next step is to approximate this surface with a tessellation of sphere units. Again, a grasshopper script was employed which maps a hexagon pattern to the surface. On limitation of this script is the hexagons are allowed to deform significantly when mapped to the surface, thus resulting in unideal sphere units which would require either custom shaped connections or spars to accommodate this difference in form. After the pattern is in place, a modified version of the centerline frame generation script, explained in chapter 3, was employed to create the spar frame.

Following method's procedure, the frame was used as an input for Karamba to perform direct stiffness method analysis. Output data used in this study was model energy, which gives a rough approximation of this configuration's structural efficiency.

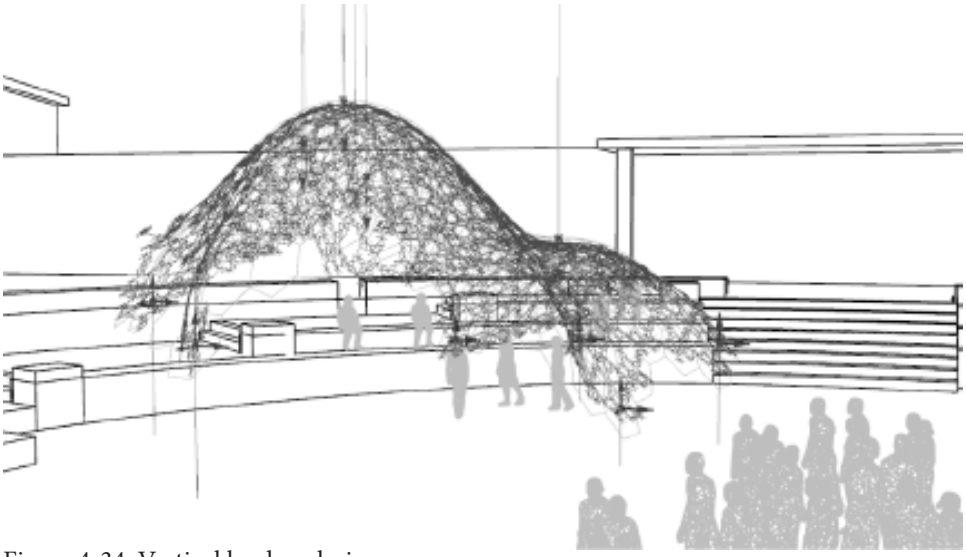

Figure 4-34: Vertical load analysis.

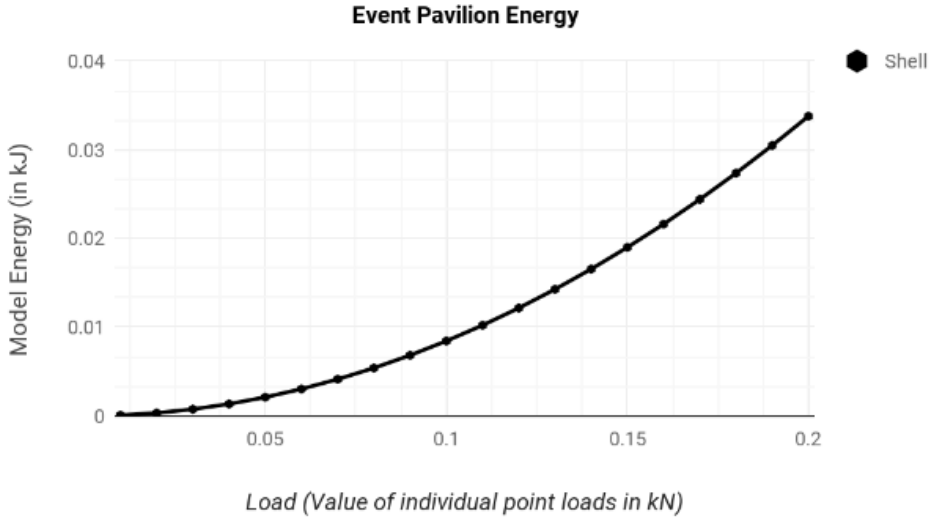

Figure 4-35: Energy versus force curve.

The final step in this workflow is to produce perspective study views where the architectural quality of this configuration can be studied. It may be helpful in future work to produce several standard views (figure 4-36); for instance in the case of the public square, views from each street corner and exiting the mall would be important to study. Plugging this entire workflow into an iterative design process gives designers qualitative and quantitative performance evaluations for each design option. This wealth of information can be used to steer the project down the most fruitful path during the very onset of the process. In this way, the designer can avoid major hiccups later in the process such as enormous unforeseen costs, or worse, a structurally impossible design, both of which could end in a project's premature termination. This design process has the potential to yield a design which satisfies the parameters laid out at the beginning of this exercise, while providing additional the additional value of space making.

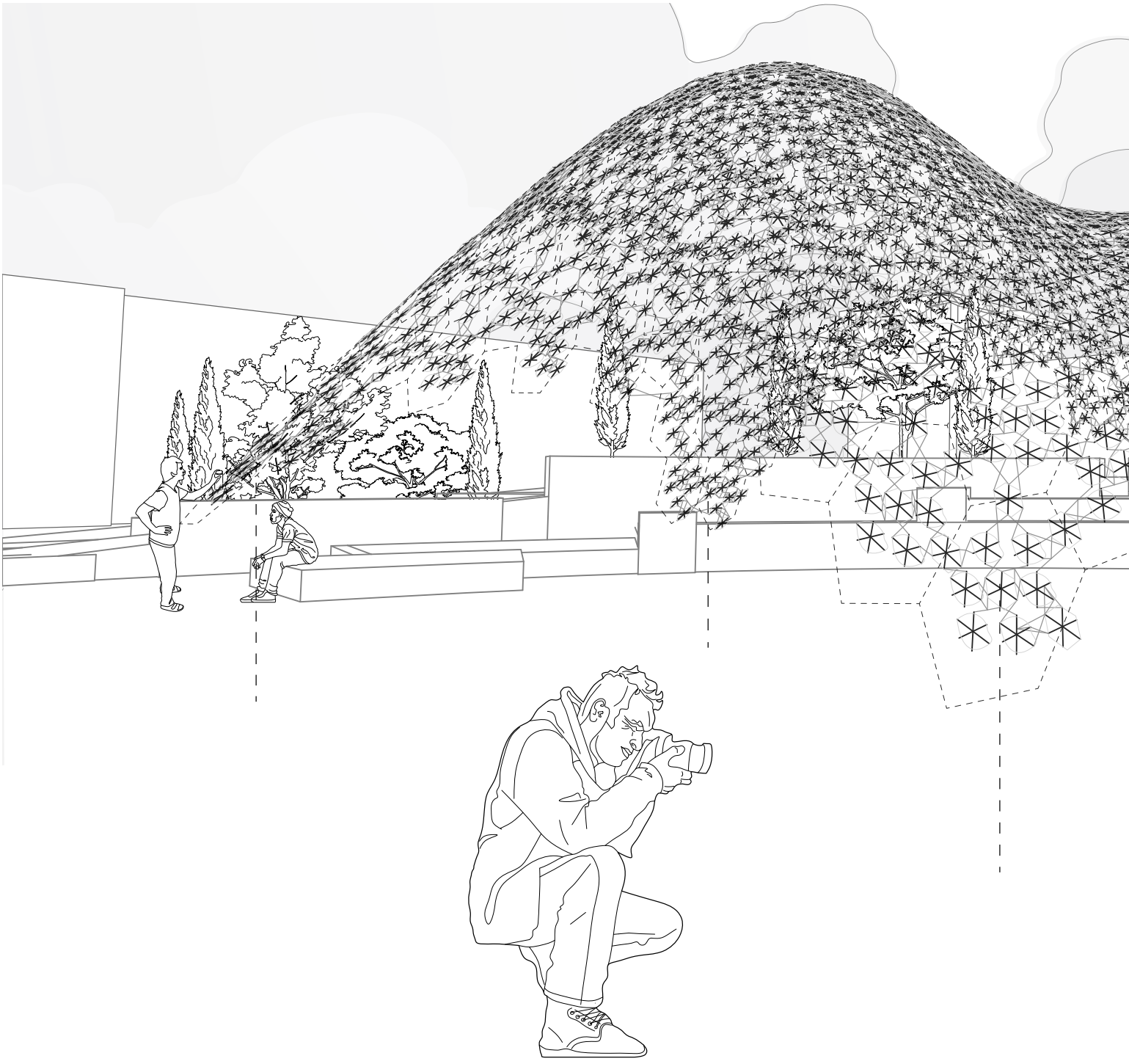

Figure 4-36: Pavilion rendering.

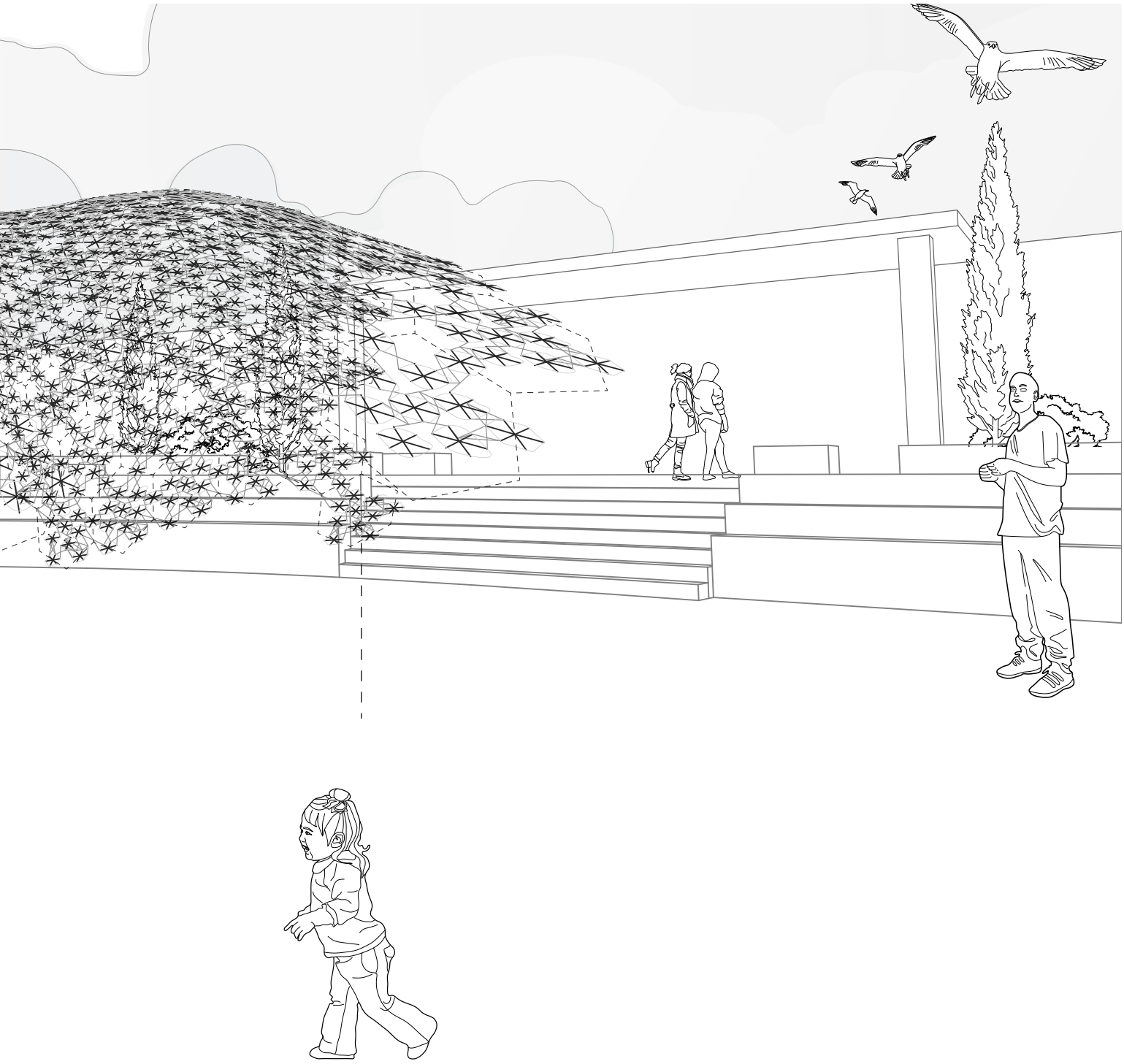

Endnotes

1 Open Streets Uptown Waterloo, accessed September 19, 2017, https://www.facebook.com/pg/OSWaterloo/about/?ref=page_internal

part 5
FUTURE WORK

5.1 RECOMMENDATIONS FOR FUTURE WORK

This thesis presented the PTAF method, a simplified approximate structural analysis method for complex frames, to integrate structural performance analysis into the form study processes of the LAS. In addition to pushing the boundaries of what is possible to build, the PTAF method could help the LAS save costs on the structure; which would allow for greater investments in mechatronic systems, equipment, and dressing. It was shown that, while various software and techniques exist for architectural and engineering design, none of them are particularly suited to providing performance analysis of complex frames that complement the architectural iterative design process. The research in this area points towards purpose built solutions, rather than general use applications. The methodologies explored in this research attempt to propose one such method for the LAS. The method was developed for the Grasshopper parametric modelling workflow because it was the main CAD software used by the LAS team. The process has two parts: the first is parametric frame generation via Grasshopper and the second is frame analysis through Karamba. The parametric script was constructed in such a way that it accepts the polygons already used by the LAS for composition modelling as input. The output is a line model representing what is known as a sphere unit by the researchers of the LAS.

The second part of this method was to make the analysis compute more quickly. It is known that if two analytical models have components that closely approximate one another, by enforcing continuity on the finite element approximation, the behaviour of these models will also be similar. A detailed FEA model and a simplified FEA model were made. The stiffness of the simplified model was manipulated to achieve the same force displacement curve as the detailed model. Once all these stiffness values are known, they are encoded into the line model from grasshopper in order to approximate the behaviour of the entire frame.

Two studies were conducted: the first was a direct collaboration with the LAS on the Amatria installation at Luddy Hall, and the second was the design study of a hypothetical pavilion. The Amatria project was the research project which laid the foundation for this thesis. Key structural components of Amatria were identified and designed for various loading conditions for increased ease of installation. During this process, it was found that FEA modeling could not keep up with the pace of design exploration. Furthermore, the FEA models created were so taxing on computer hardware to run that it was not possible to simulate more than a few spars at a time. These findings lead to the development of the PTAF method. The pavilion was a study of how the combination of parametric

modeling and approximate analysis could be used to design a free standing pavilion from typical LAS produced components. Catenary formfinding was proposed because forms derived through this technique are generally more strong and stable then free form surfaces and flat frames.

There is still significant work to be done to ensure accuracy of analysis and integration with the design process of the LAS. Delving deeply into each portion of the analytical procedure could become an entire research project on its own.

The purpose of this research was to outline a viable technique, resulting in the PTAF method, moving forward, the research diverges into specific fields which can be recombined into an improved PTAF method. These areas are: linking topology optimization into the polygon tessellation

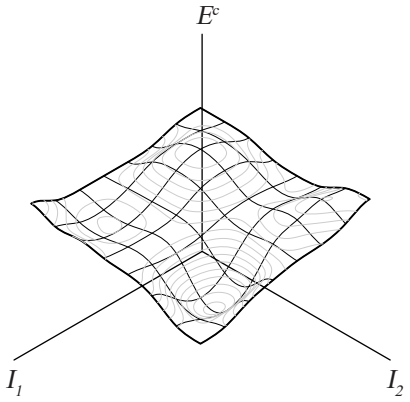

Where E^c is the function of error.

$$E^c = \int_0^f [m_\alpha^c - m_\beta^c]^2 df$$

We want to find m_β^c such that E^c is minimized.

Since $m_\beta^c\ (I_1, I_2)$, $E^c\ (I_1, I_2)$

We shall find $\frac{\partial E^c}{\partial I_1} = 0$, $\frac{\partial E^c}{\partial I_2} = 0$

Figure 5-1: Minimization of a multi-variable function of error.

process, improving the accuracy of the spar approximation, and creating custom solver algorithms. The PTAF method was based around using polygons as input because it was how LAS designers explored new compositions. In order to broaden the design space, new types of spar combination polygons and their combinatorics could be explored. Topology optimization algorithms could potentially be employed to approximate input surfaces as tessellations of several input polygon types. These tools would open the door to even more exploration.

The metal expansion process, relating the cut pattern to expanded form, of the Spar elements would require a series of lab tests in order to calibrate further numerical analysis. During these lab experiments, it would be important to map the strain within the steel, and compare it to values derived from FEA. One possible method would be to use digital image correlation (DIC) to create a strain map of the test specimen. Physical testing on already formed spars is also required to calibrate the linear elastic FEA simulations. Strain mapping such as DIC may also be useful as a measurement tool for these experiments as well. The connection FEA simulations should also be calibrated through physical testing in a similar manner.

The equivalent stiffness method used in this thesis only approximated the bending stiffness of each component. In the future, each component should have a stiffness approximation for bending in the other axes, as well as torsion. In this way, the function of error becomes a multi-dimensional function, making it more difficult to derive the equivalent stiffness.
The current approximation models do not give any information about structural failure. Unfortunately, there is no straightforward method to achieve this information; however, the following outline might serve as a starting point: First, load the component in question until yield occurs. Next, record the displacement matrix of the nodes which can also be found on the approximation model. Finally, write a program that compares these nodal displacement values of the model to the displacement matrix corresponding to yielding, and returns an indicator if any of these values has been exceeded. In this way, it might possible to approximately predict yielding.

Further research should consider the non-linear behaviour of the entire frame. The current model is only valid for the frame subjected to small deformations; however, a complex frame has the ability to undergo large deformations because the stresses have many paths to redistribute. For this reason, the behaviour of the frame is non linear because the effective

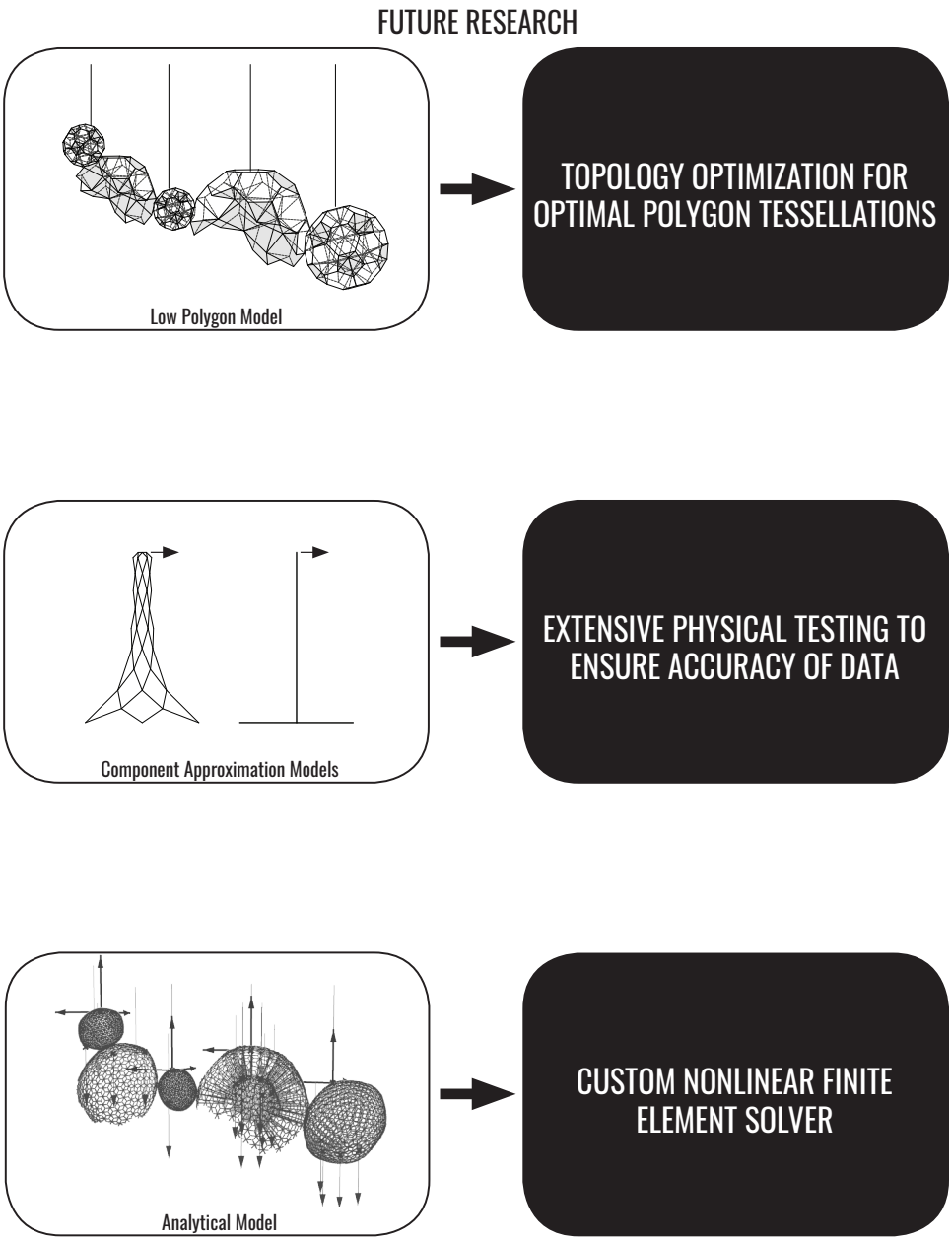

Figure 5-2: Each component of the PTAF method has the potential to become an entire field of future research.

stiffness changes while the body is deforming. The current model does not take advantage of this and will inevitably lead to over designed frames. In this way, the material efficiency of these types of structures are somewhat lost.

The PTAF method can directly contribute to the LAS body of work. This research has provided the possibility of self supporting structures, based on the system of components currently being used in LAS testbeds. Employing PTAF in future testbeds will provide invaluable information leading to new fields of design exploration.

BIBLIOGRAPHY

Abdelhameed, Wael. "Reciprocal Relationship of Conceptualization and Design Problem Definition." *CAAD Futures 2009* (2009): 410-422, http://papers.cumincad.org/cgi-bin/works/paper/cf2009_410.

"AISI Type 304 Stainless Steel," *ASM Aerospace Specification Metals*, accessed March 20, 2018, http://asm.matweb.com/search/SpecificMaterial.asp?bassnum=mq304a.

Barnes, Michael. "Form Finding and Analysis of Tension Structures by Dynamic Relaxation," *International Journal of Space Structures* 14, no. 2, (1999): 89-104. Accessed November 2, 2017. http://journals.sagepub.com.proxy.lib.uwaterloo.ca/doi/abs/10.1260/0266351991494722.

Bathe, Klaus-Jürgen. *Finite Element Procedures* (Utgivningsort Okänd: Utgivare Okänd, 2006).

Bialkowski, Sebastian. "Structural Optimisation Methods as a New Toolset for Architects." *Proceedings of the 34th ECAADe Conference* 2 (2016): 255-264. http://papers.cumincad.org/cgi-bin/works/paper/ecaade2016_098.

Block, Philippe. "Thrust Network Analysis Exploring Three-dimensional Equilibrium," PhD diss., Massachusetts Institute of Technology (437415216) accessed October 3, 2017,https://dspace.mit.edu/handle/1721.1/49539. 37.

Brown, Nathan. "Design Space Exploration User Manual Version 1.1," *Massachusetts Institute of Technology*, 2017, accessed November 2, 2017, http://digitalstructures.mit.edu/page/tools#design-space-exploration-tool-suite-for-grasshopper.

Canadian Wood Council, *The Span Book: Span Tables for Canadian Dimension Lumber and Glued-Laminated Timber*, 6th ed. (Ottawa, Ontario.: Canadian Wood Council, 2009)

Changiz, Navid, and Mehdi Jalalpou. "Robust topology optimization of frame structures undergeometric or material properties uncertainties," *Structural and Multidisciplinary Optimization* 56, Issue 4, (2017): 791–807. Accessed January 12, 2018. doi:10.1007/s00158-017-1686-4

"Comparative Building Costs," *Buildings*, accessed June 18, 2019, https://www.buildings.com/news/industry-news/articleid/21528/title/comparative-building-costs.

Danhaive, Renaud, and Caitlin T. Mueller. “Combining Parametric Modeling and Interactive Optimization for High-Performance and Creative Structural Design,” *Proceedings of the IASS Symposium* 2015 (2015). Accessed November 11, 2017, http://digitalstructures.mit.edu/files/2015-09/iass2015-524698.pdf.

Eyre, Jim. “Architecture or Engineering,” *WilkinsonEyre*, accessed June 18, 2019. https://www.wilkinsoneyre.com/thoughts/essays/architecture-or-engineering.

Fischer, Thomas. “Generation of Apparently Irregular Truss Structures,” *Computer Aided Architectural Design Futures 2005* (2005): 229-238, doi:10.1007/1-4020-3698-1_21.

Fish, Jacob, and Ted Belytschko. *A First Course in Finite Elements* (Pacific Grove, CA: Content Technologies, 2007).

Hui, Deng, Li Hongyang, Su Cheng and Yiping Jiang. “Monitoring and Analyzing Displacement of Large-Span Spoke-Type Cable Structure Roof,” *Journal of Surveying Engineering* 142, no.4 (2017). Accessed November 2, 2017, http://ascelibrary.org/doi/10.1061/%28ASCE%29SU.1943-5428.0000237.

Hibbeler, Russell C. *Structural Analysis*, 10th ed. (Upper Saddle River, N.J: Pearson Prentice Hall, 2017).

Hibbeler, Russell C., and Kai Beng Yap, *Mechanics of Materials* (Harlow, United Kingdom: Pearson, 2018).

Januszkiewicz, Krystyna, and Marta, Banachowicz. “Nonlinear Shaping Architecture Designed with Using Evolutionary Structural Optimization Tools.” *IOP Conference Series: Materials Science and Engineering* 245 (2017): 082042. doi:10.1088/1757-899x/245/8/082042.

Kilian, Axel, and John Ochsendorf. “Particle-Spring Systems for Structural Form Finding,” *Journal of the International Association for Shell and Spatial Structures* 46, no.147 (2005). Accessed November 11, 2017, http://designexplorer.net/newscreens/cadenarytool/KilianOchsendorfIASS.pdf.

Kociecki, Maggie, and Hojjat Adeli. "Two-phase Genetic Algorithm for Size Optimization of Free-form Steel Space-frame Roof Structures." *Journal of Constructional Steel Research* 90 (2013): 283-96. doi:10.1016/j.jcsr.2013.07.027.

Kociecki, Maggie, and Hojjat Adeli. "Two-phase Genetic Algorithm for Topology Optimization of Free-form Steel Space-frame Roof Structures with Complex Curvatures." *Engineering Applications of Artificial Intelligence* 32 (2014): 218-27. doi:10.1016/j.engappai.2014.01.010.

Reddy, J.N., *Introduction to the Finite Element Method* (Europe: McGraw-Hill Education, 2018).

Mueller, Caitlin T. "Computational Exploration of the Structural Design Space," PhD diss., Massachusetts Institute of Technology (893430996). Accessed October 3, 2017, http://hdl.handle.net/1721.1/91293.

Ren, Shibo, Salomé Galjaard, Sander Hofman, and Neil Perry. "Topology Optimisation for Steel Structural Design with Additive Manufacturing." *Proceedings of the IASS Symposium 2015* (2015): 35-44. doi:10.1007/978-3-319-24208-8_3.

Ontario Association of Architects, *Canadian Handbook of Practice for Architects* (Ottawa: Royal Architectural Institute of Canada, 2009).

Open Streets Uptown Waterloo, accessed September 19, 2017, https://www.facebook.com/pg/OSWaterloo/about/?ref=page_internal.

"R.R.O. 1990, Reg. 941: General," *Government of Ontario*, made March 23, 2018, https://www.ontario.ca/laws/regulation/900941.

Veenendaal, Diederik, Jack Bakker and Philippe Block. "Structural Design of the Flexibly Formed, Mesh-reinforced Concrete Sandwich Shell Roof Of Nest HiLo," *Journal of the International Association for Shell and Spatial Structures* 58, no.1(2017). Accessed November 2, 2017, http://www.block.arch.ethz.ch/brg/files/Jiass_2017_vol58_no1_08_Veenedaal_Mesh-reinforced-sandwich-shell-roof-NEST-HiLo_1491482576.pdf.

Wellington, Arthur M. *The Economic Theory of the Location of Railways: An Analysis of the Conditions Controlling the Laying out of Railways to Effect the Most Judicious Expenditure of Capital* (New York: J. Wiley & Sons, 1887).